

Understanding the chemical impacts of biogenic volatile organic
compounds and the physical drivers of their observed seasonality

Deborah F. McGlynn

Dissertation submitted to the Faculty of the
Virginia Polytechnic Institute and State University
in partial fulfillment of the requirements for the degree of

Doctor of Philosophy

in

Civil and Environmental Engineering

Gabriel Isaacman-VanWertz, Chair

Linsey C. Marr

John Little

Sally Pusede

May 6, 2022

Blacksburg, Virginia

Keywords: biogenic volatile organic compounds, gas chromatography flame ionization
detector, atmospheric reactivity, ozone, secondary organic aerosol, atmospheric composition

Copyright 2022, Deborah F. McGlynn

Understanding the chemical impacts of biogenic volatile organic compounds and the physical drivers of their observed seasonality

Deborah F. McGlynn

(ABSTRACT)

Emissions from natural ecosystems, broadly classified as biogenic volatile organic compounds (BVOCs), contribute 90% to the VOC budget. Individual BVOCs vary widely in their reaction rates with atmospheric oxidants, making their atmospheric impact highly dependent on VOC composition. Their emissions are also dependent on vegetative make up and a number of meteorological and ecological variables. However, the ecological and physical drivers of their emissions is becoming more variable in a changing climate, leading to greater uncertainties in models. Increasing the monitoring of individual compounds can improve our understanding of the drivers of these emissions and the impact of individual chemical species on atmospheric composition. Improved understanding of BVOC composition can better emission models and, SOA and ozone formation predictions. To study the atmospheric impacts and physical drivers of BVOCs, a GC-FID was adapted for automated hourly sampling and analysis. The details of the hardware and software used for the system are described in detail to enable future long-term BVOC measurements in additional locations. The instrument was deployed at a measurement tower in a forest in central Virginia for year-round collection of BVOC concentrations. Using two years of collected hourly data, this work assesses the chemical impacts of individual BVOCs on time scales ranging from hour to year. This work identifies the importance of both concentration and chemical structure in determining atmospheric impacts. Additionally, seasonality in the concentration of some biogenic species has large implications for atmospheric reactivity in the warmest months of the year, particularly ozone reactivity. Using ecological and meteorological data collected at

the site in conjunction with the BVOC data, the drivers of BVOC concentrations and their seasonality are identified. Comparison between this data and current models, reveal important deviations which may lead to large modeled uncertainties. Furthermore, the collected data has been made publicly available to aid in future research regarding BVOCs.

Understanding the chemical impacts of biogenic volatile organic compounds and the physical drivers of their observed seasonality

Deborah F. McGlynn

(GENERAL AUDIENCE ABSTRACT)

The earth hosts a number of sources of atmospheric emissions. These range from human-driven sources such as vehicles and factories, to natural sources such as trees and grass. The content of these emissions, amongst others, become a part of a large reactor (the atmosphere), that interact with each other. The interaction of these emissions with atmospheric oxidants forms a gas (ozone) with implications for human and ecosystem health, and secondary organic aerosol (the leading component to smog). However, the extent to which these emissions react with atmospheric oxidants is largely dependent on the structure of individual compounds. A major focus of this dissertation is to show that compounds with reactive structures can have a large impact on atmospheric composition, and that the quantity of emissions can be as important as compound structure. Understanding the impact of individual compounds in the atmosphere requires improved measurement techniques, capable of detecting the compounds of interest over long time periods. Therefore, another focus of this work was the adaptation and deployment of an instrument capable of detecting some of the most reactive species in the atmosphere, volatile organic compounds emitted from forests. The instrument deployed in this work was a gas chromatography flame ionization detector (GC-FID), which detects compounds largely composed of carbon and hydrogen. The instrument was adapted to run automatically through the development of an electronics box and software program interfaced with the GC-FID. Following development, the instrument was deployed to a remote forest research site for two years. The data collected from this work was used to determine the impact of individual compounds on atmospheric composition.

Findings from this work could be used to improve a range of atmospheric models. Small changes in emissions (human or plant) contribute to the total VOC budget which can have large implications for the formation of ozone and SOA. Therefore, increased understanding of the BVOC concentrations and emission driver will aid in predicting these atmospheric components.

Acknowledgments

The work would not have been made possible without the assistance, guidance, and friendship from a number of people. My partner Brad has been by my side from undergraduate through two different graduate programs. He is always up for a conversation about coding while walking down to the local coffee shop for a matcha-break from work. When we are not working, he is happy to try out a local brewery with me, a new hike with some friends or attempt to make ethiopean food. He is always excited and supportive of trying a new hobby such a coffee roasting or gardening, to name a few. These degrees would not have been possible without his endearing love and friendship.

My adviser, Gabe provided years of guidance, support, and suggestions for my work which always yielded results beyond which I thought I was capable of. He is always optimistic even when a situation is not ideal, making it little easier to keep going. He also has an incredible eye for story telling which is something that I hope to have picked up. He has been beyond supportive throughout my academic career and in my job search.

I would like to thank my committee (Dr. Marr, Dr. Little, and Dr. Pusede) for their feedback and guidance on my work. Dr. Marr has also been incredibly helpful and supportive when applying for fellowships and jobs. Dr. Manual Lerdau was not on my committee but was an incredibly supportive collaborator. He provided insightful advice and thoughts on the biological side of the work I was doing, which substantially improved the depth of my investigations. He also was quick to provide feedback or sit down for a conversation whenever I asked.

As one of the first two students in Gabe's lab, I was really excited to see the lab grow with new students and postdocs. The labmates I have worked with throughout my time at Virginia Tech have been great to talk to about work and other things. I am incredibly happy

that our grad school time has overlapped.

I have made a lot of wonderful friends during my grad school years which has made my time in Blacksburg a lot of fun and filled with great memories. If it weren't for their willingness to go to trivia, day-trip to Roanoke, or go hiking, the time would have passed very slowly.

The CEE department at Virginia Tech is like no other academic department I have been apart of. Everyone is very welcoming, optimistic, and excited to be here and working together; it truly is a wonderful academic environment. Specifically, I would like to thank Jody Smiley and Beth Lucas for their assistance during my time in the department. Jody, for analytical instruction and assistance; Beth, for administrative assistance.

About half of my grad school years have been during COVID. When COVID first started, the local animal shelter was in need people to foster cats. Since then, I have had 4 long-term fosters (Curtis, Mr. Fitz, Pearl, and Kiara). They'll never know it, but they have given to me more than I have given to them.

My parents, sister, and Brad's mom (Sherry) have supported both of us in every step of our academic journey's. When we were closer to home, they would have us over for dinner while letting us use their washing machine. After we moved to Virginia, they have come to visit us, which I know is a long drive. My sister in particular has always picked of the phone whenever I needed someone to talk for everything from professional advice to just casual conversation. This was incredibly helpful when I was driving back from Charlottesville after a long day at the tower.

Thank you again to everyone who has helped to get me here.

Contents

List of Figures	xii
List of Tables	xviii
1 Introduction	1
1.1 Volatile organic compounds	1
1.1.1 Biogenic volatile organic compounds	2
1.2 Methods for detection of atmospheric volatile organic compounds	4
1.3 Importance of BVOCs for ozone and SOA models	8
1.4 Objectives	9
1.5 Organization of the Dissertation	10
1.6 References	11
2 An autonomous remotely operated gas chromatograph for chemically re- solved monitoring of atmospheric volatile organic compounds	20
2.1 Abstract	20
2.2 Introduction	21
2.3 Methods	24
2.3.1 Instrument overview	24
2.3.2 Adsorbent trap and desorption program	27
2.3.3 Electronic design	27
2.3.4 Automated data analysis	30
2.3.5 Data collection and calibration	32
2.3.6 FID signal integration to concentration	33

2.4	Results and Discussion	34
2.4.1	The species detected	34
2.4.2	Calibration curve	35
2.4.3	Stable calibration	37
2.4.4	Additional recommendations for improved long-term deployment	38
2.5	Conclusions	40
2.6	Acknowledgements	41
2.7	References	41
3	Variability in the composition of biogenic volatile organic compounds in a Southeastern US forest and their role in atmospheric reactivity	47
3.1	Abstract	48
3.2	Introduction	49
3.3	Methods	52
3.3.1	Instrument location and operation	52
3.3.2	Calibration and compound identification	55
3.3.3	Atmospheric oxidant reactivity and reaction rate calculations	56
3.4	Results and Discussion	57
3.4.1	Temporal trends in BVOC mixing ratios	57
3.4.2	Calculated reactivity with atmospheric oxidants	63
3.4.3	Isomer composition of monoterpenes	67
3.5	Conclusion	70
3.6	Acknowledgements	71
3.7	References	72
4	Minor contributions of daytime monoterpenes are major contributors to atmospheric reactivity	84

4.1	Abstract	84
4.2	Introduction	85
4.3	Methods	89
4.3.1	Data collection and preparation	89
4.3.2	Positive Matrix Factorization	89
4.3.3	Ozone reactivity calculations	90
4.4	Results and discussion	91
4.4.1	Monoterpene seasonality	91
4.4.2	Light dependent and light independent monoterpene concentration	94
4.4.3	Ozone and OH reactivity	96
4.5	Conclusion	100
4.6	Acknowledgements	102
4.7	References	102
5	Conclusions	110
5.1	Outcomes of objective 1	111
5.2	Outcomes of objective 2	112
5.3	Outcomes of objective 3	112
5.4	Recommendations for future work	113
	Appendices	115
	Appendix A Supplemental Information for Chapter 2	116
	Appendix B Supplemental Information for Chapter 3	119
	Appendix C Figures associated with the updated ozone reaction rate constant with limonene in chapter 3	122

List of Figures

2.1	Instrument overview. A depiction of the gas chromatograph (GC) connections and plumbing. A zoomed in representation of the trap, which is found on the 6-port valve, can be found to the left of the dashed line. The trap connects externally to a 6-port valve, situated on-top of the GC oven, and is cooled by a 24V fan. The flame ionization detector (FID) and column are supplied by gases using electronic pressure controllers (EPC) operated by the GC. Sample and calibrant flows are controlled by mass flow controllers (MFC). A valve (V1) is used for calibrants and zero air.	26
2.2	The trap heating profile for sample desorption. The red line depicts the set point, and the blue line depicts the trap temperature as it heats and cools at the beginning of a run.	28
2.3	Diagram of the control electronics. Connections between the data acquisition board and controlled instrument components are shown. A 24V relay board controls 6 directly switched circuits, including those used for the fan and valves, and 2 switched solid state relays (SSR) that control 110V power for the heaters. Additional connections include the 6-port valve, thermocouple (TC) hub, mass flow controllers (MFC), FID signals, and GC start and stop signals.	29
2.4	An example chromatogram with a label for a range of compounds detected by the instrument. “A” denotes that the compound is anthropogenic, “I”, “M”, “S” are terpenes or isoprene, monoterpene, and sesquiterpene, and “O” are oxygenated species.	34

2.5	A linear regression plot between the integrated FID signal and the calibrant concentration for one week of calibrations. The slope from this linear regression is multiplied by each integration during that week and divided by the effective carbon number to yield ppb. The shading represents the standard error (4.4 ± 0.2) of the residuals to account for the uncertainty of the slope of the linear regression. Colors represent different calibration levels (i.e., different dilution flows) and symbols represent calibrants.	36
2.6	A tracking standard for limonene, trimethylbenzene, and α -cedrene each day between January and May 2021.	37
3.1	A schematic of the VOC-GC-FID set up at the Virginia Forest Research Lab. MFC, mass-flow controller; V1, valve; GC, gas chromatograph; FID, flame ionization detector; EPC, electronic pressure controller; He, helium gas; H ₂ , hydrogen gas. Small, dashed lines around the inlet, denote the portion that is heated. The large grey dashed line denotes the indicates that the inlet is within the canopy and the rest of the instrument is in the shed, the boxed-in grey dashed line denotes the components that are part of the GC.	54
3.2	A typical GC chromatogram of sampled ambient air collected at the site. The compounds identified on the figure show the range of species found by the instrumental methods. These include isoprene (I), isoprene oxidation products (IOP), monoterpenes (M), and sesquiterpenes (S). Unlabeled peaks were not identified to be terpenes or isoprene oxidation products and are, in most cases, identifiable as a belonging to a different compound class.	58

3.3	24-hour average concentrations of (a) isoprene, (b) isoprene oxidation products (methyl vinyl ketone and methacrolein), (c) sum of monoterpenes, and (d) sum of sesquiterpenes between September 15th, 2019 and September 15th, 2020	60
3.4	Binned hourly boxplots for the four BVOC classes, divided into (left) the growing season, May-October and (right) the non-growing season, November-April. Classes shown are: (a-b) isoprene, (c-d) isoprene oxidation products, (e-f) monoterpenes, and (g-h) sesquiterpenes. The plots show the median value as a horizontal line, the bottom and top of each box indicates the 25 th and 75 th percentiles while the whisker represent 1.5 times the interquartile range. Each box represents the data for each hour of the day.	62
3.5	(a) Timeseries of 24-hour averaged calculated OH reactivity of all measured terpene classes and the monoterpene class, as well as the monthly mean of calculated OH reactivity. (b) Relative contribution of each of the BVOC classes to OH reactivity.	63
3.6	(a) Timeseries of 24-hour averaged calculated ozone reactivity of all terpene classes and the monoterpene class, as well as the monthly mean of calculated ozone reactivity. (b) Relative contribution of each of the BVOC classes to ozone reactivity.	65
3.7	(a) Timeseries of 24-hour averaged calculated nitrate reactivity of all terpene classes and the monoterpene class, as well as the monthly mean of calculated nitrate reactivity. (b) Relative contribution of each of the BVOC classes to nitrate reactivity.	66

3.8	A breakdown of detected monoterpene isomers in the growing and non-growing seasons for (a-b) concentration, (c-d) OH reactivity, (e-f) ozone reactivity, (g-h) nitrate reactivity. Values are rounded to the nearest percent and values below 1% are not depicted.	68
4.1	The mean (a) α -pinene and (b) limonene concentration in the four seasons of the northern hemisphere between September 2019 and September 2021. . . .	92
4.2	The 12-hour average of α -pinene and limonene between April 2021 and August 2021. The averaging period for each compound was between 7 AM and 7 PM.	93
4.3	Time series of isoprene concentration, the two positive matrix factorization factors between September 2019 and September 2020 and the breakdown of the monoterpene species that contribute to each factor.	95
4.4	A four-day period in July 2020 of isoprene, and the two PMF factors (Light Dependent and Light Independent).	97
4.5	The 2020 summer diurnal profile of (a) measured concentration, (b) calculated monoterpene ozone reactivity and (c) OH reactivity, as well as light dependent(LD) (d) concentrations, (e) ozone reactivity, and (f) OH reactivity, and light independent (LI) (g) concentration, (h) ozone reactivity, (i) OH reactivity.	99
A.1	A linear regression plot between the integrated FID signal and the calibrant concentration for one-week of Limonene and TMB calibrations. The shading represents the standard error (3.5 ± 0.07) of the residuals to account for the uncertainty of the slope of the linear regression. Colors represent different calibration levels (i.e., different dilution flows) and symbols represent calibrants.	117

A.2	A linear regression plot between the integrated FID signal and the calibrant concentration for one-week of MVK and Nopinone calibrations. The shading represents the standard error (11 ± 1.3) of the residuals to account for the uncertainty of the slope of the linear regression. Colors represent different calibration levels (i.e., different dilution flows) and symbols represent calibrants.	118
B.1	Ambient temperature ($^{\circ}\text{C}$) and downwelling shortwave radiation (W m^{-2}) for January 1 st 2020 – September 15 th , 2020.	120
B.2	Concentration plotted against reactivity to yield the rate constant for OH (a-b), Ozone (c-d), nitrate (e-f) in the growing and non-growing season. The slope in each equation is the average reaction rate of each oxidant with total monoterpenes.	121
C.1	(a) Timeseries of 24-hour averaged calculated ozone reactivity of all terpene classes and the monoterpene class, as well as the monthly mean of calculated ozone reactivity. (b) Relative contribution of each of the BVOC classes to ozone reactivity.	123
C.2	A breakdown of detected monoterpene isomers in the growing and non-growing seasons for (a-b) concentration, (c-d) OH reactivity, (e-f) ozone reactivity, (g-h) nitrate reactivity. Values are rounded to the nearest percent and values below 1% are not depicted	124
C.3	Concentration plotted against reactivity to yield the rate constant for OH (a-b), Ozone (c-d), nitrate (e-f) in the growing and non-growing season. The slope in each equation is the average reaction rate of each oxidant with total monoterpenes.	125

D.1	The 12-hour average of α -pinene and limonene between September 2019 and September 2021. The averaging period for each compound was between 7 AM and 7 PM.	128
D.2	Time series of isoprene concentration, the two positive matrix factorization factors between January 2021 and September 2021 and the breakdown of the monoterpene species that contribute to each factor.	129
D.3	A four-day period in July 2021 of isoprene, and the two PMF factors (Light Dependent and Light Independent).	130
D.4	The diurnal profile of (a) measured monoterpene concentration and (b) ozone reactivity, (c) factor 1 monoterpene concentration and (d) ozone reactivity, and (e) factor 2 monoterpene concentration and (f) ozone reactivity for summer 2021.	131

List of Tables

2.1	Compound names and labels on the example chromatogram	34
3.1	Compound identities on an example chromatogram and associated rate constants ($cm^3molec^{-1}s^{-1}$) for OH, ozone, and nitrate.	59
3.2	Average and interquartile range of mixing ratio, OH (OHR), ozone (O ₃ R), and nitrate (NO ₃ R) reactivities in the growing and non-growing seasons . . .	61
4.1	Percent of concentrations attributed to de novo and pool emissions by compound for 2019-2020	98
B.1	Composition and pure concentration of the multi-component calibrant . . .	120
D.1	Ozone rate constants and associated compounds	127
D.2	Mapping of bootstrap factors to base factors for 2019-2020 data	127
D.3	Percent of factor attributed to light independent (%LI) and light dependent (%LD) emissions by compound for 2019-2020 data	127

List of Abbreviations

BVOC Biogenic Volatile Organic Compound

ECN Effective carbon number

EPA Environmental Protection Agency

EPC Electronic pressure controller

FID Flame Ionization Detector

GC Gas Chromatography

LOD Limit of detection

MACR Methacrolein

MDL Method detection limit

MFC Mass flow controller

MS Mass Spectrometry

MVK Methyl Vinyl Ketone

NIST National Institute for Standards and Technology

NO₃ Nitrate

NO₃R Nitrate reactivity

NO_x Nitrogen oxides (NO, NO₂)

O₃ Ozone

O₃R Ozone reactivity

OH Hydroxyl Radical

OHR Hydroxyl Reactivity

PMF Positive matrix factorization

ppb parts per billion

ppbC parts per billion by carbon

ppm parts per million

ppt parts per trillion

SOA Secondary Organic Aerosol

TERN TAG ExploreR and iNtegration package

TMB Trimethylbenzene

VFL Virginia Forest Laboratory; Pace Tower

VOC Volatile Organic Compound

Chapter 1

Introduction

1.1 Volatile organic compounds

Volatile organic compounds (VOC) are a diverse group of carbon containing compounds that are gas phase at room temperature. They are divided into subcategories based on their vapor pressures where more volatile species have higher vapor pressure. These sub categories roughly divide compounds by whether they are expected to partition to the particle phase at normal ambient temperatures (Donahue et al. [2011](#), [2012](#)). Volatile organic compounds (VOC) are found in the gas phase at ambient temperature, intermediate volatile organic compounds (IVOC) have lower vapor pressures than VOCs but are also in the gas phase at ambient temperatures, and semi-volatile organic compounds (SVOC) tend to partition between the gas and particle phase at these same temperatures (Donahue et al. [2011](#)). They are emitted from both anthropogenic and natural sources, though natural sources comprise 90% of emissions globally (Guenther et al. [1995](#)). VOCs are not only classified by their volatility, but also their source. For example, anthropogenic VOCs (AVOC) are emitted from human sources and include emissions from paint and perfumes, amongst others. Oxygenated VOCs (OVOC) constitute oxygen containing compounds and can be emitted directly or formed through reactions between VOCs and atmospheric oxidants. Biogenic VOCs (BVOC) are comprised of all VOCs that are emitted from natural sources such as trees and grasses and are the major focus of this work.

1.1.1 Biogenic volatile organic compounds

Plants emit a wide range of reactive gases known as biogenic volatile organic compounds. The importance of these emissions to atmospheric composition was described at least as early as 1960, with the blue haze phenomenon identified over forested regions (Went 1960a,b). The implication of their atmospheric impact is also notable for a number of geographic regions such as the Blue Mountains, Great Smoky Mountains, and the Blue Ridge Mountains of the US, and the Blue Mountains of Australia.

BVOCs include, terpenes, phenols, and nitrogenous compounds (Niinemets and Monson 2013), though this work focuses largely on terpenes. Terpenes are the dominant form of reactive carbon, and constitute a range of volatile organic compounds including, isoprene (C_5H_8), and larger, more varied chemical classes consisting of multiple isoprene units: monoterpenes ($C_{10}H_{16}$), sesquiterpenes ($C_{15}H_{24}$), and diterpenes ($C_{20}H_{32}$). The composition of volatile organic compounds is largely dependent on the vegetative composition of an ecosystem. Generally speaking, monoterpenes and larger classes are emitted through volatilization from resin ducts of needles from coniferous trees (Ghirardo et al. 2010; Niinemets and Monson 2013; Staudt et al. 1999). Isoprene is emitted after formation within the plant through plant stomata of dicotyledon trees such as poplars and oaks (Ghirardo et al. 2010; Niinemets and Monson 2013). Furthermore, studies looking at the types of species emitted from different plants largely find that plants that emit isoprene are not large emitters of monoterpenes and sesquiterpenes, and visa versa. However, this represents only a general trend and there may be outliers (Brilli et al. 2009; Ghirardo et al. 2010; Kesselmeier and Staudt 1999; Niinemets and Monson 2013).

As BVOCs react with atmospheric oxidants such as OH, Ozone (O_3) and Nitrate (NO_3), they begin to form OVOCs, which tend to have lower vapor pressures (Seinfeld and Pandis 2006). The importance of oxidation by atmospheric oxidants is dependent on whether sun-

light is present or not. For example, oxidation by OH and ozone is most important during the day, due to photooxidation. Despite lower reaction rates between ozone and VOCs as compared to OH with VOCs, the higher concentration of this compound makes alkenes just as likely to be oxidized by ozone during the day. Oxidation of VOCs by ozone can also have a major impact on the ozone budget, leading to ozone formation (as a byproduct of photo-oxidation) and destruction (through direct reaction with ozone). During the evening, oxidation by NO_3 dominates due to a decrease in OH radical recycling from photooxidation (Seinfeld and Pandis 2006).

VOC oxidation is complex, with significant and non-linear impacts of nitrogen oxides (NO_x), typically present due to anthropogenic combustion-driven emissions. When the ratio VOC: NO_x is high (i.e., relatively low NO_x environment), VOCs reactions with OH undergo a competition between subsequent reactions with HO_2 (a "relative" of OH) that quickly yield stable, lower volatility OVOCs, and subsequent reactions with NO that facilitate production of ozone and further oxidation toward higher volatility OVOCs (Seinfeld and Pandis 2006). Conversely, with a low ratio of VOC: NO_2 (NO_x rich environment), the latter reactions dominate, efficiently producing ozone and propagating chemical reactions. Under very high NO_x conditions, increased reactions between OH and NO_2 to form stable nitric acid can actually limit OH and HO_2 cycling and decrease the efficiency of ozone production (Seinfeld and Pandis 2006). However, the ratio of VOC: NO_2 that determines whether a system is NO_x poor or NO_x rich is dependent on the mix of individual VOCs available for reaction and their relative reaction rate with atmospheric oxidants. Therefore both the ozone budget and SOA formation are partly dependent on the structure and the resulting chemistry of individual VOCs. Further research into VOC composition will enable a better understanding of both of these domains.

Continued oxidation of these species results in partitioning to the particle phase, ultimately leading to the formation of biogenic secondary organic aerosol (BSOA). However,

the contribution of each BVOC to SOA formation is largely dependent on compound structure (Seinfeld and Pandis 2006). For example, SOA yields of aromatic VOCs increase with increasing carbon atoms, and SOA yields for non-aromatic VOCs are lower due to compound fragmentation during reaction (Seinfeld and Pandis 2006). However, SOA yields of branched compounds are lower than non-branched compounds due to fragmentation into even smaller, higher volatility compounds. Conversely, rings may increase SOA yields by preserving the carbon backbone even when the compound fragments (Lim and Ziemann 2009). BVOC classes with more than one isomer (e.g., monoterpenes, sesquiterpenes, diterpenes) can have 3 or more degrees of unsaturation, split between hydrocarbon rings and double bonds. This variability in structure can have critical impacts on atmospheric reactions, and subsequently, atmospheric composition. Compounds such as myrcene, with three double bonds and no rings, react quickly with atmospheric oxidants (Friedman and Farmer 2018; Lee et al. 2006; Lim and Ziemann 2009) but might be expected to fragment into high volatility OVOCs which are not significant contributors to SOA. Compounds with fewer double bonds and/or one or more rings, while less reactive, might be expected to have higher aerosol formation potential (Friedman and Farmer 2018; Lee et al. 2006; Lim and Ziemann 2009). However, these are general trends in expected yields and observed SOA yields of BVOC isomers do not appear to follow these trends consistently, and are not always in agreement between publications (Faiola et al. 2018; Friedman and Farmer 2018). Consequently, while variability in yields between isomers almost certainly exists, it is difficult to quantify these impacts.

1.2 Methods for detection of atmospheric volatile organic compounds

A range of analytical methods exist for capturing and quantifying VOCs. Offline sampling methods include sampling onto sorption tubes or into canisters. The tubes and canisters

are analyzed in a lab typically on a GC-MS system to characterize species, providing high chemical resolution. However, this approach is generally associated with poor temporal resolution, as it relies on an operator to collect and/or transport each sample. Nevertheless, whole air samples and multi-bed adsorbent traps allows for detection of a wide range of VOCs. Consequently, sampling coupled with offline analyses can yield detailed information for short-term measurement campaigns. Additionally, a few measurement campaigns have used sorbent tubes to measure daily or weekly for months to years at a time, providing improved understanding of seasonal and interannual variability of VOCs (Holdren, Westberg, and Zimmerman 1979; Simpson et al. 2012).

In contrast to the low temporal resolution of offline measurements, a number of online measurement options exist and have been widely used to provide measurements on timescales of seconds to hours. Most widely used amongst these tools are proton transfer reaction mass spectrometry (PTR-MS), chemical ionization mass spectrometry (CIMS), and field-deployable gas chromatography mass spectrometry/flame ionization detection (GC-MS/FID) (Apel 2003; Ayres et al. 2015; Bouvier-Brown et al. 2009; Davison et al. 2009; De Blas et al. 2011; Fischbach et al. 2002; Goldan et al. 2004; Gouw and Warneke 2007; Kalogridis et al. 2014; Liebmann et al. 2019; Mehra et al. 2020; Millet et al. 2005; Riches, Lee, and Farmer 2020; Tanner et al. 2006; Yuan et al. 2017). Each of these tools carries different advantages and disadvantages. For example, proton transfer reaction mass spectrometry (PTR-MS) offers high temporal resolution and has been used in the atmospheric chemistry field for a number of VOC measurement campaigns (Davison et al. 2009; Gouw and Warneke 2007; Kalogridis et al. 2014; Mielke et al. 2010; Park et al. 2013; Yu et al. 2017). Much like PTR-MS, other direct-sampling mass spectrometric instruments have been used widely in recent years, including CIMS and derivatives of CIMS (Ayres et al. 2015; Liebmann et al. 2019; Mehra et al. 2020; Riches, Lee, and Farmer 2020). These instruments classify the composition of the atmosphere by molecular formulas on timescales as fast as 10 Hz. Therefore, their

use has significantly advanced understanding of tropospheric VOC composition and enabled techniques that require extremely fast measurements such as eddy covariance measurements of emission and deposition. However, these instruments, and any instrument that relies on mass spectrometry for chemical resolution, cannot provide resolution of isomers with the same chemical formula, which limits their utility for understanding some of the impacts of VOCs on oxidant and aerosol budgets.

While gas chromatography has lower temporal resolution (\sim hourly), it has the benefit of separating compounds with the same molecular formula. This is made possible by flowing the sample in an inert carrier gas (the mobile phase) through a column coated in a polar or non-polar stationary phase while simultaneously increasing the oven temperature. Separation of the compounds in the sample is a function of vapor pressure of each compound and their affinities for the stationary phase. When a compound reaches the end of the column it can either be detected by a wide range of available detectors that provide varying degrees of chemical resolution and/or universal response factors. This work focuses on the two most widely used detectors for field-deployable GC-MS in atmospheric studies, flame ionization detector (FID) and mass spectrometer (MS).

In the case of an FID, eluting compounds are combusted in a hydrogen flame, in which high temperature hydrogen radicals split larger hydrocarbons C_1 fragments that combust to form ions (Holm 1999). The ions create a current and are then measured at the detector's electrode (Scanlon and Willis 1985; Sternberg, Gallaway, and Jones 1962). The current produced is a function of the number of carbons in the compound and compounds with functional groups reduce the response generated by the attached carbon (Scanlon and Willis 1985; Sternberg, Gallaway, and Jones 1962). An FID is robust and stable for long periods of time, and provides approximately universal response per mass for all hydrocarbons. Furthermore, the response is predictable even for non-hydrocarbons, making it an ideal universal detector. To account for the detector response of hydrocarbon and non-hydrocarbon

compounds, the effective carbon number concept was developed (Sternberg, Gallaway, and Jones 1962). This method quantifies the number of aliphatic carbons that would produce the same detector response as the non-hydrocarbon compound (Sternberg, Gallaway, and Jones 1962).

If the GC is coupled to a mass spectrometer, eluting compounds from the GC column are ionized, typically by electrons, photons, or a charged reagent gas. Ionized analytes may or may not fragment depending on the ionization energy, and the resulting ions separated according to their mass-to-charge ratio (m/z) based on their interactions with a magnetic and/or electric field (Gross 2004). The ions are detected by some form of electron amplification (e.g., secondary electron multiplier or multi-channel plate detector), which uses impinging ions to generate a measurable current (Gross 2004). Results are displayed as spectra of the relative abundance of detected ions as a function of the mass-to-charge ratio; in nearly all cases ions are reasonably assumed to carry only one charge, allowing de facto classification by ion mass (Gross, 2004). With sufficient mass resolution, ion mass may be used to infer molecular formulas. Most field-deployable GC-MS systems ionize analytes through collision with electrons ("electronic impact ionization", or EI) due to the ease of generating electrons using a tungsten filament and its relatively universal response to organic compounds. This approach typically fragments analytes, generating a spectrum of mass fragments that can be used to identify a compound through comparison to known mass spectral libraries (*NIST mass spec data center* 2012). Alternately, soft ionization techniques (e.g., CIMS) can be used that preserve the analyte ion for classification by molecular weight or formula, but do not provide the fragmentation information that facilitates identification.

Gas chromatography with flame ionization detection and/or mass spectrometry have been used in a number of field campaigns. The combination of GC-MS allows for the identification of individual isomers at concentrations typical of rural and urban environments. The major issue with mass spectrometry is the limited period of time the instrument can

be left unattended before requiring tuning and maintenance (a few weeks). GC-FID is a robust analytical technique that allows for unattended maintenance for months at a time, allowing for improved understanding of seasonal and interannual variability. The source of maintenance required for unattended measurement is usually for gas replacement or pertain more to extraneous issues (i.e. sampling, calibration). The major hurdle with unattended monitoring with GC-FID is the lack of compound identification. In this work, periodic deployment of a MS coupled to the GC-FID allowed for identification of the most commonly detected compounds, though transient variability in BVOC emissions are lost through this method.

1.3 Importance of BVOCs for ozone and SOA models

Given the impact of BVOCs on the ozone budget, BVOC observational data is important for ozone modeling. For example, high ozone deposition velocities were observed on rainy days at Harvard Forest (Clifton et al. 2019). This was predicted to be the result of BVOCs with fast reaction rates, not captured in emission models (Clifton et al. 2019). It is likely that the ratios of emitted compounds vary after rain events or during other periods of stress (Brilli et al. 2009; Faiola et al. 2018; Goldstein et al. 2000; Schade and Goldstein 2003), possibly increasing emissions of highly reactive compounds. The work by (Clifton et al. 2019) suggest that monitoring BVOCs during ecosystem stress and sub-seasonal changes can assist in mitigating ozone modeling inaccuracies. Long term monitoring will also capture emission variability during stress events such as rain, drought, or increased herbivory (Faiola et al. 2019).

Two BVOC emissions models are available for estimating plant emissions in a range of ecosystem: the Model for Emissions of Gases and Aerosols from Nature (MEGAN) (Guenther et al. 2012; Guenther et al. 2006) and the Biogenic Emission Inventory System (BEIS) of the Environmental Protection Agency (Biogenic Emission Inventory System (BEIS)) (Guenther

et al. 1996). Models such as these make it possible to estimate biogenic emissions beyond the constraints of observational data. These models were built off years of laboratory leaf level experiments, field-based flux measurements, vegetation cataloging, and whole ecosystem campaigns, to name a few (Geron et al. 2000; Goldstein et al. 2000; Greenberg et al. 2003; Guenther, Monson, and Fall 1991; Schade, Goldstein, and Lamanna 1999; Zhihui, Yuhua, and Shuyu 2003). Emission models, such as these can be coupled with chemical degradation models, such as F0AM (Wolfe et al. 2016), to predict the fate of VOCs and understand their impact on ozone and SOA formation. (Bai et al. 2017; Guenther et al. 1996; Sakulyanontvittaya et al. 2016; Sinderlarova et al. 2014; Wolfe et al. 2011; Wolfe et al. 2016; Yu et al. 2017). While emissions and chemical degradation models require observational data, there are few long-term, interseasonal, or interannual measurements of VOCs to validate predictions on these temporal scales.

1.4 Objectives

This work seeks to increase understanding of O₃ chemical loss and production through the development of a long-term site for biogenic volatile organic compounds. This work also seeks to understand the variability in biosphere and atmosphere interactions on diurnal, seasonal and interannual scales from the collected data.

Specific objectives are as follows:

1. Develop and validate an automated, online, gas-chromatography flame ionization detector for detection of atmospheric volatile organic compounds across the volatility range of most BVOC classes.
2. Increase our understanding of atmospheric reactivity of BVOC species and how it varies intra-annually.
3. Understand the biological drivers of diurnal, seasonal, and interannual changes in

BVOC concentrations and their impacts on atmospheric reactivity.

1.5 Organization of the Dissertation

Chapter 2, *An autonomous remotely operated gas chromatograph for chemically resolved monitoring of atmospheric volatile organic compounds*, addresses research objective 1. In this chapter, we describe the hardware and software involved in developing a GC-FID for remote automated monitoring of atmospheric volatile organic compounds ranging between C₅-C₁₅. We examine the viability of remote automation of the instrument over a two year period. We also provide suggestions to limit downtime and speed up data analysis and calibration. For brevity, the instrument will be referred to as the VOC-GC-FID.

Chapter 3, *Variability in the composition of biogenic volatile organic compounds in a Southeastern US forest*, addresses objective 2. In this work we present the first year of hourly BVOC measurements collected by the VOC-GC-FID. The data present was collected between 15 September 2019 and 15 September 2020 at a research tower in Central Virginia (The Virginia Forest Lab) in a mixed forest representative of ecosystems in the Southeastern US. Furthermore, we present the mixing ratios of isoprene, isoprene oxidation products, monoterpenes, and sesquiterpenes between two different seasons, the growing and non-growing season. BVOC classes were examined for their impact on the hydroxyl radical (OH), ozone, and nitrate reactivity. and their role in atmospheric reactivity. Monoterpenes were found to have particular impact on atmospheric reactivity so this class was examined by individual compound.

Chapter 4, *Minor contributions of daytime monoterpenes are major contributors to atmospheric reactivity*, we examine the diurnal, seasonal, and interannual impact of individual monoterpenes on atmospheric reactivity. Using two years of speciated hourly BVOC data collected at the Virginia Forest Lab, in Fluvanna County, Virginia, we examine how minor changes in the composition of monoterpenes between seasons are found to have profound

impacts on ozone reactivity. The concentration of a range of BVOCs in the summer were found to have two different diurnal profiles, largely driven by temperature- versus light-dependent emissions. Factor analysis was used to separate the two observed diurnal profiles and determine the contribution from each driver. Highly reactive BVOCs were found to exert outsize influence on ozone and OH reactivity in the summer, particularly during the daytime. These findings reveal a need to monitor species with high atmospheric reactivity but have low concentrations and to more accurately capture their emission trends in models.

Chapter 5 brings this dissertation to a conclusion. We summarize major outcomes of each chapter and make recommendations for future work.

1.6 References

- Apel, E. C. (2003). “A fast-GC/MS system to measure C 2 to C 4 carbonyls and methanol aboard aircraft”. In: *Journal of Geophysical Research* 108.D20, p. 8794. ISSN: 0148-0227. DOI: [10.1029/2002JD003199](https://doi.org/10.1029/2002JD003199). URL: <http://doi.wiley.com/10.1029/2002JD003199>.
- Ayres, B. R. et al. (2015). “Organic nitrate aerosol formation via NO₃ + biogenic volatile organic compounds in the southeastern United States”. In: *Atmospheric Chemistry and Physics* 15.23, pp. 13377–13392. ISSN: 1680-7324. DOI: [10.5194/acp-15-13377-2015](https://doi.org/10.5194/acp-15-13377-2015). URL: <https://www.atmos-chem-phys.net/15/13377/2015/>.
- Bai, Jianhui et al. (2017). “Seasonal and interannual variations in whole-ecosystem BVOC emissions from a subtropical plantation in China”. In: *Atmospheric Environment* 161, pp. 176–190. ISSN: 18732844. DOI: [10.1016/j.atmosenv.2017.05.002](https://doi.org/10.1016/j.atmosenv.2017.05.002).
- Bouvier-Brown, N. C. et al. (2009). “In-situ ambient quantification of monoterpenes, sesquiterpenes, and related oxygenated compounds during BEARPEX 2007: implications for gas- and particle-phase chemistry”. In: *Atmospheric Chemistry and Physics* 9.15, pp. 5505–5518. ISSN: 1680-7324. DOI: [10.5194/acp-9-5505-2009](https://doi.org/10.5194/acp-9-5505-2009). URL: <https://acp.copernicus.org/articles/9/5505/2009/>.

- Brilli, Federico et al. (2009). “Constitutive and herbivore-induced monoterpenes emitted by *Populus × euroamericana* leaves are key volatiles that orient *Chrysomela populi* beetles”. In: *Plant, Cell and Environment* 32.5, pp. 542–552. ISSN: 01407791. DOI: [10.1111/j.1365-3040.2009.01948.x](https://doi.org/10.1111/j.1365-3040.2009.01948.x).
- Clifton, O. E. et al. (2019). “Spatiotemporal Controls on Observed Daytime Ozone Deposition Velocity Over Northeastern U.S. Forests During Summer”. In: *Journal of Geophysical Research: Atmospheres* 124.10, pp. 5612–5628. ISSN: 21698996. DOI: [10.1029/2018JD029073](https://doi.org/10.1029/2018JD029073).
- Davison, B. et al. (2009). “Concentrations and fluxes of biogenic volatile organic compounds above a Mediterranean Macchia ecosystem in western Italy”. In: *Biogeosciences* 6.8, pp. 1655–1670. ISSN: 17264189. DOI: [10.5194/bg-6-1655-2009](https://doi.org/10.5194/bg-6-1655-2009).
- De Blas, Maite et al. (2011). “Automatic on-line monitoring of atmospheric volatile organic compounds: Gas chromatography-mass spectrometry and gas chromatography-flame ionization detection as complementary systems”. In: *Science of the Total Environment* 409.24, pp. 5459–5469. ISSN: 00489697. DOI: [10.1016/j.scitotenv.2011.08.072](https://doi.org/10.1016/j.scitotenv.2011.08.072).
- Donahue, N. M. et al. (2011). “A two-dimensional volatility basis set: 1. organic-aerosol mixing thermodynamics”. In: *Atmospheric Chemistry and Physics* 11.7, pp. 3303–3318. ISSN: 1680-7324. DOI: [10.5194/acp-11-3303-2011](https://doi.org/10.5194/acp-11-3303-2011). URL: <https://acp.copernicus.org/articles/11/3303/2011/>.
- Donahue, N. M. et al. (2012). “A two-dimensional volatility basis set – Part 2: Diagnostics of organic-aerosol evolution”. In: *Atmospheric Chemistry and Physics* 12.2, pp. 615–634. ISSN: 1680-7324. DOI: [10.5194/acp-12-615-2012](https://doi.org/10.5194/acp-12-615-2012). URL: <https://acp.copernicus.org/articles/12/615/2012/>.
- Faiola, C. L. et al. (2018). “Terpene Composition Complexity Controls Secondary Organic Aerosol Yields from Scots Pine Volatile Emissions”. In: *Scientific Reports* 8.1, pp. 1–13. ISSN: 20452322. DOI: [10.1038/s41598-018-21045-1](https://doi.org/10.1038/s41598-018-21045-1).

- Faiola, Celia L. et al. (2019). “Secondary Organic Aerosol Formation from Healthy and Aphid-Stressed Scots Pine Emissions”. In: *ACS Earth and Space Chemistry* 3.9, pp. 1756–1772. ISSN: 24723452. DOI: [10.1021/acsearthspacechem.9b00118](https://doi.org/10.1021/acsearthspacechem.9b00118).
- Fischbach, Robert Josef et al. (2002). “Seasonal pattern of monoterpene synthase activities in leaves of the evergreen tree *Quercus ilex*”. In: *Physiologia Plantarum* 114.3, pp. 354–360. ISSN: 00319317. DOI: [10.1034/j.1399-3054.2002.1140304.x](https://doi.org/10.1034/j.1399-3054.2002.1140304.x). URL: <http://doi.wiley.com/10.1034/j.1399-3054.2002.1140304.x>.
- Friedman, Beth and Delphine K. Farmer (2018). “SOA and gas phase organic acid yields from the sequential photooxidation of seven monoterpenes”. In: *Atmospheric Environment* 187. January, pp. 335–345. ISSN: 18732844. DOI: [10.1016/j.atmosenv.2018.06.003](https://doi.org/10.1016/j.atmosenv.2018.06.003). URL: <https://doi.org/10.1016/j.atmosenv.2018.06.003>.
- Geron, Chris et al. (2000). “A review and synthesis of monoterpene speciation from forests in the United States”. In: *Atmospheric Environment* 34.11, pp. 1761–1781. ISSN: 13522310. DOI: [10.1016/S1352-2310\(99\)00364-7](https://doi.org/10.1016/S1352-2310(99)00364-7).
- Ghirardo, Andrea et al. (2010). “Determination of de novo and pool emissions of terpenes from four common boreal/alpine trees by ^{13}C CO₂ labelling and PTR-MS analysis”. In: *Plant, Cell & Environment* 33.5, pp. 781–792. ISSN: 01407791. DOI: [10.1111/j.1365-3040.2009.02104.x](https://doi.org/10.1111/j.1365-3040.2009.02104.x). URL: <https://onlinelibrary.wiley.com/doi/10.1111/j.1365-3040.2009.02104.x>.
- Goldan, Paul D. et al. (2004). “Nonmethane hydrocarbon and oxy hydrocarbon measurements during the 2002 New England Air Quality Study”. In: *Journal of Geophysical Research: Atmospheres* 109.D21, n/a–n/a. ISSN: 01480227. DOI: [10.1029/2003JD004455](https://doi.org/10.1029/2003JD004455). URL: <http://doi.wiley.com/10.1029/2003JD004455>.
- Goldstein, A. H. et al. (2000). “Effects of climate variability on the carbon dioxide, water, and sensible heat fluxes above a ponderosa pine plantation in the Sierra Nevada (CA)”.

- In: *Agricultural and Forest Meteorology* 101.2-3, pp. 113–129. ISSN: 01681923. DOI: [10.1016/S0168-1923\(99\)00168-9](https://doi.org/10.1016/S0168-1923(99)00168-9).
- Gouw, Joost de and Carsten Warneke (2007). “Measurements of volatile organic compounds in the earth’s atmosphere using proton-transfer-reaction mass spectrometry”. In: *Mass Spectrometry Reviews* 26.2, pp. 223–257. ISSN: 0277-7037. DOI: [10.1002/mas.20119](https://doi.org/10.1002/mas.20119). URL: <https://onlinelibrary.wiley.com/doi/10.1002/mas.20119>.
- Greenberg, J. P. et al. (2003). “Eddy flux and leaf-level measurements of biogenic VOC emissions from mopane woodland of Botswana”. In: *Journal of Geophysical Research: Atmospheres* 108.13, pp. 1–9. ISSN: 01480227. DOI: [10.1029/2002jd002317](https://doi.org/10.1029/2002jd002317).
- Gross, Jurgen H. (2004). *Mass Spectrometry*. Third Edit. Cham, Switzerland: Springer International Publishing, p. 986. ISBN: 978-3-319-54397-0.
- Guenther, A. et al. (1996). “Leaf, branch, stand and landscape scale measurements of volatile organic compound fluxes from U.S. woodlands”. In: *Tree Physiology* 16.1-2, pp. 17–24. ISSN: 0829318X. DOI: [10.1093/treephys/16.1-2.17](https://doi.org/10.1093/treephys/16.1-2.17).
- Guenther, A. B. et al. (2012). “The model of emissions of gases and aerosols from nature version 2.1 (MEGAN2.1): An extended and updated framework for modeling biogenic emissions”. In: *Geoscientific Model Development* 5.6, pp. 1471–1492. ISSN: 1991959X. DOI: [10.5194/gmd-5-1471-2012](https://doi.org/10.5194/gmd-5-1471-2012).
- Guenther, Alex et al. (1995). “A global model of natural volatile organic compound emissions”. In: *J. Geophys. Res.* 100.94, pp. 8873–8892.
- Guenther, Alex et al. (2006). “Estimates of global terrestrial isoprene emissions using MEGAN (Model of Emissions of Gases and Aerosols from Nature)”. In: DOI: [10.5194/acp-6-3181-2006](https://doi.org/10.5194/acp-6-3181-2006).
- Guenther, Alex B., Russell K. Monson, and Ray Fall (1991). “Isoprene and monoterpene emission rate variability: Observations with eucalyptus and emission rate algorithm de-

- velopment”. In: *Journal of Geophysical Research* 96.D6, p. 10799. ISSN: 0148-0227. DOI: [10.1029/91jd00960](https://doi.org/10.1029/91jd00960).
- Holdren, M W H, H H Westberg, and P R Zimmerman (1979). “Analysis of Monoterpene Hydrocarbons in Rural Atmospheres”. In: 84.9, pp. 1–6.
- Holm, Torkil (1999). “Aspects of the mechanism of the flame ionization detector”. In: *Journal of Chromatography A* 842.1-2, pp. 221–227. ISSN: 00219673. DOI: [10.1016/S0021-9673\(98\)00706-7](https://doi.org/10.1016/S0021-9673(98)00706-7). URL: <https://linkinghub.elsevier.com/retrieve/pii/S0021967398007067>.
- Kalogridis, C. et al. (2014). “Concentrations and fluxes of isoprene and oxygenated VOCs at a French Mediterranean oak forest”. In: *Atmospheric Chemistry and Physics* 14.18, pp. 10085–10102. ISSN: 16807324. DOI: [10.5194/acp-14-10085-2014](https://doi.org/10.5194/acp-14-10085-2014).
- Kesselmeier, J and M Staudt (1999). “An Overview on Emission, Physiology and Ecology.pdf”. In: *Journal of Atmospheric Chemistry* 33, pp. 23–88. ISSN: 01677764. DOI: [10.1023/A:1006127516791](https://doi.org/10.1023/A:1006127516791). arXiv: 0005074v1 [arXiv:astro-ph]. URL: <https://link-springer-com.ez27.periodicos.capes.gov.br/content/pdf/10.1023{\%}2FA{\%}3A1006127516791.pdf>.
- Lee, Anita et al. (2006). “Gas-phase products and secondary aerosol yields from the ozonolysis of ten different terpenes”. In: 111.Ci, pp. 1–18. DOI: [10.1029/2005JD006437](https://doi.org/10.1029/2005JD006437).
- Liebmann, Jonathan et al. (2019). “Alkyl nitrates in the boreal forest: Formation via the NO₃, OH, and O₃ induced oxidation of BVOCs and ambient lifetimes”. In: *Atmospheric Chemistry and Physics* 19.15, pp. 10391–10403. ISSN: 1680-7324. DOI: [10.5194/acp-19-10391-2019-463](https://doi.org/10.5194/acp-19-10391-2019-463). URL: <https://acp.copernicus.org/articles/19/10391/2019/>.
- Lim, Yong B. and Paul J. Ziemann (2009). “Effects of Molecular Structure on Aerosol Yields from OH Radical-Initiated Reactions of Linear, Branched, and Cyclic Alkanes in the Presence of NO_x”. In: *Environmental Science & Technology* 43.7, pp. 2328–2334. ISSN: 0013-936X. DOI: [10.1021/es803389s](https://doi.org/10.1021/es803389s). URL: <https://pubs.acs.org/doi/10.1021/es803389s>.

- 5194/amt-13-4123-2020. URL: <https://amt.copernicus.org/articles/13/4123/2020/>.
- Sakulyanontvittaya, Tanarit et al. (2016). “An assessment of enhanced biogenic emissions influence on ozone formation in central Alberta, Canada”. In: *Air Quality, Atmosphere and Health* 9.2, pp. 117–127. ISSN: 18739326. DOI: [10.1007/s11869-015-0324-9](https://doi.org/10.1007/s11869-015-0324-9).
- Scanlon, J. T. and D. E. Willis (1985). “Calculation of Flame Ionization Detector Relative Response Factors Using the Effective Carbon Number Concept”. In: *Journal of Chromatographic Science* 23.8, pp. 333–340. ISSN: 0021-9665. DOI: [10.1093/chromsci/23.8.333](https://doi.org/10.1093/chromsci/23.8.333). URL: <https://academic.oup.com/chromsci/article-lookup/doi/10.1093/chromsci/23.8.333>.
- Schade, Gunnar W. and Allen H. Goldstein (2003). “Increase of monoterpene emissions from a pine plantation as a result of mechanical disturbances”. In: *Geophysical Research Letters* 30.7, pp. 10–13. ISSN: 00948276. DOI: [10.1029/2002GL016138](https://doi.org/10.1029/2002GL016138).
- Schade, Gunnar W., Allen H. Goldstein, and Mark S. Lamanna (1999). “Are Monoterpene Emissions influenced by Humidity?” In: *Geophysical Research Letters* 26.14, pp. 2187–2190. ISSN: 00948276. DOI: [10.1029/1999GL900444](https://doi.org/10.1029/1999GL900444).
- Seinfeld, John H and S N Pandis (2006). *Atmospheric Chemistry and Physics: From Air Pollution to Climate Change*. Second edi. Hoboken: John Wiley & Sons, Inc. ISBN: 9780471720171.
- Simpson, Isobel J. et al. (2012). “Long-term decline of global atmospheric ethane concentrations and implications for methane”. In: *Nature* 488.7412, pp. 490–494. ISSN: 00280836. DOI: [10.1038/nature11342](https://doi.org/10.1038/nature11342). URL: <http://dx.doi.org/10.1038/nature11342>.
- Sinderlarova, K et al. (2014). *Global data set of biogenic VOC emissions calculated by the MEGAN model over the last 30 years*. URL: <https://acp.copernicus.org/articles/14/9317/2014/>.
- Staudt, M. et al. (1999). “Seasonal Variation in Amount and Composition of Monoterpenes Emitted by Young Pinus pinea Trees – Implications for Emission Modeling”. In: *Plant,*

- Cell and Environment* 35, pp. 77–99. ISSN: 0140-7791. DOI: <https://doi.org/10.1023/A:1006233010748>.
- Sternberg, JC, WS Gallaway, and DTL Jones (1962). “The mechanism of response of flame ionization detectors”. In: *Gas chromatography: third international symposium*. Ed. by N. Brenner, J. E. Callen, and M. D. Weiss. New York, NY: Academic Press.
- Tanner, David et al. (2006). “Gas chromatography system for the automated, unattended, and cryogen-free monitoring of C2 to C6 non-methane hydrocarbons in the remote troposphere”. In: *Journal of Chromatography A* 1111.1, pp. 76–88. ISSN: 00219673. DOI: [10.1016/j.chroma.2006.01.100](https://doi.org/10.1016/j.chroma.2006.01.100).
- Went, F. W. (1960a). “Blue Hazes in the Atmosphere”. In: *Nature* 187.4738, pp. 641–643. ISSN: 0028-0836. DOI: [10.1038/187641a0](https://doi.org/10.1038/187641a0). URL: <https://pnas.org/doi/full/10.1073/pnas.46.2.212><https://www.nature.com/articles/187641a0>.
- (1960b). “Organic Matter in the Atmosphere, and Its Possible Relation To Petroleum Formation”. In: *Proceedings of the National Academy of Sciences* 46.2, pp. 212–221. ISSN: 0027-8424. DOI: [10.1073/pnas.46.2.212](https://doi.org/10.1073/pnas.46.2.212).
- Wolfe, G. M. et al. (2011). “Forest-atmosphere exchange of ozone: Sensitivity to very reactive biogenic VOC emissions and implications for in-canopy photochemistry”. In: *Atmospheric Chemistry and Physics* 11.15, pp. 7875–7891. ISSN: 16807316. DOI: [10.5194/acp-11-7875-2011](https://doi.org/10.5194/acp-11-7875-2011).
- Wolfe, Glenn M. et al. (2016). “The framework for 0-D atmospheric modeling (F0AM) v3.1”. In: *Geoscientific Model Development* 9.9, pp. 3309–3319. ISSN: 19919603. DOI: [10.5194/gmd-9-3309-2016](https://doi.org/10.5194/gmd-9-3309-2016).
- Yu, Haofei et al. (2017). “Airborne measurements of isoprene and monoterpene emissions from southeastern U.S. forests”. In: *Science of the Total Environment* 595, pp. 149–158. ISSN: 18791026. DOI: [10.1016/j.scitotenv.2017.03.262](https://doi.org/10.1016/j.scitotenv.2017.03.262).

- Yuan, Bin et al. (2017). “Proton-Transfer-Reaction Mass Spectrometry: Applications in Atmospheric Sciences”. In: *Chemical Reviews* 117.21, pp. 13187–13229. ISSN: 0009-2665. DOI: [10.1021/acs.chemrev.7b00325](https://doi.org/10.1021/acs.chemrev.7b00325). URL: <https://pubs.acs.org/doi/10.1021/acs.chemrev.7b00325>.
- Zhihui, Wang, Bai Yuhua, and Zhang Shuyu (2003). “A biogenic volatile organic compounds emission inventory for Beijing”. In: *Atmospheric Environment* 37.27, pp. 3771–3782. ISSN: 13522310. DOI: [10.1016/S1352-2310\(03\)00462-X](https://doi.org/10.1016/S1352-2310(03)00462-X).

Chapter 2

An autonomous remotely operated gas chromatograph for chemically resolved monitoring of atmospheric volatile organic compounds

Deborah F. McGlynn¹, Namrata Panji¹, Graham Frazier¹, Chenyang Bi¹, Gabriel Isaacman-VanWertz¹

¹Civil and Environmental Engineering, Virginia Tech, Blacksburg, VA, 24061, USA

2.1 Abstract

Volatile organic compounds range in their reaction rates with atmospheric oxidants by several orders of magnitude, even for isomers of the same chemical class. Therefore, inventorying their atmospheric concentration between seasons and years requires isomer resolution to understand their impact on oxidant budgets and secondary organic aerosol formation. An automated gas-chromatography flame ionization (GC-FID) detector was developed for hourly sampling and analysis of C₅-C₁₅ hydrocarbons at remote locations. Samples are collected on an air-cooled multibed adsorbent trap for preconcentration of hydrocarbons in the target volatility range, specifically designed to minimize dead volume and enable rapid heating and sample flushing. Instrument control uses custom electronics designed to allow

flexible autonomous operation at moderate cost, with automated data transfer and processing. The instrument has been deployed for over two years with samples collected mid-canopy from the Virginia Forest Laboratory located in the Pace research forest in central Virginia. We present here the design of the instrument itself, control electronics, and calibration and data analysis approaches to facilitate the development of similar systems by the atmospheric chemistry community. Detection limits of all species are in the range of a few to tens of ppt and is suitable for detection of a wide range of biogenic, lightly oxygenated, and anthropogenic (predominantly hydrocarbon) compounds. Data from calibrations are examined to provide understanding of instrument stability and quantify uncertainty. In this work, we present challenges and recommendations for future deployments of this instrument, as well as suggested adaptations to decrease required maintenance. The presented design is particularly suitable for long-term and remote deployment campaigns where access, maintenance, and materials transport are difficult.

2.2 Introduction

VOCs are emitted from both anthropogenic and natural sources, though natural sources contribute $\sim 90\%$ to VOC emissions (Guenther et al. 2012). VOCs include a wide range of species, with rate constants and mixing ratios varying by several orders of magnitude, which impact their tendencies to form secondary organic aerosol. Furthermore, in the case of biogenic emissions, concentrations and the types of species emitted is dependent on vegetation type, seasonality, and a range of external stimuli (Guenther et al. 2012; Loreto et al. 1998; Schuh et al. 1997). These factors make understanding their role in oxidant and aerosol budget difficult. In particular, understanding long-term, interannual, and interseasonal trends in the emissions and concentrations of these compounds is critical for understanding their potential changes in a changing climate. Furthermore, due to the widely variable physical and chemical properties of these compounds, it is critical to understand these temporal and

spatial patterns not only for compound classes as a whole, but for individual compounds. Unfortunately, collection of such long-term datasets is difficult due to instrument capabilities which makes long-term, chemically resolved datasets of VOCs relatively scarce.

A wide range of methods for detecting and monitoring VOCs are available. They vary in their ability to detect speciated VOCs and to run autonomously for extended periods of time. Additionally, they vary in their ability to detect species at low concentration, high volatility, and/or low volatility. For example, offline methods such as sampling onto canisters or adsorbent tubes for later analysis on gas chromatography/mass spectrometry systems have been used for many years. This type of sampling allows for speciated analysis, but requires substantial manual labor and on-site access (Kalogridis et al. 2014). Therefore, the temporal resolution of the resulting data from these types of offline measurements is at the discretion of the researcher, and typically on the order of daily to weekly for long-term sampling (Holdren, Westberg, and Zimmerman 1979; Simpson et al. 2012). There is also long history of sampling campaigns using offline GC-FID for VOC detection (Goldan et al. 2004; Millet et al. 2005; Schade and Goldstein 2001, 2003; Tanner et al. 2006). While these campaigns significantly increased our understanding of VOCs, they did not have the benefit of technological advances utilizing automation and advanced data processing techniques.

There are available instruments to measure VOCs in real-time (time resolution of minutes, seconds, or faster). For example, proton transfer reaction mass spectrometry (PTR-MS) offers high temporal resolution and has seen wide use in the field of atmospheric chemistry for fast measurements of a wide range of VOCs (Davison et al. 2009; Gouw and Warneke 2007; Kalogridis et al. 2014; Mielke et al. 2010; Park et al. 2013; Yuan et al. 2017). Like PTR-MS, other forms of direct-sampling mass spectrometric instruments have recently seen substantial increase in use in field measurements of VOCs (Ayres et al. 2015; Liebmann et al. 2019; Mehra et al. 2020). These instruments have significantly advanced understanding of VOC composition by providing time resolution sufficiently high to enable emission

and deposition flux measurements through eddy-covariance techniques (which require multiple measurements per second). However, instruments such as these that rely on mass spectrometry for chemical resolution and cannot provide resolution of isomers with the same chemical formula, which limits their utility for understanding impacts on oxidant and aerosol budgets. Furthermore, instruments relying on mass spectrometry often require significant maintenance and tuning, which complicates their use for reliable deployment longer than a few weeks to a few months (Kalogridis et al. 2014; Mielke et al. 2010; Millet et al. 2005).

In contrast, gas chromatographic tools provide high chemical resolution by enabling resolution of individual compounds, though at the cost of lower temporal resolution (typically \sim hourly). These tools may be coupled to a mass spectrometer for high chemical resolution, though this suffers the same difficulty in long-term deployments for any mass spectrometric tool. A GC may also be coupled to a flame ionization detector (FID) or other single-channel detector that provides no additional chemical resolution (Gross 2004). While the latter decreases the capabilities of chemical resolution, they offer stable, predictable response over long periods of time with relatively little maintenance (Faiola et al. 2012; Sternberg, Gallaway, and Jones 1962). These features make them an attractive detector for automated, remote, and online measurement campaigns.

Due to their higher chemical resolution, many modern field deployable gas chromatographic systems rely on mass spectrometric detection (Apel 2003; De Blas et al. 2011; Goldan et al. 2004; Millet et al. 2005; Wang et al. 2014; Williams et al. 2006), but such an approach frequently requires higher degrees of maintenance and operator intervention than is not ideal for long-term, remote measurement sites. Many modern reported systems focus on high volatility hydrocarbons (C_2 - C_{10}) for weeks to months at a time without cryogen trapping and with reported detection limits between 5-150 ppt (De Blas et al. 2011; Roest and Schade 2017; Tanner et al. 2006). For the most part, these systems rely on similar physical features such as varied adsorbent trap composition to capture compounds that vary

in volatility and Nafion dryers to remove condensation. The reported detection limit of these systems ranged from ~ 1 ppt to ~ 0.4 ppb (Tanner et al. 2006). Additional works detail the development of a system to increase the range of detected hydrocarbon species to C_2 - C_{12} (Panopoulou et al. 2020; Wang et al. 2014). Both systems had two separate preconcentration traps to capture high volatility and intermediate volatility hydrocarbons (Panopoulou et al. 2020; Wang et al. 2014).

In this work we present an automated, online, GC-FID system capable of detecting hydrocarbons and lightly oxygenated hydrocarbons between C_5 - C_{15} designed in particular to capture major biogenic VOC classes including isoprene, monoterpenes, and sesquiterpenes, and other anthropogenic hydrocarbon compounds within this target range. This work relies on a preconcentration trap previously described in the literature (Wernis et al. 2021) that efficiently collects high volatility species such as pentane and isoprene as well as intermediate volatile compounds. We present details of the design of the instrument and trap, the custom electronics, and the calibration and data processing approach, with the goal of expanding the availability of long-term chemically resolved VOC measurements by facilitating the collection of such measurements by other researchers. We also detail automated data processing approaches implemented in the freely available TERN software program in IGOR (Isaacman-VanWertz et al. 2017) to decrease the time required to integrate the amount of data produced from an automated GC.

2.3 Methods

2.3.1 Instrument overview

An overview of the instrument is provided in Figure 2.1. Air is pulled by a pump through a multi-bed adsorbent trap described in detail below at the maximum flow rate enabled by the trap, roughly 150 sccm. During sampling, the GC column is isolated by a 6-port

valve within a valve oven held at 150 °C. The GC column flow is connected directly to the 6-port valve from the GC oven and uses helium as a carrier gas. The trap is desorbed by actuating from the 6-port valve, purging the preconcentrated sample to the head of the GC column with no additional focusing or trapping. After 30 seconds, the trap is heated to 165 °C (± 10 °C) for a period of 2 minutes; heating is uncontrolled (i.e., not managed by a PID controller), prioritizing rapid heating to or beyond the desired setpoint as opposed to stable maintenance at a given setpoint (Figure 2.2). Following the heating period, the trap is fan-cooled for a period of 3 minutes. The entire desorption, heat, and cool time of the trap takes 5.5 minutes, after which the valve is actuated back to the sampling position to isolate the GC operation and begin a new sample. The GC oven temperature increases from 35 °C to 250 °C at 6°C per minute with a 10-minute hold at the maximum temperature, making the sample analysis 46.33 minutes, followed by a cooling period of about 9 minutes prior to the start of the next analysis. A sample is collected for the duration of the GC analysis and cooling, providing ~55 minutes of sampling (~8 liters of sampled air) when operating with hourly time resolution. Analytes are separated using a mid-polarity GC column (Rtx-624, 60m x 0.32mm x 1.8 μ m, Restek Inc.) and detected by a flame ionization detector (FID).

The instrument is built on a commercially available GC-FID, in this case an Agilent 7820A or Agilent 7890B outfitted with an FID (both have been tested in this work). GC flow is controlled by an electronic pressure controller (EPC) on-board the GC. The heated valve oven and 6-port valve may be integrated into and controlled by the GC or may be an independently controlled oven and valve (e.g., commercially available through Vici Valco); both configurations have been tested in this work. Positioning of the valve box directly on top of the GC oven provides a contiguous heated zone for the column to pass into the oven with no connections or cold spots (Figure 2.1). The carrier and make up gas used for this setup is helium while hydrogen fuels the FID, both gases are supplied by AirGas (5.0 grade). Air for the FID is generated onsite at 125 psig with a zero-air generator (Parker 75-83NA).

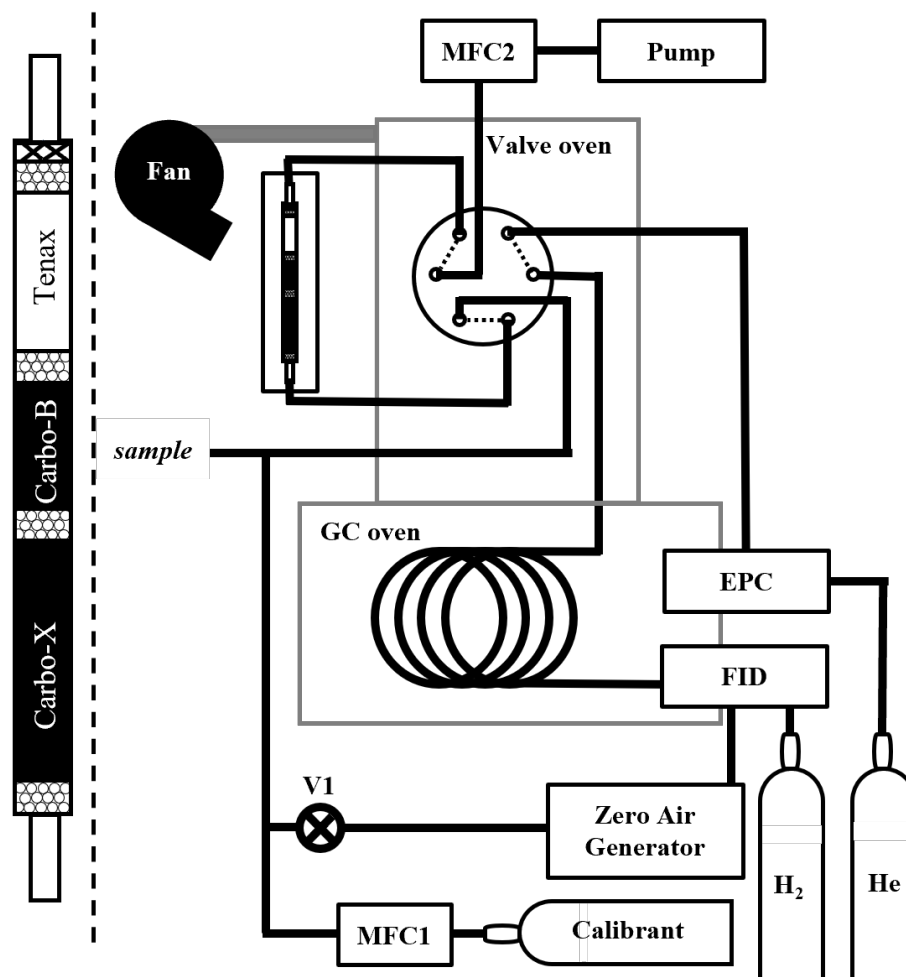


Figure 2.1 Instrument overview. A depiction of the gas chromatograph (GC) connections and plumbing. A zoomed in representation of the trap, which is found on the 6-port valve, can be found to the left of the dashed line. The trap connects externally to a 6-port valve, situated on-top of the GC oven, and is cooled by a 24V fan. The flame ionization detector (FID) and column are supplied by gases using electronic pressure controllers (EPC) operated by the GC. Sample and calibrant flows are controlled by mass flow controllers (MFC). A valve (V1) is used for calibrants and zero air.

The instrument as configured for this work includes a single trap, column, and detector. However, inclusion of a second channel operating in parallel would require minimal modification by adding an additional trap and valve, and outfitting the GC with a second column and FID. Though not yet implemented here, the instrument electronics, described in detail below, are designed to enable expansion to a two-channel system with minimal modification.

2.3.2 Adsorbent trap and desorption program

The design of the preconcentration trap uses a combination of features to capture species with a range in volatilities including layering of adsorbents with different adsorptive strength (Gentner et al. 2012; Wernis et al. 2021). The trap design follows that of Wernis et al. 2021, with an adsorbent bed consisting of 10 mg of Tenax® TA (60-80 mesh), 20 mg of Carbopack™ B (60-80 mesh), and at least 50 mg of Carbopack™ X (60-80 mesh) with each adsorbent surrounded by ~10mg of glass beads (50-70 sieve) (Figure 2.1, left). Adsorbents are held in place by packing the outlet of the trap with glass beads (50-70 sieve) and then glass wool.

Because the system is not a two-step purge-and-trap system and has no focusing between the sample trap and the head of the GC column, any compound not strongly retained by the column is immediately mobile once desorbed. Desorption of the trap consequently affects peak shape of high volatility compounds, and the rapid heating and flushing of the trap is a critical instrument design. To minimize retention in the trap during desorption, the trap (manufactured by Aerosol Dynamics Inc.) consists of a partially flattened 1/8" passivated metal tube, with low swept volume and minimal dead volume (Wernis et al. 2021). The trap is heated using two 1/8" diameter, 100-watt cartridge heaters within an aluminum manifold designed to have low thermal mass and be thermally isolated from any other instrument component in order to minimize heating and cooling times, with heating achieved in under 30 seconds. The manifold also hosts a 1/32" K-type thermocouple which is used to monitor the temperature and control the desorption heating of the trap.

2.3.3 Electronic design

A moderate cost data acquisition board (LabJack U6 Pro) is the central interface between the hardware and software, controlling instrument components (Figure 2.3) and housed within a standalone electronics enclosure. An 8-channel relay board powered by a 24 VDC

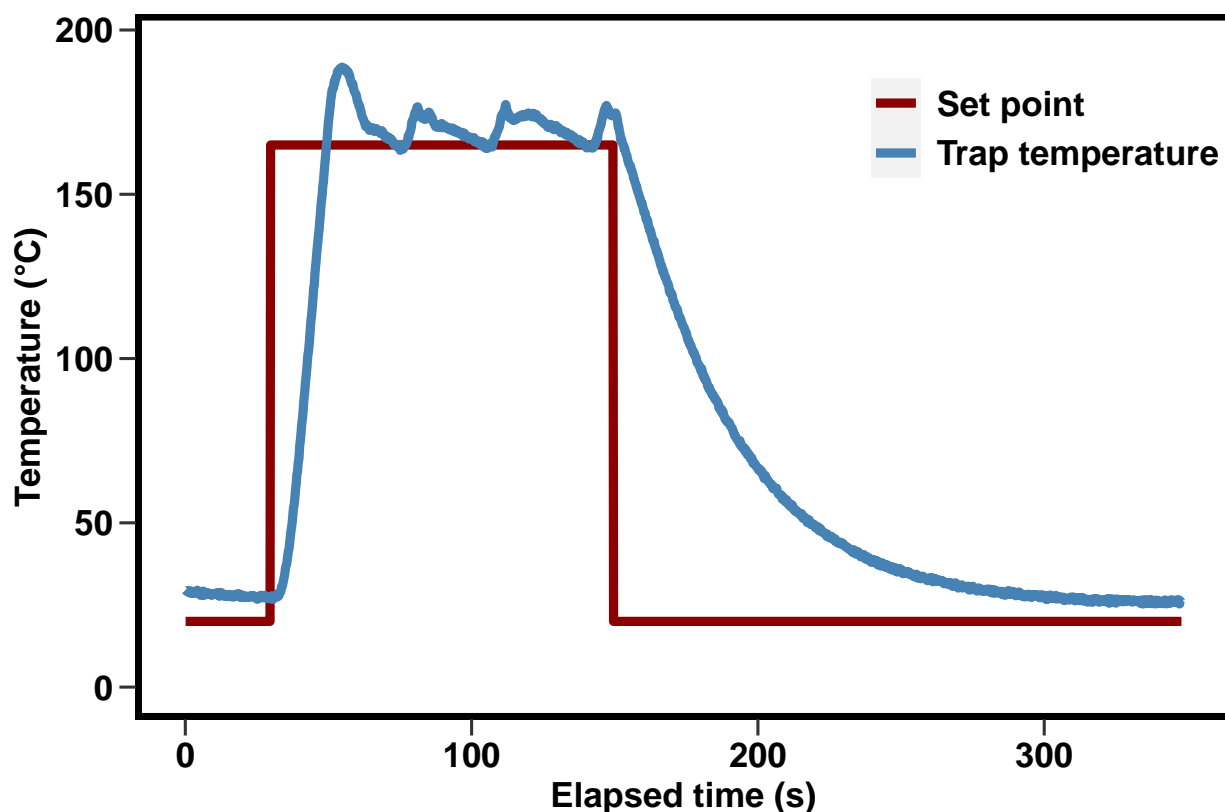


Figure 2.2 The trap heating profile for sample desorption. The red line depicts the set point, and the blue line depicts the trap temperature as it heats and cools at the beginning of a run.

power supply controls six switched 24 VDC channels, and two switched 110 VAC channels; all channels are independently fused, accessed by screw terminals on the face of the enclosure, and controlled by digital out (DO) channels. The fan and valve shown in Figure 2.1 are controlled by two of the 24 VDC channels. The cartridge heaters are controlled by one of the 110 VAC channels, in which a 24 VDC relay is used to switch two independent solid-state relays (SSRs, Sensata-Crydom) to provide better heat dissipation.

Additional connections provide an interface with other instrument components. Starting and stopping of the GC-FID is enabled through a DB9 remote start/stop controlled by two digital out channels, which are pulled low to drive a change in state. Additional digital

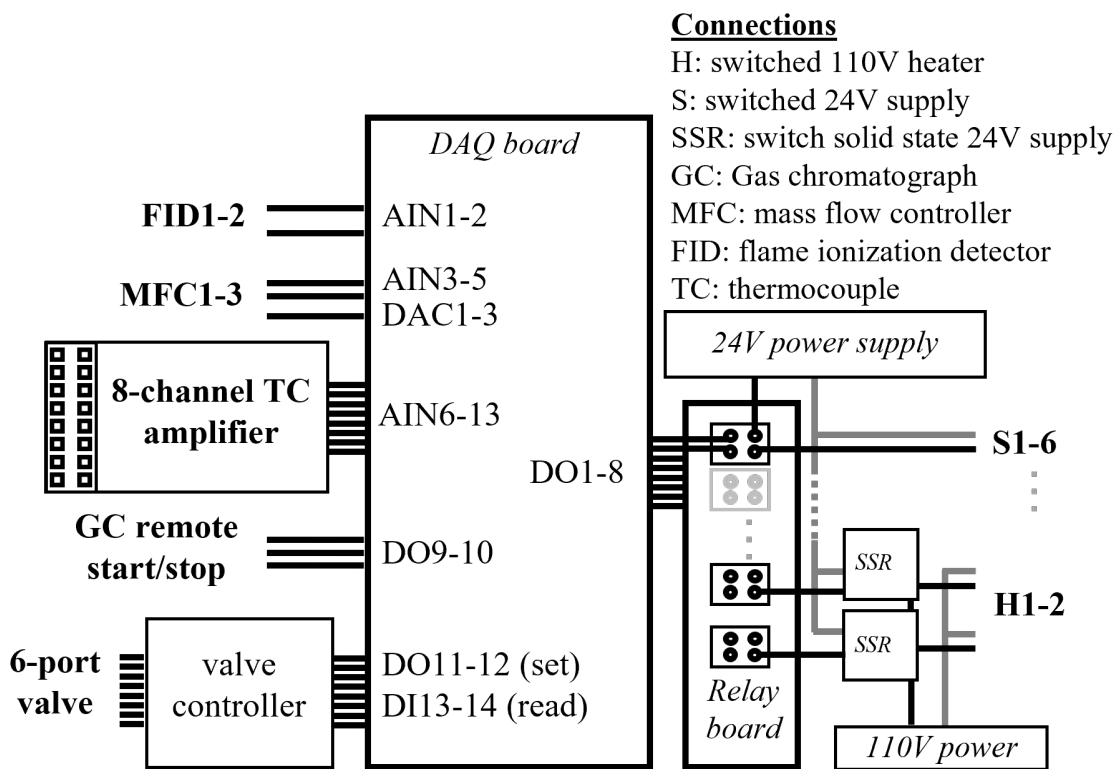


Figure 2.3 Diagram of the control electronics. Connections between the data acquisition board and controlled instrument components are shown. A 24V relay board controls 6 directly switched circuits, including those used for the fan and valves, and 2 switched solid state relays (SSR) that control 110V power for the heaters. Additional connections include the 6-port valve, thermocouple (TC) hub, mass flow controllers (MFC), FID signals, and GC start and stop signals.

out (DO) and in (DI) channels interface with an independent controller for a heated valve box (Vici Valco HVE2), situated on top of the GC, to set and read back the state of the 6-port valve. Temperatures are monitored by thermocouples connected to a commercially available thermocouple hub (HGSI TCA-MS-K-8-A4) mounted onto the enclosure in order to amplify signals from 8 thermocouples and convert to standard (i.e., 0-5V) analog input (AIN); thermocouple connections could be made directly to the data acquisition board, but the approach used here simplifies the system by avoiding the need for independent cold junction compensation and the need to separately mount thermocouple connectors on the

face of the enclosure. Two mass flow controllers (MFC) are each controlled by digital-to-analog converters (DAC), with flow readback using an AIN channel. An additional AIN is available for flow measurement using a third MFC, though no DAC is available to set this flow on the data acquisition board used in this setup. Signal from up to two FIDs is read by analog inputs configured as differential-ended signals (i.e., two AI channels for detector). Many of these components are not used in the present configuration, and are instead reserved to enable expansion to a two-channel system with no additional changes; these reserved components include: one of the FID readback channels (for a second detector), the MFC readback channel (to measure flow on a second trap), up to four of the 24 VDC switched channels (for a second fan and additional valves), and one of the 110 VAC switched channels (for heating a second trap). All electronics, and by extension the instrument itself, are controlled through custom LabVIEW code (National Instruments), which sets digital outputs on a set schedule and reads back analog inputs to store as datafiles.

2.3.4 Automated data analysis

A key advance in the autonomous deployment is automated data processing, as the reduction and analysis of chromatographic data is time consuming and labor intensive. Automated data processing is achieved here through several software advances. First, data is automatically uploaded to an online repository using a custom, standalone executable that is configurable and compiled from open-source Python code. The code is provided through GitHub (<https://github.com/gabrielivw/>) and the executable is available online at <https://ivw.cee.vt.edu/>. This program monitors a folder on the instrument computer and syncs any new data files to a repository, while the same program running on an analytical computer syncs the repository to a local folder. This code is designed to interface with storage space in Amazon Web Services through the data repository DigitalOcean (<https://www.digitialocean.com/>), and is referred to for simplicity as “DOsync.” File types,

folder locations, and digital repository locations are specified by a configuration file.

Files added to the local analytical computer are processed using an updated version of TERN, a freely-available and customizable chromatographic data analysis package in the Igor Pro programming environment (Wavemetrics, Inc.). The most recent publicly available version of this software package is available at <https://sites.google.com/site/ternigor/>. Several advances to this package since originally described (Isaacman-VanWertz et al. 2017) have been implemented here to enable automated data processing. A number of new autonomous features include:

1. Monitoring a data acquisition folder for automated ingestion of newly collected data files
2. Ingestion of metadata by monitoring a spreadsheet and/or file names
3. Fitting of peaks using default parameters that are allowed to vary between analytes to improve fits
4. Preliminary calibration and application to integrated data
5. Generation and saving of user-specific plots

Once a file is downloaded from the repository by DOsync, the new file is automatically ingested into TERN (1) and assigned metadata (i.e., ambient sample, calibrant level, etc.) based on its filename (2). Chromatographic peaks in these samples representing known analytes of interest (e.g., those in the calibration standard) are integrated by fitting them to idealized peak shapes (Gaussian or Gaussian convolved with an exponential decay) following the previously published approach (Isaacman-VanWertz et al. 2017), with fitting improved by specifying compound-specific default fit parameters (e.g., peak width or fitting window) (3). Integrated data are approximately calibrated using a user-provided response factor (4), and calibrated results are plotted and saved to a folder (5).

In short, data generated by the instrument is automatically processed into preliminary calibrated data and figures for the user to monitor with little operator interaction. This represents a significant step forward in the viability of long-term deployment of GC based instrumentation such as the instrument described here.

2.3.5 Data collection and calibration

The data used to evaluate and examine the instrument in this work is collected during an ongoing, multi-year field deployment at the Virginia Forest Lab (VFL), located in central Virginia. The VFL sits on the east side of the Blue Ridge Mountains and is about 25 km east-southeast of Charlottesville, VA. The site receives some anthropogenic emissions from nearby towns and roadways. The instrument sits at the base of a 40-meter meteorological tower, inside a climate-controlled, internet-connected lab that is supplied by line power. Samples are collected mid-canopy from a heated inlet with a sample flow of 1350 sccm. The instrument subsamples off this bypass flow at a sample flow rate of ~ 150 sccm. Instrument performance is monitored and evaluated by the automated calibration procedure described in section 2.4. In the present deployment, a calibration sample occurs every seventh hour at one of five different calibrant levels. Two of the calibrations performed each day are a zero and tracking standard. The third daily calibrant varies between three rotating calibrant mixing ratios. For each non-zero calibration, a zero-air sample mixes with a multi-component calibrant (Apel-Riemer Environmental Inc.) at one of four different flow rates, generating four different mixing ratios of calibrant mixtures. The composition and pure volume mixing ratio of the multi-component calibrant used for this instrument range between 4.35–17.60 ppb for monoterpene, anthropogenic, oxygenated, and sesquiterpene species while isoprene is at 40.3 ppb. The flow rates of 5, 20, 50, and 100 sccm dilute the calibrant into ~ 1350 sccm of zero air to create the 4 different calibrant levels. Estimated limits of detection for isoprene, oxidation products, monoterpenes, and sesquiterpenes are 20, 4.3, 2.2, and 2.7 ppt,

respectively (McGlynn et al. 2021).

2.3.6 FID signal integration to concentration

The calibration measurements from each week identify any sub-optimal instrument performance and aide conversion of the integrated FID signal to concentration (ppb). To do so, the concentration ($C_{\text{samp,cal}}$) of each calibrant compound sent to the trap is calculated by multiplying the concentration in the calibrant supply tank ($C_{\text{supply,cal}}$) by the calibrant flow (Q_{cal}) and dividing by the total sample flow rate (Q_{tot}).

$$C_{\text{samp,cal}}[\text{ppb}] = \frac{C_{\text{supply,cal}} \times Q_{\text{cal}}}{Q_{\text{tot}}} \quad (2.1)$$

Calibrant compounds are converted from FID signal to concentration in ppbC by factoring in an effective carbon number (ECN) (Faiola et al. 2012; Scanlon and Willis 1985). This normalizes the detector response to a per carbon basis, generating a unified calibration curve that can be used to calibrate compounds for which no authentic standard is available.

$$C_{\text{samp,cal}}[\text{ppbC}] = \frac{C_{\text{supply,cal}} \times Q_{\text{cal}} \times \text{ECN}}{Q_{\text{tot}}} \quad (2.2)$$

The slope from a linear regression between the integrated FID signal and the known calibrant concentration (in ppbC) is obtained from one week of calibration data at a time. This slope then becomes a conversion multiplier for the data collected in that same week. Once the slope of the linear fit is multiplied by all integrations matching that week, the adjusted FID signal is divided by the effective carbon number to convert from ppbC to ppb (Faiola et al. 2012; Scanlon and Willis 1985).

2.4 Results and Discussion

2.4.1 The species detected

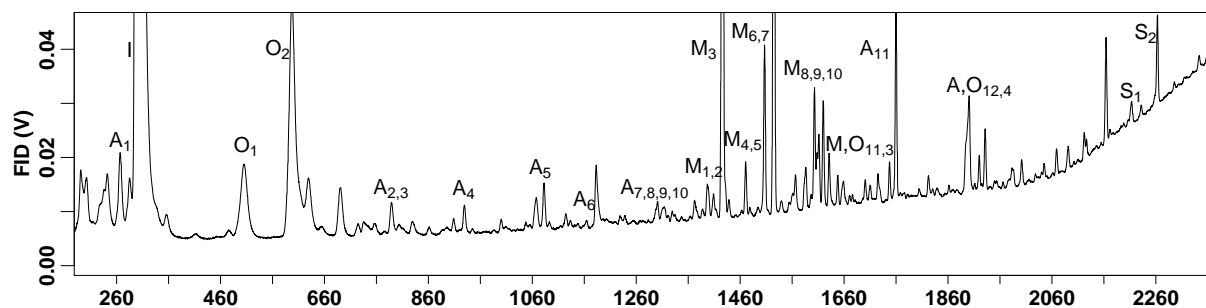


Figure 2.4 An example chromatogram with a label for a range of compounds detected by the instrument. “A” denotes that the compound is anthropogenic, “I”, “M”, “S” are terpenes or isoprene, monoterpene, and sesquiterpene, and “O” are oxygenated species.

Table 2.1 Compound names and labels on the example chromatogram

Terpenes		Anthropogenic		Oxygenated	
Compound	Symbol	Compound	Symbol	Compound	Symbol
isoprene	I	pentane	A1	methacrolein	O1
thujene	M1	carbon tetrachloride	A2	methyl vinyl ketone	O2
tricyclene	M2	benzene	A3	eucalyptol	O3
α -pinene	M3	pentanal	A4	methyl salicylate	O4
fenchene	M4	toluene	A5		
camphene	M5	hexanal	A6		
sabinene	M6	PCBTF	A7		
β -pinene	M7	ethylbenzene	A8		
limonene	M8	m-xylene	A9		
cymene	M9	o-xylene	A10		
β -phellandrene	M10	decanal	A11		
γ -terpinene	M11				
α -cedrene	S1				
β -cedrene	S2				

A wide range of species are detected on this instrument, including a number of BVOCs

which were previously reported (McGlynn et al. 2021). Additional detected compounds include several anthropogenic species such as Benzene, Toluene, Ethylbenzene, (o, m)-Xylene (BTEX) (Table 2.1). We also detect a handful of oxygenated species such as eucalyptol and methyl salicylate (Table 2.1), in addition to those previously reported. An example chromatogram with peak labels can be found in Figure 2.4. Additional species beyond those reported in Figure 2.4 and Table 2.1 are detected, and those reported here are simply to provide an indication of the range and capability of the instrument and methodology.

2.4.2 Calibration curve

All hydrocarbon compounds in the calibration tank fit a linear regression of FID signal as a function of carbon concentration (ppbC) figure 2.5. For compounds present in ambient samples, this average slope (4.4 in the provided example) can be used to convert peak integrations into mixing ratios in ppbC for any hydrocarbon analyte, which can then be converted to ppb using a known or estimated effective carbon number for each compound (Faiola et al. 2012; Sternberg, Gallaway, and Jones 1962). Between the start of sample collection on September 15th, 2019, and June 25th, 2020, the instrument did not have a calibration tank installed. However, manual calibrations performed at the beginning of this period were compared to the online calibration approach described here and found to be in reasonable agreement. The use of a unified calibration curve allows for simple calibration of compounds for which no authentic standard is available, enabling quantification with low uncertainty for a wide range of ambient compounds. However, compounds without authentic standards will have somewhat higher uncertainty in accuracy. Note in Figure 2.5 the lower slope for limonene and trimethylbenzene. Faiola et al. 2012 report measured effective carbon numbers of 9.5 for limonene and 9.22 for trimethylbenzene, but 9.76 for α -pinene, so some difference in slope is expected, though this does not fully explain the observed differences. Nonetheless, calibrating these compounds using the unified slope method results in a bias of $\sim 20\%$

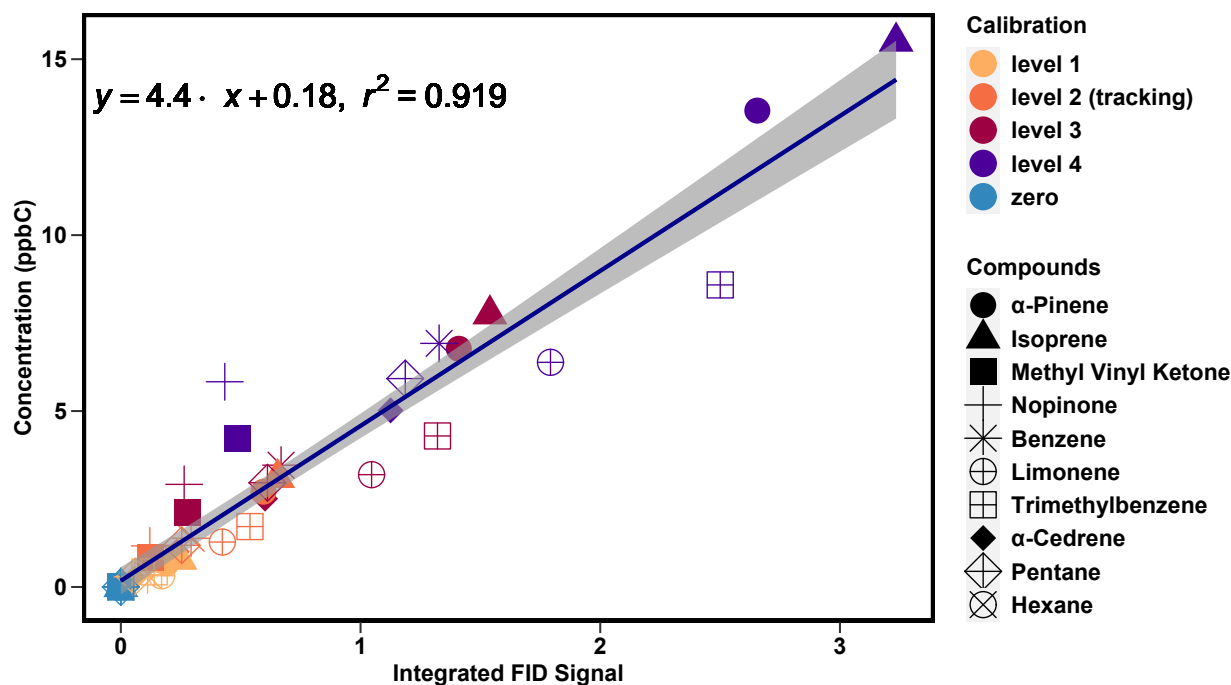


Figure 2.5 A linear regression plot between the integrated FID signal and the calibrant concentration for one week of calibrations. The slope from this linear regression is multiplied by each integration during that week and divided by the effective carbon number to yield ppb. The shading represents the standard error (4.4 ± 0.2) of the residuals to account for the uncertainty of the slope of the linear regression. Colors represent different calibration levels (i.e., different dilution flows) and symbols represent calibrants.

(Figure A.1). Similarly, the unified calibration method does not perform well for oxygenated compounds. The slope for MVK and nopinone is found to be 11 (Figure A.2). The ECNs of these compounds are roughly 25% (MVK) and 10% (nopinone) lower than their carbon number, so some reduced signal per ppbC (yielding a higher calibration slope) is expected, but this issue alone does not account for the larger difference in observed slope. Instead, reduced signal from oxygenates is likely due to partial removal by the ozone scrubber, an issue that has been previously observed (Pollmann, Ortega, and Helmig 2005) and suggests that oxygenates should be calibrated using the response of an oxygenated calibrant and not simply the unified calibration curve.

2.4.3 Stable calibration

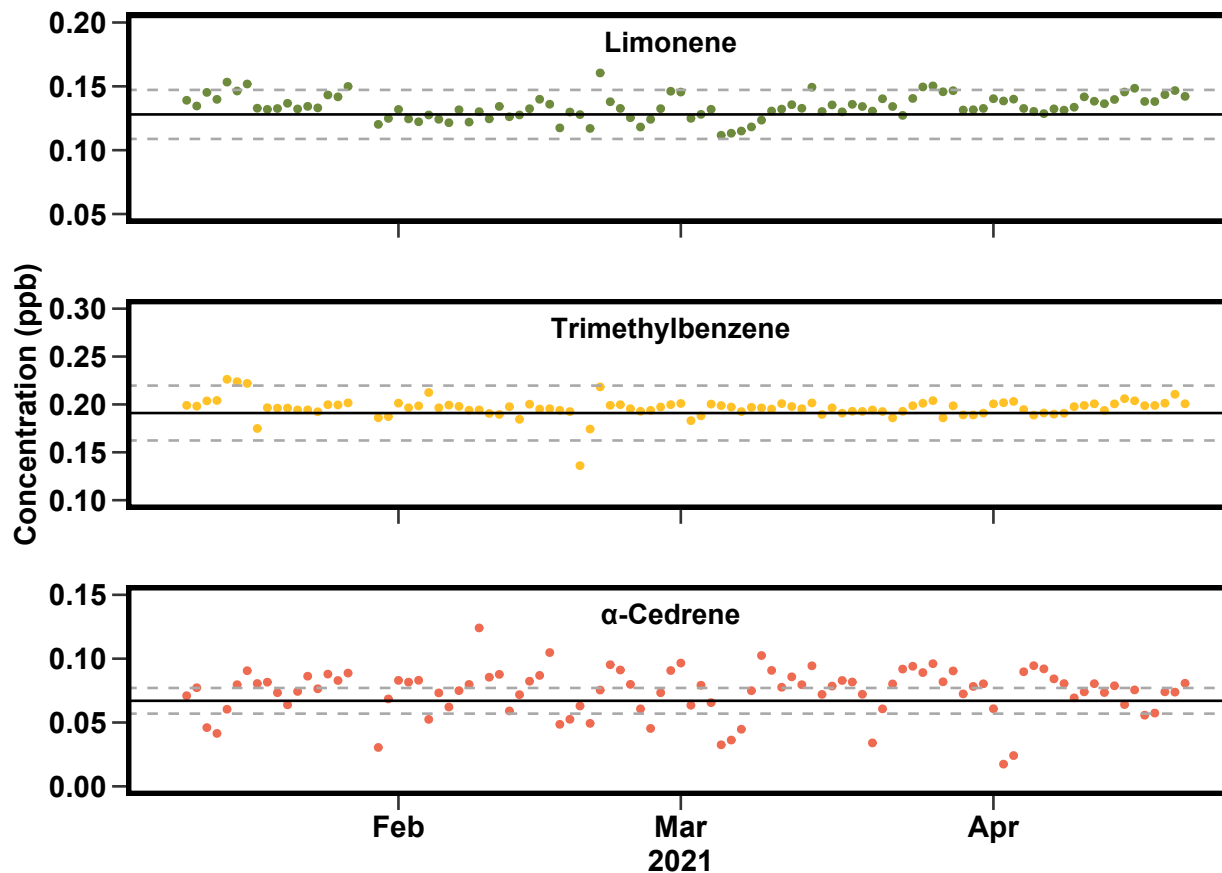


Figure 2.6 A tracking standard for limonene, trimethylbenzene, and α -cedrene each day between January and May 2021.

To evaluate the long-term stability and precision of this instrument, concentrations measured in the tracking standard are compared to expected values (Figure 2.6). In this comparison, calibration curves for each individual compound are used in order to assess instrument precision without the confounding issue of potential biases or errors in accuracy due to using a unified calibration curve, as discussed above. Across the 4 month period, the concentration measured is in good agreement with the expected value, shown in Figure 2.6 for a biogenic VOC (limonene), an anthropogenic VOC (1,3,5-trimethylbenzene), and a compound at the low-volatility edge of the instrument capabilities (α -cedrene). For compounds in the middle

of the instrument range (e.g., limonene and trimethylbenzene), nearly all points fall within 15% of the expected value. For compounds at the edges of instrument capability have somewhat lower precision, roughly 15%, likely due to sticking in inlet lines and/or incomplete transfer through the valve oven.

Overall, the data presented in Figures 2.5 and 2.6 suggest instrument uncertainty of roughly 10% for most compounds, at least during periods of near-optimal instrument operation. Harder-to-measure compounds may suffer somewhat higher uncertainty, and compounds for which no authentic standard or known response factor is available suffer an additional 20% in accuracy. These values are consistent with known uncertainties in chromatographic peak integration (impacting precision) and effective carbon number (impacting accuracy for uncalibrated compounds).

2.4.4 Additional recommendations for improved long-term deployment

Several components in this system require regular maintenance due to constant use, and represent weak spots in the autonomous remote operation of a GC instrument for VOC measurements. Particular failure points in this system include the oil-free vacuum pump used to pull sample flow, the zero-air generator, and the computer. Regular maintenance on the schedules recommended by the suppliers, or preferably more frequently can mitigate some failures and reduce downtime. We nevertheless identify here the issues surrounding maintenance and component failure for which backup and/or maintenance plans should be considered in developing long-term VOC measurements as described here.

Ozone scrubbing

Ozone must be removed from the sample flow to mitigate reactions in sampled air. Presently, 4 quartz-fiber filters infused with sodium thiosulfate (Pollmann, Ortega, and

Helmig 2005) are placed at the front of the inlet. This has been shown to effectively remove ozone for up to 6 weeks. Further details on validation of this method can be found in (McGlynn et al. 2021). This is the primary reason for regular visits to the site, suggesting that addressing the issues below should enable long-term operation with onsite operators visiting fewer than 10 times per year.

Sampling pump

Critically, the vacuum pump used in this work tends to fail within approximately one year, consistent with typical pump lifetimes of $\sim 10,000$ hours. Downtime due to pump failure has been mitigated in our system by including a backup pump in parallel, with a three-way electronic valve controlling which pump is used and a relay-controlled outlet providing power to the backup pump (commercially available or custom-built). One of the 24 VDC channels can be remotely activated to switch the electronic valve and turn on the backup pump, allowing continued sample flow without the need for an onset visit; in principle, activation of this relay could be an automated function of measured sample flow, but this level of complexity is in practice unnecessary as long as the generated data are being regularly monitored.

Zero-air generator

Regular maintenance on timescales of 6-9 months is necessary. This source of downtime has not been mitigated in our system. A compressor with an inline activated charcoal trap can provide temporary clean air during maintenance but has not been found to be an effective long-term solution.

Computer

Allowing computer updates during operation risks interrupting the data collection. Consequently, updates need to be disabled, but doing so has led to intermittent failures of the

operating system. Therefore, the computer used to run the instrument should be allowed to update during periods of ozone filter changes (every 4-6 weeks); careful remote updating may be possible to extend this period but has not been tested in our system.

Gases

Required flows of helium and hydrogen are minimal, but do require delivery of gas tanks for the instrument. In this system, each cylinder was found to last approximately 6 months, so gas delivery need only be coordinated roughly once or twice per year, which is reasonable for the present field site. However, for remote field sites, or sites to which gas delivery is infeasible, the system could be run without the regular use of gas tanks by generating hydrogen onsite with the use of a commercial hydrogen generator. Hydrogen could also serve as the FID carrier gas, thus eliminating the need for any onsite cylinders. However, this method requires purification with oxygen, water, and hydrocarbon scrubbers (Tanner et al. 2006). Furthermore, a hydrogen generator requires the addition of water, and the capacity of most generators would require the addition of larger water reservoirs to decrease site visitations. Though these modifications would eliminate the need to transport gas tanks to remote locations, the frequency of visits would likely increase relative to cylinder-dependent operation given the need to swap out purifiers and add water to reservoirs.

2.5 Conclusions

Remote and online monitoring of C_5 - C_{15} , including lightly oxygenated species was achieved through the development of an automated gas chromatograph using a flame ionization detector. Sample preconcentration is achieved using a recently developed adsorbent trap carefully designed to minimize swept volumes and thermal mass (Wernis et al. 2021). This instrument enables hourly measurement of volatile organic compounds spanning four to five orders of magnitude in volatility, without cryogen or thermoelectric cooling.

The instrument described here is designed to make collection of VOCs at high temporal and chemical resolution feasible in a wide range of locations, with the goal of broadening the availability of long-term measurements of reactive carbon. The instrument is highly adaptable and could be expanded and tuned to enable additional detection ranges, for instance through selecting different columns and/or trapping materials. Additionally, making the described minor changes to the instrument in order to operate it as a two-channel system would further broaden the potential use cases by enabling measurements at two inlet locations simultaneously, or onto two separate traps or columns. Development and deployment of instruments similar to the one presented here could vastly improve understanding of spatial and temporal distributions of VOC concentrations and emissions, and have the potential to improve VOC, ozone and secondary organic aerosol predictions.

2.6 Acknowledgements

This research was funded by the National Science Foundation (AGS 1837882 and AGS 1837891). Tower maintenance and operation were supported in part by the Pace Endowment. Deborah F. McGlynn is supported in part by Virginia Space Grant Consortium Graduate Research Fellowships.

2.7 References

- Apel, E. C. (2003). “A fast-GC/MS system to measure C₂ to C₄ carbonyls and methanol aboard aircraft”. In: *Journal of Geophysical Research* 108.D20, p. 8794. ISSN: 0148-0227. DOI: [10.1029/2002JD003199](https://doi.org/10.1029/2002JD003199). URL: <http://doi.wiley.com/10.1029/2002JD003199>.
- Ayres, B. R. et al. (2015). “Organic nitrate aerosol formation via NO₃ + biogenic volatile organic compounds in the southeastern United States”. In: *Atmospheric Chemistry and Physics* 15.23, pp. 13377–13392. ISSN: 1680-7324. DOI: [10.5194/acp-15-13377-2015](https://doi.org/10.5194/acp-15-13377-2015). URL: <https://www.atmos-chem-phys.net/15/13377/2015/>.

- Davison, B. et al. (2009). “Concentrations and fluxes of biogenic volatile organic compounds above a Mediterranean Macchia ecosystem in western Italy”. In: *Biogeosciences* 6.8, pp. 1655–1670. ISSN: 17264189. DOI: [10.5194/bg-6-1655-2009](https://doi.org/10.5194/bg-6-1655-2009).
- De Blas, Maite et al. (2011). “Automatic on-line monitoring of atmospheric volatile organic compounds: Gas chromatography-mass spectrometry and gas chromatography-flame ionization detection as complementary systems”. In: *Science of the Total Environment* 409.24, pp. 5459–5469. ISSN: 00489697. DOI: [10.1016/j.scitotenv.2011.08.072](https://doi.org/10.1016/j.scitotenv.2011.08.072).
- Faiola, C. L. et al. (2012). “Quantification of biogenic volatile organic compounds with a flame ionization detector using the effective carbon number concept”. In: *Atmospheric Measurement Techniques* 5.8, pp. 1911–1923. ISSN: 18671381. DOI: [10.5194/amt-5-1911-2012](https://doi.org/10.5194/amt-5-1911-2012).
- Gentner, Drew R et al. (2012). “Elucidating secondary organic aerosol from diesel and gasoline vehicles through detailed characterization of organic carbon emissions”. In: *Proceedings of the National Academy of Sciences* 109.45, pp. 18318–18323. ISSN: 0027-8424. DOI: [10.1073/pnas.1212272109](https://doi.org/10.1073/pnas.1212272109). URL: <http://www.pnas.org/cgi/doi/10.1073/pnas.1212272109>.
- Goldan, Paul D. et al. (2004). “Nonmethane hydrocarbon and oxy hydrocarbon measurements during the 2002 New England Air Quality Study”. In: *Journal of Geophysical Research: Atmospheres* 109.D21, n/a–n/a. ISSN: 01480227. DOI: [10.1029/2003JD004455](https://doi.org/10.1029/2003JD004455). URL: <http://doi.wiley.com/10.1029/2003JD004455>.
- Gouw, Joost de and Carsten Warneke (2007). “Measurements of volatile organic compounds in the earth’s atmosphere using proton-transfer-reaction mass spectrometry”. In: *Mass Spectrometry Reviews* 26.2, pp. 223–257. ISSN: 0277-7037. DOI: [10.1002/mas.20119](https://doi.org/10.1002/mas.20119). URL: <https://onlinelibrary.wiley.com/doi/10.1002/mas.20119>.
- Gross, Jurgen H. (2004). *Mass Spectrometry*. Third Edit. Cham, Switzerland: Springer International Publishing, p. 986. ISBN: 978-3-319-54397-0.

- Guenther, A. B. et al. (2012). “The model of emissions of gases and aerosols from nature version 2.1 (MEGAN2.1): An extended and updated framework for modeling biogenic emissions”. In: *Geoscientific Model Development* 5.6, pp. 1471–1492. ISSN: 1991959X. DOI: [10.5194/gmd-5-1471-2012](https://doi.org/10.5194/gmd-5-1471-2012).
- Holdren, M W H, H H Westberg, and P R Zimmerman (1979). “Analysis of Monoterpene Hydrocarbons in Rural Atmospheres”. In: 84.9, pp. 1–6.
- Isaacman-VanWertz, Gabriel et al. (2017). “Automated single-ion peak fitting as an efficient approach for analyzing complex chromatographic data”. In: *Journal of Chromatography A* 1529, pp. 81–92. ISSN: 0021-9673. DOI: [10.1016/j.chroma.2017.11.005](https://doi.org/10.1016/j.chroma.2017.11.005). URL: <http://dx.doi.org/10.1016/j.chroma.2017.11.005>.
- Kalogridis, C. et al. (2014). “Concentrations and fluxes of isoprene and oxygenated VOCs at a French Mediterranean oak forest”. In: *Atmospheric Chemistry and Physics* 14.18, pp. 10085–10102. ISSN: 16807324. DOI: [10.5194/acp-14-10085-2014](https://doi.org/10.5194/acp-14-10085-2014).
- Liebmann, Jonathan et al. (2019). “Alkyl nitrates in the boreal forest: Formation via the NO₃, OH, and O₃ induced oxidation of BVOCs and ambient lifetimes”. In: *Atmospheric Chemistry and Physics* 19.15, pp. 10391–10403. ISSN: 1680-7324. DOI: [10.5194/acp-19-10391-2019-463](https://doi.org/10.5194/acp-19-10391-2019-463). URL: <https://acp.copernicus.org/articles/19/10391/2019/>.
- Loreto, Francesco et al. (1998). “On the monoterpene emission under heat stress and on the increased thermotolerance of leaves of *Quercus ilex* L. fumigated with selected monoterpenes”. In: *Plant, Cell and Environment* 21.1, pp. 101–107. ISSN: 01407791. DOI: [10.1046/j.1365-3040.1998.00268.x](https://doi.org/10.1046/j.1365-3040.1998.00268.x).
- McGlynn, Deborah F. et al. (2021). “Measurement report: Variability in the composition of biogenic volatile organic compounds in a Southeastern US forest and their role in atmospheric reactivity”. In: *Atmospheric Chemistry and Physics* 21.20, pp. 15755–15770. ISSN: 1680-7324. DOI: [10.5194/acp-21-15755-2021](https://doi.org/10.5194/acp-21-15755-2021). URL: <https://acp.copernicus.org/articles/21/15755/2021/>.

- Mehra, Archit et al. (2020). “Oligomer and highly oxygenated organic molecule formation from oxidation of oxygenated monoterpenes emitted by California sage plants”. In: *Atmospheric Chemistry and Physics* 20.18, pp. 10953–10965. ISSN: 1680-7324. DOI: [10.5194/acp-20-10953-2020](https://doi.org/10.5194/acp-20-10953-2020). URL: <https://acp.copernicus.org/articles/20/10953/2020/>.
- Mielke, Levi H et al. (2010). “Quantitative Determination of Biogenic Volatile Organic Compounds in the Atmosphere Using Proton-Transfer Reaction Linear Ion Trap Mass”. In: 82.19, pp. 8835–8840. DOI: [10.1029/2006GL025976](https://doi.org/10.1029/2006GL025976). (14).
- Millet, Dylan B. et al. (2005). “Atmospheric volatile organic compound measurements during the Pittsburgh Air Quality Study: Results, interpretation, and quantification of primary and secondary contributions”. In: *Journal of Geophysical Research Atmospheres* 110.7, pp. 1–17. ISSN: 01480227. DOI: [10.1029/2004JD004601](https://doi.org/10.1029/2004JD004601).
- Panopoulou, Anastasia et al. (2020). “Yearlong measurements of monoterpenes and isoprene in a Mediterranean city (Athens): Natural vs anthropogenic origin”. In: *Atmospheric Environment* 243.July, p. 117803. ISSN: 13522310. DOI: [10.1016/j.atmosenv.2020.117803](https://doi.org/10.1016/j.atmosenv.2020.117803). URL: <https://linkinghub.elsevier.com/retrieve/pii/S1352231020305379>.
- Park, J.-H. et al. (2013). “Active Atmosphere-Ecosystem Exchange of the Vast Majority of Detected Volatile Organic Compounds”. In: *Science* 341.6146, pp. 643–647. ISSN: 0036-8075. DOI: [10.1126/science.1235053](https://doi.org/10.1126/science.1235053). URL: <https://www.science.org/doi/10.1126/science.1235053>.
- Pollmann, Jan, John Ortega, and Detlev Helmig (2005). “Analysis of atmospheric sesquiterpenes: Sampling losses and mitigation of ozone interferences”. In: *Environmental Science and Technology* 39.24, pp. 9620–9629. ISSN: 0013936X. DOI: [10.1021/es050440w](https://doi.org/10.1021/es050440w).
- Roest, Geoffrey and Gunnar Schade (2017). “Quantifying alkane emissions in the Eagle Ford Shale using boundary layer enhancement”. In: *Atmospheric Chemistry and Physics* 17.18, pp. 11163–11176. ISSN: 1680-7324. DOI: [10.5194/acp-17-11163-2017](https://doi.org/10.5194/acp-17-11163-2017). URL: <https://acp.copernicus.org/articles/17/11163/2017/>.

- Scanlon, J. T. and D. E. Willis (1985). “Calculation of Flame Ionization Detector Relative Response Factors Using the Effective Carbon Number Concept”. In: *Journal of Chromatographic Science* 23.8, pp. 333–340. ISSN: 0021-9665. DOI: [10.1093/chromsci/23.8.333](https://doi.org/10.1093/chromsci/23.8.333). URL: <https://academic.oup.com/chromsci/article-lookup/doi/10.1093/chromsci/23.8.333>.
- Schade, Gunnar W. and Allen H. Goldstein (2001). “Fluxes of oxygenated volatile organic compounds from a ponderosa pine plantation”. In: *Journal of Geophysical Research Atmospheres* 106.D3, pp. 3111–3123. ISSN: 01480227. DOI: [10.1029/2000JD900592](https://doi.org/10.1029/2000JD900592).
- (2003). “Increase of monoterpene emissions from a pine plantation as a result of mechanical disturbances”. In: *Geophysical Research Letters* 30.7, pp. 10–13. ISSN: 00948276. DOI: [10.1029/2002GL016138](https://doi.org/10.1029/2002GL016138).
- Schuh, G. et al. (1997). “Emissions of volatile organic compounds from Sunflower and Beech: dependence on temperature and light intensity”. In: *Journal of Atmospheric Chemistry* 27, pp. 291–318. DOI: [10.1023/A:1005850710257](https://doi.org/10.1023/A:1005850710257).
- Simpson, Isobel J. et al. (2012). “Long-term decline of global atmospheric ethane concentrations and implications for methane”. In: *Nature* 488.7412, pp. 490–494. ISSN: 00280836. DOI: [10.1038/nature11342](https://doi.org/10.1038/nature11342). URL: <http://dx.doi.org/10.1038/nature11342>.
- Sternberg, JC, WS Gallaway, and DTL Jones (1962). “The mechanism of response of flame ionization detectors”. In: *Gas chromatography: third international symposium*. Ed. by N. Brenner, J. E. Callen, and M. D. Weiss. New York, NY: Academic Press.
- Tanner, David et al. (2006). “Gas chromatography system for the automated, unattended, and cryogen-free monitoring of C2 to C6 non-methane hydrocarbons in the remote troposphere”. In: *Journal of Chromatography A* 1111.1, pp. 76–88. ISSN: 00219673. DOI: [10.1016/j.chroma.2006.01.100](https://doi.org/10.1016/j.chroma.2006.01.100).
- Wang, Ming et al. (2014). “Development and validation of a cryogen-free automatic gas chromatograph system (GC-MS/FID) for online measurements of volatile organic com-

- pounds”. In: *Analytical Methods* 6.23, pp. 9424–9434. ISSN: 17599679. DOI: [10.1039/c4ay01855a](https://doi.org/10.1039/c4ay01855a).
- Wernis, Rebecca A. et al. (2021). “Development of an in situ dual-channel thermal desorption gas chromatography instrument for consistent quantification of volatile, intermediate-volatility and semivolatile organic compounds”. In: *Atmospheric Measurement Techniques* 14.10, pp. 6533–6550. ISSN: 18678548. DOI: [10.5194/amt-14-6533-2021](https://doi.org/10.5194/amt-14-6533-2021).
- Williams, Brent J. et al. (2006). “An In-Situ Instrument for Speciated Organic Composition of Atmospheric Aerosols: Thermal Desorption Aerosol GC/MS-FID (TAG)”. In: *Aerosol Science and Technology* 40.8, pp. 627–638. ISSN: 0278-6826. DOI: [10.1080/02786820600754631](https://doi.org/10.1080/02786820600754631). URL: <http://www.tandfonline.com/doi/abs/10.1080/02786820600754631>.
- Yuan, Bin et al. (2017). “Proton-Transfer-Reaction Mass Spectrometry: Applications in Atmospheric Sciences”. In: *Chemical Reviews* 117.21, pp. 13187–13229. ISSN: 0009-2665. DOI: [10.1021/acs.chemrev.7b00325](https://doi.org/10.1021/acs.chemrev.7b00325). URL: <https://pubs.acs.org/doi/10.1021/acs.chemrev.7b00325>.

Chapter 3

Variability in the composition of biogenic volatile organic compounds in a Southeastern US forest and their role in atmospheric reactivity

Deborah F. McGlynn¹, Laura E.R. Barry², Manuel T. Lerdau^{2,3}, Sally E. Pusede², Gabriel Isaacman-VanWertz¹

¹Civil and Environmental Engineering, Virginia Tech, Blacksburg, VA, 24061, USA

²Department of Environmental Sciences, University of Virginia, Charlottesville, VA, 22904, USA

³Department of Biology, University of Virginia, Charlottesville, VA, 22904, USA

(This chapter reproduces work with permission published as: D.F. McGlynn, L. E. R. Barry, M. T. Lerdau, S. E. Pusede, and G. Isaacman-VanWertz: Measurement report: Variability in the composition of biogenic volatile organic compounds in a Southeastern US forest and their role in atmospheric reactivity. *Atmospheric Chemistry and Physics*. 21 (20), 15755–15770, doi: 10.5194/acp-21-15755-2021, 2021.

Since publication, we recommend a revised limonene ozone reaction rate, which impacts some of the figures and calculated values of this work. This chapter reproduces the work as published. The updated recommended rate is noted in Table 1, and figures associated with this updated value can be found in Appendix B. The updated value is used in Chapter 4.)

3.1 Abstract

Despite the significant contribution of biogenic volatile organic compounds (BVOCs) to organic aerosol formation and ozone production and loss, there are few longterm, year-round, ongoing measurements of their volume mixing ratios and quantification of their impacts on atmospheric reactivity. To address this gap, we present 1 year of hourly measurements of chemically resolved BVOCs between 15 September 2019 and 15 September 2020, collected at a research tower in Central Virginia in a mixed forest representative of ecosystems in the Southeastern US. Mixing ratios of isoprene, isoprene oxidation products, monoterpenes, and sesquiterpenes are described and examined for their impact on the hydroxy radical (OH), ozone, and nitrate reactivity. Mixing ratios of isoprene range from negligible in the winter to typical summertime 24 h averages of 4–6 ppb, while monoterpenes have more stable mixing ratios in the range of tenths of a part per billion up to 2 ppb year-round. Sesquiterpenes are typically observed at mixing ratios of <10 ppt, but this represents a lower bound in their abundance. In the growing season, isoprene dominates OH reactivity but is less important

for ozone and nitrate reactivity. Monoterpenes are the most important BVOCs for ozone and nitrate reactivity throughout the year and for OH reactivity outside of the growing season. To better understand the impact of this compound class on OH, ozone, and nitrate reactivity, the role of individual monoterpenes is examined. Despite the dominant contribution of α -pinene to total monoterpene mass, the average reaction rate of the monoterpene mixture with atmospheric oxidants is between 25% and 30% faster than α -pinene due to the contribution of more reactive but less abundant compounds. A majority of reactivity comes from α -pinene and limonene (the most significant low-mixing-ratio, high-reactivity isomer), highlighting the importance of both mixing ratio and structure in assessing atmospheric impacts of emissions.

3.2 Introduction

Biogenic volatile organic compounds (BVOCs) are a dominant source of reactive carbon in the atmosphere, with an estimated 90% of BVOCs emitted from natural ecosystems (Guenther et al. 2012; Guenther et al. 1995). In the presence of nitrogen oxides ($\text{NO}_x \equiv \text{NO} + \text{NO}_2$), BVOCs can react to form tropospheric ozone (O_3), which has deleterious effects on human health and ecosystems (Avnery et al. 2011a,b; Kroll and Seinfeld 2008; Lim et al. 2012). These reactions also result in the formation of lower volatility gases and secondary organic aerosol (SOA) (Atkinson and Arey 2003a; Guenther et al. 1995; Hallquist, Wängberg, and Ljungström 1997; Kroll and Seinfeld 2008), which have direct and indirect effects on the radiative balance of the atmosphere (The Intergovernmental Panel on Climate Change 2013). Once emitted, BVOCs react with and destroy O_3 or produce O_3 through reactions with other oxidants (in particular, the hydroxyl radical) (Kurpius and Goldstein 2003; Wolfe and Thornton 2011; Wolfe et al. 2011). The impact of plant emissions on net O_3 production versus loss depends on mixing ratios of NO_x , as well as the specific chemistry of the BVOCs emitted (Peake and Sandhu 1983; Pusede et al. 2014; Trainer et al. 1993). Changes in environmental conditions, pollution levels, phenology and ecological succession

affect plants and ecosystems in ways that change their BVOC emissions and ozone uptake (Faiola et al. 2019; Lerdau, Guenther, and Monson 1997; Sadiq et al. 2017; Zheng et al. 2017).

BVOC emissions consist largely of terpenes, including isoprene (C_5H_8), monoterpenes ($C_{10}H_{16}$), sesquiterpenes ($C_{15}H_{24}$), and diterpenes ($C_{20}H_{32}$) (Guenther et al. 2012; Kesselmeier and Staudt 1999; Laothawornkitkul et al. 2009). These compounds vary widely in their reaction rates with atmospheric oxidants, so the impacts of BVOC emissions on regional atmospheric chemistry and composition vary with atmospheric composition and species composition of the dominant vegetation (Atkinson et al. 1992; Claeys et al. 2004; Geron et al. 2000; Goldstein and Galbally 2007; Hoffmann et al. 1997; Lee et al. 2006). Compounds that are acyclic or cyclic with endocyclic double bonds tend to react faster with oxidants due to the higher substitution of the alkenyl carbons in contrast to exocyclic double bonds, which often have one unsubstituted alkenyl carbon (Hatakeyama et al., 1989). Endocyclic monoterpenes (e.g., myrcene, limonene and Δ^3 -carene) and sesquiterpenes (e.g., α -humulene and β -caryophyllene) (Atkinson and Arey 2003b; Matsumoto 2014) also have a greater aerosol formation potential because C-C scission of the double bond is less likely to produce high-volatility fragments (Friedman and Farmer 2018). Additionally, previous studies that have assessed the reactivity of OH and O_3 have found that higher molecular weight BVOCs are emitted at lower rates, but that they make up an outsize percentage of OH and O_3 reactive loss due to their faster reaction rates (Helmig et al. 2006; Holzke et al. 2006; Yee et al. 2018). Therefore, detailed speciated BVOC data are important for understanding reactivity and formation of ozone and SOA. Furthermore, long-term and detailed measurements of BVOCs can assist in reducing inaccuracies in modeled BVOC emissions and in understanding their contribution in ozone and SOA formation (Porter, Safieddine, and Heald 2017).

The chemical complexity of BVOCs presents a challenge in understanding both atmospheric oxidant interactions and SOA production and composition. This problem becomes

more complex in a changing climate and, subsequently, with changing ecosystems. For example, emissions have been found to increase during a forest thinning event (Goldstein et al. 2004) and decrease during times of severe drought and elevated CO₂ (Demetillo et al. 2019; Holopainen et al. 2018). Additionally, increased herbivory has been shown to increase both total plant emissions as well as the relative proportion of sesquiterpenes, which in turn affects SOA production and composition (Faiola et al. 2018; Faiola et al. 2019). Therefore, understanding oxidant budgets, SOA formation, and future changes to ecosystems and atmospheric composition requires a detailed chemical understanding of BVOCs.

BVOCs have been the subject of a large number of measurements and studies, and an exhaustive overview of available datasets is outside of the scope of this manuscript. Generally, measurement campaigns make tradeoffs between temporal resolution, chemical resolution, and long-term instrument stability. Many campaigns of a few weeks to a few months have provided chemically detailed (i.e., isomer-resolved) measurements of BVOCs with time resolution on the order of hourly (Gilman et al. 2009; Goldstein et al. 2004; Park, Schade, and Boedeker 2010; Schade and Goldstein 2003; Schade, Goldstein, and Lamanna 1999), while longer-term (multi-season or multi-year) measurements tend to achieve lower temporal resolution (Guenther et al. 1996; Holdren, Westberg, and Zimmerman 1979; Simpson et al. 2012). Some measurements have provided temporal resolution on the order of minutes by using direct mass spectrometry (e.g., proton transfer reaction mass spectrometry, (Davison et al. 2009; Fares et al. 2010; Ghirardo et al. 2010; Greenberg et al. 2003; Kalogridis et al. 2014), but these instruments are unable to resolve isomers that may differ substantially in their reactivity and physicochemical properties. A few measurement campaigns have collected long-term (many month), temporally resolved (hourly), and chemically detailed (isomer-resolved) measurements of a range of BVOCs (Hellén et al. 2018; Kramer et al. 2015; Maria Yanez-Serrano et al. 2018; Millet et al. 2005; Panopoulou et al. 2020; Plass-Dülmer et al. 2002; Read et al. 2009; Schade and Goldstein 2001), but the number of such campaigns is

fairly limited and very few are currently ongoing. These long-term, temporally and chemically detailed measurements are important for understanding the impacts and behavior of BVOCs on time scales relevant to atmospheric processes, from intra-daily to inter-annually. Therefore, to further advance understanding of the role of biogenic emissions with reactions of atmospheric oxidants on timescale of hours to season, we present one year of temporally and chemically resolved BVOC measurements in a forest canopy that is representative of many ecosystems in the eastern and southeastern U.S., as part of an ongoing measurement site with measurements planned to continue for the indefinite future. We examine here the temporal and seasonal patterns of BVOCs that drive oxidant reactivity. The specific focus of this work is to understand the extent to which composition of major BVOC classes may vary and how minor but reactive components may drive oxidant chemistry. A major outcome of this work is a detailed characterization of monoterpenes that may allow model descriptions and non-isomer-resolved measurements of this chemical class to more accurately capture its impacts on tropospheric chemistry.

3.3 Methods

3.3.1 Instrument location and operation

In-canopy BVOC volume mixing ratios were measured at the Virginia Forest Research Facility (37.9229 °N, 78.2739 °W), located in Fluvanna County, Virginia. The site is located on the east side of the Blue Ridge Mountains and receives some anthropogenic influence from Charlottesville, VA, and surrounding counties, located 25 km to the west of the site. Ambient temperature in the winter and spring months of January-April (due to data availability), was 9.6 ± 9.4 °C, and in the summer and fall months (May-October) was 24.3 ± 7.1 °C (Fig. B.1). Downwelling shortwave radiation was lower in the winter and spring months (141.4 ± 214.8 W m⁻²) than the summer and fall months (January-April) on average (235.6 ± 455.4

W m^{-2}) and exhibited lower variability (Fig. B.1). The forest canopy consists predominantly of maple, oak, and pine and is approximately 24 m tall (Chan 2011). Roughly three-quarters of trees in the forest are species that shed their leaves in the fall and winter months. Tree species found at the site range from being predominantly isoprene emitters, such as oak to predominantly monoterpene and sesquiterpene emitters, such as conifers (Fuentes et al. 1999). Further information pertaining to tree species at the site can be found in (Chan 2011). The site houses a 40-meter meteorological tower, with a climate-controlled, internet-connected lab at the bottom that is supplied by line power, known alternately as “Virginia Forest Research Lab” (VFRL) and “Pace Tower”. The measurement period included in this work extends from September 15, 2019, to September 15, 2020, though measurements are ongoing and are anticipated to continue for several years. All results describing seasonality are divided into two separate seasons based on approximate frost dates: the growing season (May-October) and non-growing season (November-April).

Figure 3.1 depicts the sampling and instrumentation configuration for the automated gas chromatograph-flame ionization (GC-FID) detector used to quantify BVOC volume mixing ratios (the “VOC-GC-FID”). Air is pulled from mid-canopy ($\sim 20\text{m}$ above ground level) at 1400 sccm through a 1/8” ID Teflon tube in an insulated waterproof sheath held at 45 °C. The residence time of an air sample in the inlet is about 8 seconds. Ozone is removed from the sample using a sodium thiosulfate infused quartz fiber filter (Pollmann, Ortega, and Helmig 2005) at the front of the inlet. Efficacy of the ozone scrubber was empirically tested by measuring removal over a multi-week exposure to ozone concentrations several times higher than ambient levels. Efficacy was confirmed following deployment by verifying ozone removal of removed filters. A subsample of ~ 70 sccm is concentrated onto a multibed adsorbent trap composed of: (in order of inlet to outlet) 10 mg of Tenax TA, 20 mg of Carboxen 1000, and 20 mg of Carboxen B, with 15 mg of glass beads between each layer and at the inlet (from Sigma-Aldrich); prior work (Guenther et al. 2012) used a trap composition and analytical

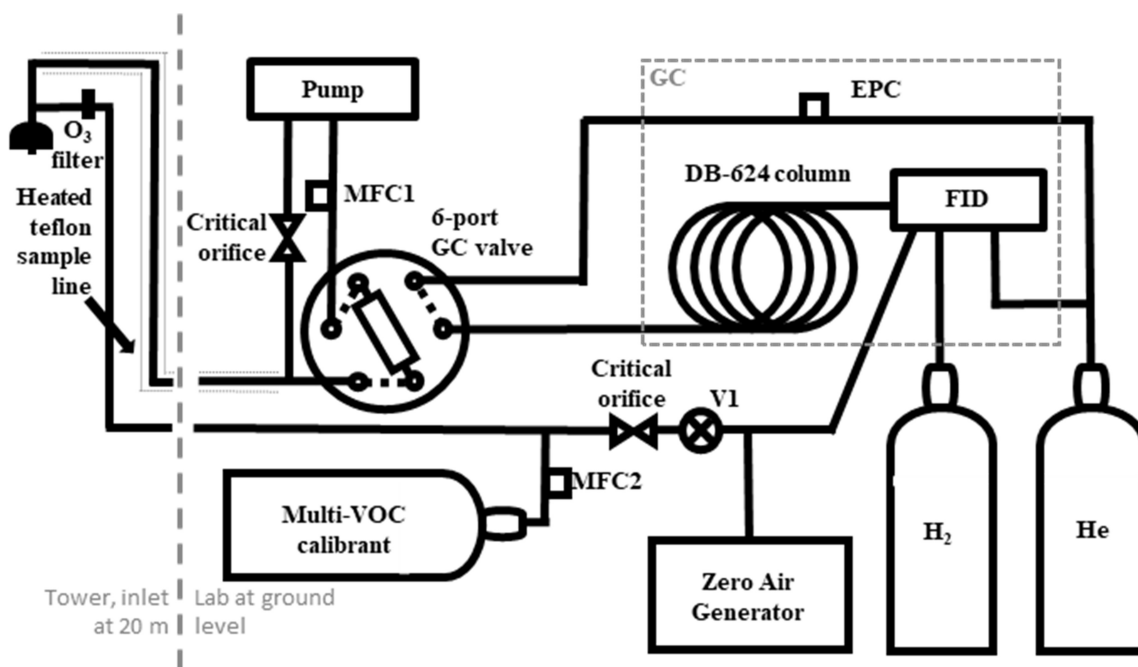


Figure 3.1 A schematic of the VOC-GC-FID set up at the Virginia Forest Research Lab. MFC, mass-flow controller; V1, valve; GC, gas chromatograph; FID, flame ionization detector; EPC, electronic pressure controller; He, helium gas; H₂, hydrogen gas. Small, dashed lines around the inlet, denote the portion that is heated. The large grey dashed line denotes the indicates that the inlet is within the canopy and the rest of the instrument is in the shed, the boxed-in grey dashed line denotes the components that are part of the GC.

system similar to this instrument to sample compounds between C₅ and C₁₄. A custom LabVIEW program (National Instruments) operates the instrument for automated sample collection and analysis, with sample collected for 54.5 minutes of each hour (total sample volume: 3.8 L). Following sample collection, the trap is thermally desorbed under a helium backflush at 140±10 °C for 5.5 minutes, transferring analytes through a heated 6-port valve (150 °C) to the head of the gas chromatography column in a GC oven (Agilent 7890B) with a helium flow rate of 5.5 sccm. GC analysis begins at the end of thermal desorption and proceeds throughout the subsequent sample collection, enabling hourly sample collection and analysis. Analytes are separated using a mid-polarity GC column (Rtx-624, 60m x 0.32mm x 1.8µm, Restek Inc.) and detected by a flame ionization detector (FID). Sample flow is

measured by a mass flow controller (MFC1 in Fig. 3.1, Alicat Scientific), and GC flow is controlled by an electronic pressure controller (EPC in Fig. 3.1) on-board the GC. Ultrapure hydrogen and helium are provided from compressed gas cylinders (5.0 grade, AirGas) as FID fuel gas (H_2), FID makeup gas (He), and GC carrier gas (He). Air for the FID is generated onsite at 30 psig with a zero-air generator (Series 7000, Environics, Inc.).

A major advantage of deploying a GC-FID in a field setting is the limited required maintenance. The most frequent maintenance required by the system is the replacement of ozone filters every 4-6 weeks. The system also requires hydrogen and helium gas tanks, which last for roughly 6-8 months (though the former could be generated on-site). GC components (traps, columns) require little to no replacement over the time period reported here under normal operation. The oil-less vacuum pump used to pull samples suffers somewhat from constant use and overheating in the warmest months of the year and therefore had to be replaced after ~ 12 months.

3.3.2 Calibration and compound identification

For calibration, the sample inlet is overblown with ~ 1400 sccm zero air from a zero-air generator, optionally mixed with a multi-component calibrant (Apel-Riemer Environmental Inc.) at one of four different flows (generating four different mixing ratios of calibrant mixtures). A calibration sample occurs each 7th hour, rotating between zero air only, a calibrant at a fixed “tracking” mixing ratio, and a calibrant at one of three other mixing ratios. Composition and pure volume mixing ratio of the multi-component calibrant are provided in Table B.1 (in brief: 40.3 ppb isoprene, 4.35-17.60 ppb monoterpenes and sesquiterpenes), and diluted into zero air at flows of 10, 25, 50, and 100 sccm to generate dilutions of approximately 140, 60, 30, and 15 times respectively. Estimated limits of detection for isoprene, isoprene oxidation products, monoterpenes, and sesquiterpenes are 20 ppt, 4.3 ppt, 2.2 ppt, and 2.7 ppt, respectively, estimated as the mixing ratio that would yield a chromatographic

peak with a height three times the standard deviation of the noise in the chromatographic baseline. Mixing ratios reported above these levels have an estimated uncertainty of 15%, primarily driven by uncertainty in chromatographic integration (Isaacman-VanWertz et al. 2017). In most cases, mixing ratios calculated below these values are either reported as LOD (in cases when peaks were too small to be integrated), or reported as calculated, but can be considered to have substantial error.

While an FID provides nearly-universal quantification of analytes as a function of their carbon content (Faiola et al. 2012; Scanlon and Willis 1985), it does not provide any chemical resolution. To identify analytes in the samples, a mass spectrometer (MS, Agilent 5977) was deployed in October 2019 and September 2020 in parallel with the FID. Retention times of analytes detected by the two detectors were aligned using the retention time of known analytes (e.g., calibrants). Analytes were identified by mass spectral matching with the 2011 NIST MS Library and reported retention indices (NIST Chemical Kinetics Database, 2020). All analytes reported in this work matched the identified compound within the range of reported retention indices and with a cosine similarity of at least 0.85. This parameter is the preferred spectral comparison method of the widely-used NIST mass spectral library search program, and previous work has shown that a threshold of 0.85 or greater indicates a high probability of correct identification (Stein and Scott 1994; Worton et al. 2017). Data were analyzed using the freely-available TERN software packaged (Isaacman-VanWertz et al. 2017) within the Igor Pro 8 programming environment (Wavemetrics, Inc.).

3.3.3 Atmospheric oxidant reactivity and reaction rate calculations

Reactivity of an individual BVOC and/or a BVOC class to the hydroxyl radical (OHR), ozone (O₃R) and nitrate (NO₃R) is calculated as the sum of the products of the mixing ratio and oxidation reaction rate of each BVOC, i :

$$OxR_{tot}(s^{-1}) = \sum (k_{O_x+BVOC_i} [BVOC_i]) \quad (3.1)$$

Published rate constants (units: $\text{cm}^3 \text{ molec}^{-1} \text{ s}^{-1}$) at 298k were used where available (Atkinson et al. 2006; Atkinson and Arey 2003b; Atkinson, Aschmann, and Arey 1990; Corchnoy and Atkinson 1990; Kerdouci, Picquet-Varrault, and Doussin 2010; King, Canosa-Mas, and Wayne 1999; Pfrang et al. 2006; Pinto et al. 2007; Pratt et al. 2012; Shu and Atkinson 1994; U.S. EPA 2012) and were otherwise calculated from the Kwok and Atkinson structure activity relationships, as implemented by the Estimation Program Interface provided by the U.S. Environmental Protection Agency (King, Canosa-Mas, and Wayne 1999; Kwok and Atkinson 1995; U.S. EPA 2012). Rate constants calculated using structure activity relationships are estimated to be within a factor of ~ 2 of measured rate constants (King, Canosa-Mas, and Wayne 1999). However, uncertainty of estimated rate constants is not expected to significantly impact calculated reactivity as compounds with the largest contribution to atmospheric reactivity have measured rate constants.

3.4 Results and Discussion

3.4.1 Temporal trends in BVOC mixing ratios

Observed and quantified BVOCs include isoprene, two isoprene oxidation products methyl vinyl ketone and methacrolein, eleven monoterpene species, and two sesquiterpene species. Due to the nature of the sample collection, diterpenes many oxygenated species other than MVK and MACR are poorly captured. Oxygenated species either have volatilities that are too high for efficient trapping (e.g., methanol) or are removed by the ozone filter (e.g., nopinone). Many of the small, oxygenated compounds that might be expected at this site at moderately high abundance (e.g., methanol, acetone) have low reaction rate constants that imply they likely contribute only minutely to OHR and NO_3R , and not at all to O_3R .

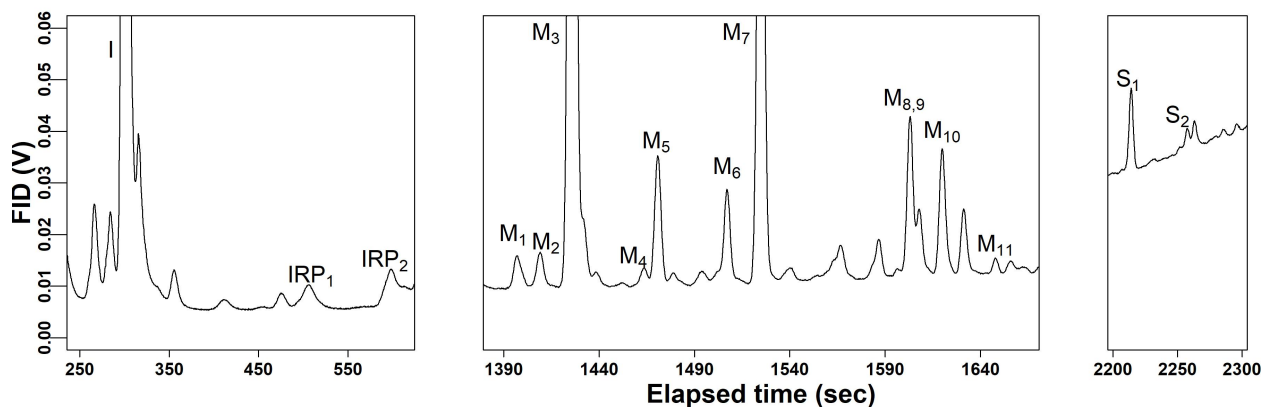


Figure 3.2 A typical GC chromatogram of sampled ambient air collected at the site. The compounds identified on the figure show the range of species found by the instrumental methods. These include isoprene (I), isoprene oxidation products (IOP), monoterpenes (M), and sesquiterpenes (S). Unlabeled peaks were not identified to be terpenes or isoprene oxidation products and are, in most cases, identifiable as belonging to a different compound class.

The exception may be acetaldehyde, which previous work has been shown to contribute non-negligibly to reactivity (Hunter et al. 2017) but is too volatile to be trapped by the instrument used in this work. A sample chromatogram is shown in Fig. 3.2. The detected monoterpene species include α -pinene, β -pinene, β -phellandrene, camphene, limonene, tricyclene, α -fenchene, thujene, cymene, sabinene, and γ -terpinene (Table B.1). The sesquiterpene species regularly detected include α -cedrene and β -cedrene, but these are generally present at very low mixing ratios. Consequently, we expect that not all sesquiterpenes are captured by this instrument and caution that all reported mixing ratios of sesquiterpenes represent lower bounds.

Daily 24-hour averaged mixing ratios of each BVOC class for the measurement period are shown in Fig. 3.3. Periods with gaps, are due to instrument issues, periods reported as zero are below the limit of detection (LOD). Many species approached the LOD in the fall and winter months due to low temperatures and decreased incoming shortwave radiation as compared to the warmest months of the year (Fig. B.1). Isoprene and its oxidation products

Table 3.1 Compound identities on an example chromatogram and associated rate constants ($cm^3molec^{-1}s^{-1}$) for OH, ozone, and nitrate.

Compound	Symbol	Retention time (s)	$k_{OH+BVOC_i}$	$k_{O_3+BVOC_i}$	$k_{NO_3+BVOC_i}$
Isoprene	I	308	$1.01 \times 10^{-10,a}$	$1.27 \times 10^{-17,a}$	$7.00 \times 10^{-13,a}$
Methyl Vinyl Ketone	IOP ₁	504	$5.60 \times 10^{-12,b}$	$1.00 \times 10^{-20,c}$	$4.70 \times 10^{-15,d}$
Methacrolein	IOP ₂	597	$5.00 \times 10^{-11,b}$	$1.00 \times 10^{-20,c}$	$9.60 \times 10^{-16,d}$
Thujene	M ₁	1397	$7.10 \times 10^{-11,e}$	$6.20 \times 10^{-17,e}$	$5.5 \times 10^{-12,f}$
Tricyclene	M ₂	1409	$2.66 \times 10^{-12,g}$	0	0
α -pinene	M ₃	1423	$5.37 \times 10^{-11,a}$	$9.00 \times 10^{-17,a}$	$6.20 \times 10^{-12,k}$
α -fenchene	M ₄	1463	$5.70 \times 10^{-11,c}$	$1.20 \times 10^{-17,c}$	$8.95 \times 10^{-13,c}$
camphene	M ₅	1470	$5.33 \times 10^{-11,g}$	$9.00 \times 10^{-19,e}$	$6.20 \times 10^{-12,e}$
sabinene	M ₆	1507	$1.17 \times 10^{-10,g}$	$8.30 \times 10^{-17,g}$	$1.00 \times 10^{-11,k}$
β -pinene	M ₇	1522	$7.89 \times 10^{-11,g}$	$2.10 \times 10^{-17,g}$	$2.50 \times 10^{-12,k}$
cymene	M ₈	1608	$1.51 \times 10^{-11,h}$	0	$9.90 \times 10^{-16,h}$
limonene*	M ₉	1600	$1.64 \times 10^{-10,g}$	$6.40 \times 10^{-16,g}$	$1.22 \times 10^{-11,k}$
β -phellandrene	M ₁₀	1620	$1.68 \times 10^{-10,g}$	$1.80 \times 10^{-16,g}$	$7.96 \times 10^{-12,k}$
γ -terpinene	M ₁₁	1648	$1.77 \times 10^{-10,g}$	$1.40 \times 10^{-16,g}$	$2.90 \times 10^{-11,k}$
α -cedrene	S ₁	2257	$6.70 \times 10^{-11,g}$	$2.78 \times 10^{-17,i}$	$8.20 \times 10^{-12,j}$
β -cedrene	S ₂	2279	$6.24 \times 10^{-11,i}$	$1.20 \times 10^{-17,i}$	$3.55 \times 10^{-13,j}$

^aAtkinson et al. (2006), ^bPaulot et al. (2009), ^cAtkinson et al. (1990), ^dKerdouci et al. (2010),

^ePinto et al. (2007), ^fPfrang et al. (2006), ^gAtkinson and Arey (2003), ^hCorchnoy and Atkinson (1990),

ⁱShu and Atkinson (1994), ^jEstimated using King et al. (1999), ^kU.S. EPA (2012)

*The ozone reaction rate constant value reported in this table is the value used in this work however, it is recommended to use $2.10 \times 10^{-16,g}$. The value $2.10 \times 10^{-16,g}$ will be used in chapter 4 of this work.

(Fig. 3.3a-b) were near or below detection limits from mid to late-October through early May. Both classes reached their seasonal peak in late July, with an average \pm interquartile range of hourly isoprene mixing ratio in the growing season of 2.13 (\pm 2.99) ppb, and near levels of detection in the non-growing season; uncertainties here and throughout represent interquartile range about the mean. The average mixing ratio of summed isoprene oxidation products was 0.27 (\pm 0.40) ppb in the growing season and 0.02 (\pm 0.03) ppb in the non-growing season. Interestingly, the ratio of isoprene oxidation products to isoprene is variable over the course of the measurement campaign. In addition to differences in their oxidation rates, these differences may be due in part to anthropogenic emissions both through the influence of NO_x on isoprene oxidation pathways and the direct emission of MVK and MACR from vehicles (Biesenthal and Shepson 1997; Ling et al. 2019). The average mixing ratio of

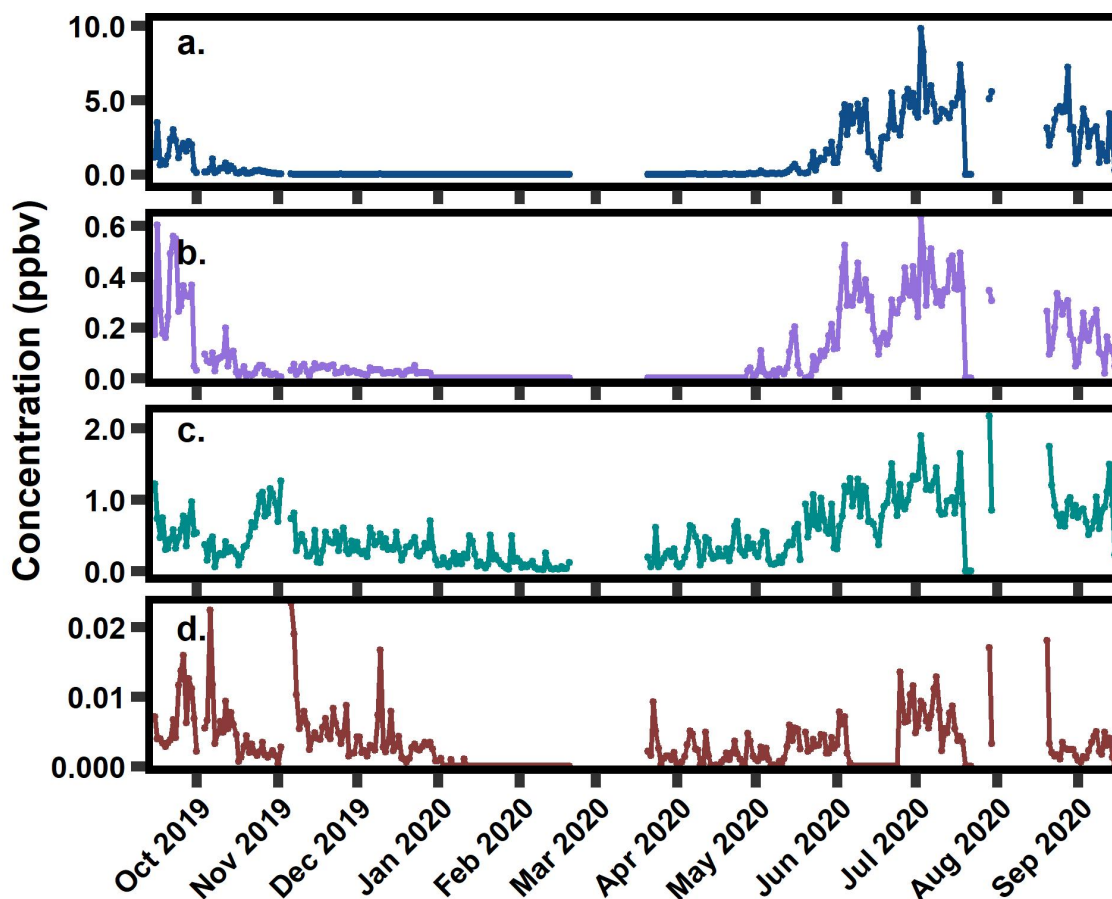


Figure 3.3 24-hour average concentrations of (a) isoprene, (b) isoprene oxidation products (methyl vinyl ketone and methacrolein), (c) sum of monoterpenes, and (d) sum of sesquiterpenes between September 15th, 2019 and September 15th, 2020

summed monoterpenes in the growing season is $0.53 (\pm 0.82)$ ppb and $0.20 (\pm 0.28)$ ppb in the non-growing season (Fig. 3.3c). Monoterpenes exhibit a similar high period during the growing season but are present throughout the non-growing season as well. The average of summer sesquiterpene mixing ratios in the growing season was $0.01 (\pm 0.02)$ ppb and $0.01 (\pm 0.01)$ ppb in the non-growing season. Sesquiterpenes, much like monoterpenes, are detected in both the growing and non-growing season. Average mixing ratios of all classes for each season are provided in Table 3.2.

Diurnal trends in mixing ratios during the growing season (May-October) and non-growing season (November-April) are shown in Fig. 3.4 for isoprene, summed isoprene

Table 3.2 Average and interquartile range of mixing ratio, OH (OHR), ozone (O₃R), and nitrate (NO₃R) reactivities in the growing and non-growing seasons

	Growing Season Average			
	Mixing ratio (ppb)	OHR (s ⁻¹)	O ₃ R (x 10 ⁻⁶ s ⁻¹)	NO ₃ R (s ⁻¹)
Isoprene	2.13 ± 2.99	5.38 ± 7.55	0.67 ± 0.95	0.04 ± 0.05
MVK + MACR	0.27 ± 0.40	0.15 ± 0.20	0.00 ± 0.00	0.00 ± 0.00
Monoterpenes	0.53 ± 0.82	1.42 ± 1.18	2.45 ± 2.13	0.11 ± 0.08
Sesquiterpenes	0.01 ± 0.02	0.01 ± 0.01	0.00 ± 0.00	0.00 ± 0.00
	Non-Growing Season Average			
	Mixing ratio (ppb)	OHR (s ⁻¹)	O ₃ R (x 10 ⁻⁶ s ⁻¹)	NO ₃ R (s ⁻¹)
Isoprene	LOD	—	—	—
MVK + MACR	0.02 ± 0.03	0.01 ± 0.02	0.00 ± 0.00	0.00 ± 0.00
Monoterpenes	0.20 ± 0.28	0.48 ± 0.49	0.78 ± 0.79	0.04 ± 0.04
Sesquiterpenes	0.01 ± 0.01	0.01 ± 0.01	0.00 ± 0.00	0.00 ± 0.00

oxidation products, summed monoterpenes, and summed sesquiterpenes (α - and β -cedrene). All terpene classes exhibited the highest mixing ratios in the growing season (May-October), when temperature and incoming shortwave radiation were highest (Fig. B.1). Isoprene and isoprene oxidation products peak in late afternoon hours, as expected due to the light dependence of isoprene (Guenther 1997; Lamb et al. 1987; Zimmerman 1979). Isoprene and oxidation product mixing ratios were typically below the limits of detection in the non-growing season, with little clear diurnal pattern.

In contrast to isoprene, monoterpenes exhibit peak values in the evening hours, which is consistent with previously reported findings (Davison et al. 2009; Panopoulou et al. 2020). Evening peak values were higher in the growing season than in the non-growing season. Additionally, daytime lows lasted for longer periods of time in the growing season than in the non-growing season due to longer daylight hours driving more photolytic reactions with OH radical and shorter-lasting nighttime boundary layers (Davison et al. 2009). Hourly monoterpene mixing ratios ranged between 0.10 ppb and 2.94 ppb throughout the year, with the lowest values occurring in the non-growing season (Fig. 3.3b).

Sesquiterpene mixing ratios also exhibited peak diurnal mixing ratios in the evening in

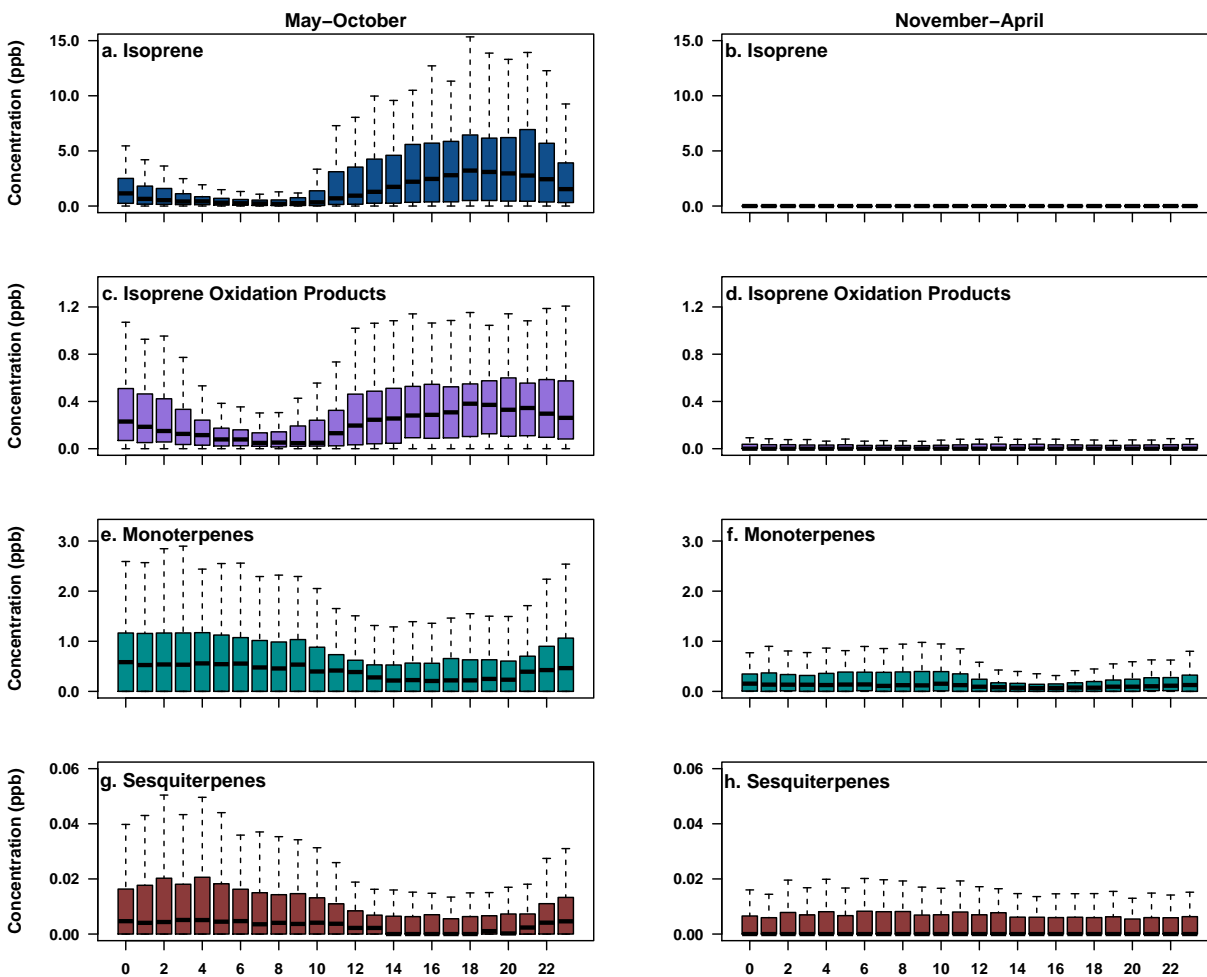


Figure 3.4 Binned hourly boxplots for the four BVOC classes, divided into (left) the growing season, May-October and (right) the non-growing season, November-April. Classes shown are: (a-b) isoprene, (c-d) isoprene oxidation products, (e-f) monoterpenes, and (g-h) sesquiterpenes. The plots show the median value as a horizontal line, the bottom and top of each box indicates the 25th and 75th percentiles while the whisker represent 1.5 times the interquartile range. Each box represents the data for each hour of the day.

the growing season. Summed mixing ratios of sesquiterpenes (Fig. 3.3g, h) include only two species, and so represent a lower bound of possible total sesquiterpene mixing ratios. However, the limit of detection for sesquiterpenes is estimated as 2.7 ppt, so other sesquiterpenes are unlikely to be present at mixing ratios significantly higher than this. Measured sesquiterpenes therefore provide some insight into the total mixing ratios of sesquiterpenes.

Mean sesquiterpene (i.e., sum of α - and β -cedrene) values were around 0.01 (\pm 0.02) ppb in the growing season and exhibited similar diurnal variability to monoterpenes. Outside the growing season, the mean sesquiterpene mixing ratio was 0.01 (\pm 0.01) ppb with little discernable diurnal variability.

3.4.2 Calculated reactivity with atmospheric oxidants

Calculated OH reactivity

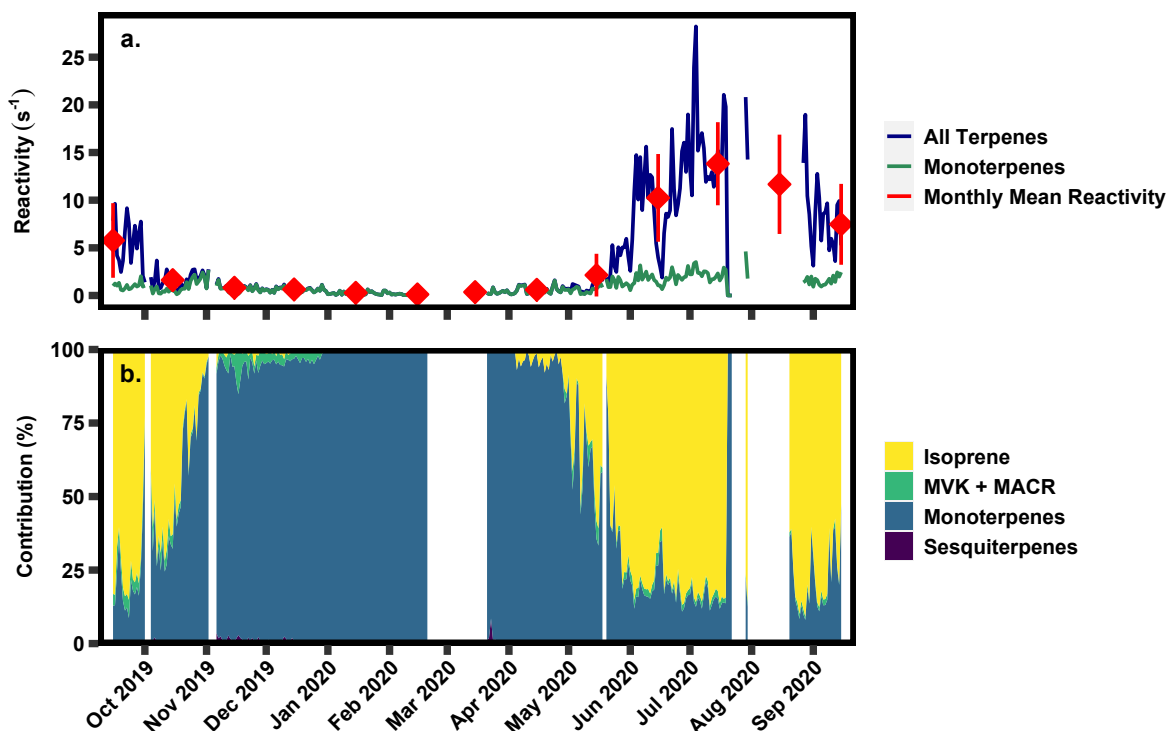


Figure 3.5 (a) Timeseries of 24-hour averaged calculated OH reactivity of all measured terpene classes and the monoterpene class, as well as the monthly mean of calculated OH reactivity. (b) Relative contribution of each of the BVOC classes to OH reactivity.

Calculated OH reactivity of total observed terpenes varies seasonally, with a 24-hour average summertime peak of ~ 27 s⁻¹ and growing season average of 8.48 (± 10.68) s⁻¹ driven by isoprene (Fig. 3.5a). Comparatively, the non-growing season OH reactivity average was 0.99 (± 1.04) s⁻¹. Reactivity of monoterpenes has weaker seasonality with higher values

occurring in the growing season, peaking at $\sim 3 \text{ s}^{-1}$. These values are roughly within the range of previously reported direct measurements of summertime OH reactivity of 1-21 s^{-1} where measurements were taken below ponderosa and coniferous forest canopies and within the canopy of a coniferous forest (Ramasamy et al., 2016; Nakashima et al., 2014; Sinha et al., 2010), though at the higher end, likely due to the measurements in this work occurring directly within the canopy. While isoprene dominates reactions with OH when present (Fig. 5b), mixing ratios of isoprene and detected sesquiterpenes are negligible in the non-growing season, causing a steep decline in reactivity. Due to the year-round presence of monoterpenes, these compounds become the dominant source of OH reactivity in the non-growing season. Generally, monoterpenes contribute $\sim 100\%$ in the non-growing season and $\sim 15\text{-}35\%$ of terpene reactivity in the growing season, with isoprene dominating the balance. Detected isoprene oxidation products and sesquiterpenes contribute, on average, $< 5\%$ to OH reactivity. While some sesquiterpenes may be below level of detection, sesquiterpenes do not generally have OH reaction rates substantially higher than other more dominant terpenes (Lee et al., 2006) and so are not likely to contribute substantially to OH reactivity.

Calculated ozone reactivity

Calculated 24-hour averaged O_3 reactivity ranges between $0.1 \times 10^{-5} \text{ s}^{-1}$ and $1.0 \times 10^{-5} \text{ s}^{-1}$ (Fig. 3.6a) and is almost entirely dominated by monoterpenes (Fig. 3.6b), even during the growing season peak (monoterpenes: $\sim 70\%$), due to the relatively slow reaction rate of isoprene and its oxidation products with ozone. Ozone reactivity decreases in the non-growing season due to both the decline in isoprene, and the decrease in monoterpenes. Average ozone reactivity with isoprene in the growing season is $0.67 \times 10^{-6} (\pm 0.95 \times 10^{-6}) \text{ s}^{-1}$ while in the non-growing season isoprene does not contribute substantially to ozone reactivity (Table 3.2). Average ozone reactivity with monoterpenes in the growing season is $2.45 \times 10^{-6} (\pm 2.13 \times 10^{-6}) \text{ s}^{-1}$ while in the non-growing season it is $0.78 \times 10^{-6} (\pm 0.79 \times 10^{-6}) \text{ s}^{-1}$.

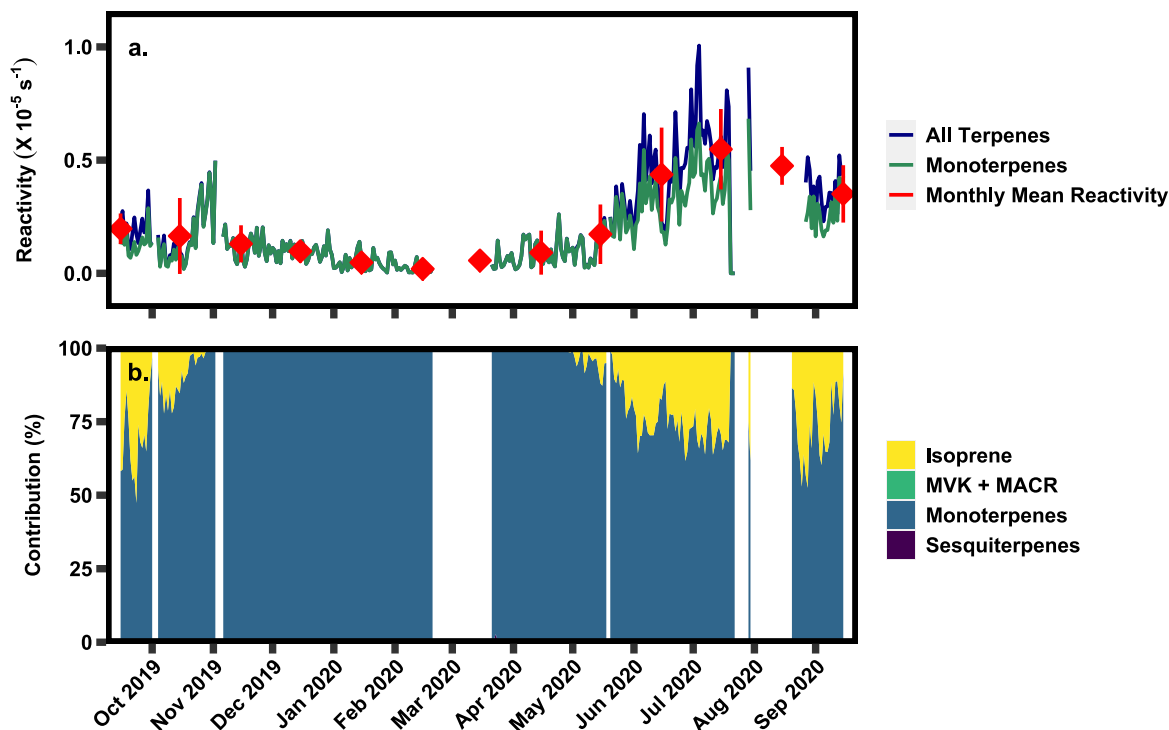


Figure 3.6 (a) Timeseries of 24-hour averaged calculated ozone reactivity of all terpene classes and the monoterpene class, as well as the monthly mean of calculated ozone reactivity. (b) Relative contribution of each of the BVOC classes to ozone reactivity.

s^{-1} The measured isoprene oxidation products and sesquiterpenes are not strongly reactive with ozone, and therefore have no significant contribution to ozone reactivity. However, unlike with OH reaction rates, O_3 reaction rates of sesquiterpenes are frequently orders of magnitude larger than dominant monoterpenes, so it is possible that low abundance, highly reactive sesquiterpenes may still contribute non-negligibly to ozone reactivity. Important contributions by low abundance, highly reactive sesquiterpenes have been previously shown in other environments, and cannot be excluded by these measurements (Arnts, Mowry, and Hampton 2013; Ortega et al. 2007; Wolfe et al. 2011; Yee et al. 2018).

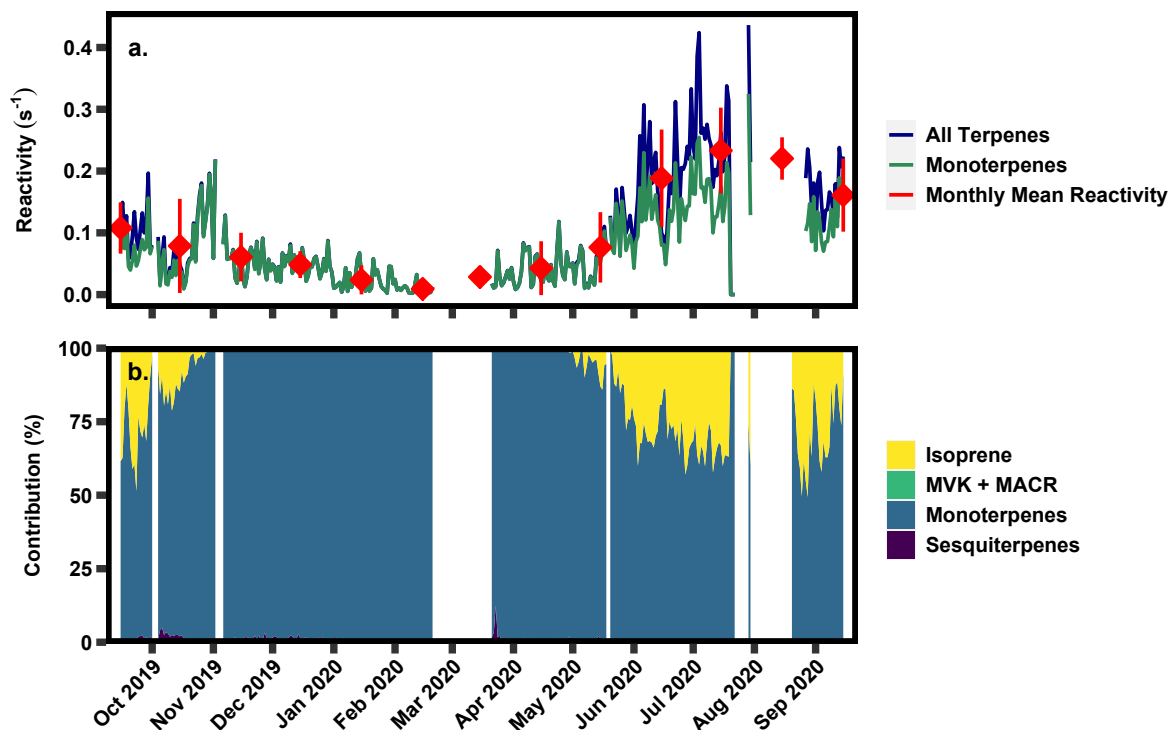


Figure 3.7 (a) Timeseries of 24-hour averaged calculated nitrate reactivity of all terpene classes and the monoterpene class, as well as the monthly mean of calculated nitrate reactivity. (b) Relative contribution of each of the BVOC classes to nitrate reactivity.

Calculated nitrate reactivity

Calculated nitrate reactivity of all detected BVOCs is shown in Fig. 3.7a in addition to the monthly average reactivity and the reactivity of the monoterpene class. The amount that each BVOC class contributes to nitrate reactivity is shown in Fig. 3.7b. Nitrate reactivity of observed BVOCs varies seasonally, with a summertime peak in 24-average reactivity of $\sim 0.4 \text{ s}^{-1}$ driven largely by monoterpenes. Reactivity of monoterpenes has strong seasonality with higher values occurring in the growing season, peaking at $\sim 0.3\text{-}0.4 \text{ s}^{-1}$. As in the case of ozone, nitrate reactivity is dominated by monoterpenes due to the slow reaction rates of isoprene and its oxidation products with NO_3 . Isoprene contributes between 20-40% to nitrate reactivity in the growing season and has a mean hourly average of $0.04 (\pm 0.05) \text{ s}^{-1}$. In

the non-growing season, isoprene, like isoprene oxidation products and sesquiterpenes do not contribute to nitrate reactivity. Monoterpenes dominate nitrate reactivity year-round and have a mean hourly average of $0.11 (\pm 0.08) \text{ s}^{-1}$ in the growing season and $0.04 (\pm 0.04) \text{ s}^{-1}$ in the non-growing season. Unmeasured and minimally detected sesquiterpenes are unlikely to contribute substantially to nitrate reactivity as their reaction rates are typically of the same order of magnitude as α -pinene and isoprene but they are present at concentrations 10-100 times lower (Yee et al. 2018).

3.4.3 Isomer composition of monoterpenes

Monoterpenes are detected year-round, but small changes in their compositional breakdown (i.e., the relative contribution of different isomers) leads to important changes in their reactivity and chemistry. Calculated 24-hour average monoterpene mixing ratios ranged between 0.10 ppb and 2.00 ppb with the lowest mixing ratios occurring in the non-growing season daytime and highest mixing ratios occurring in the growing season nights (as shown in Fig. 3.4).

Relative contributions from monoterpene isomers are similar for the highest mixing ratio species between the growing and non-growing seasons (Fig. 3.8a-b). At nearly all times, α -pinene contributes the most, followed by α -pinene, camphene, limonene, and cymene. OH reactivity (Fig. 3.8c and 3.8d) of each isomer roughly follows the distribution of mixing ratios, driven by the relatively narrow range in OH reaction rates for monoterpenes with double bonds (slowest: α -pinene – $5.37 \times 10^{-11} \text{ cm}^3 \cdot \text{molec}^{-1} \cdot \text{s}^{-1}$, fastest: β -phellandrene – $1.68 \times 10^{-10} \text{ cm}^3 \cdot \text{molec}^{-1} \cdot \text{s}^{-1}$). There is nevertheless some outsize contribution to OH reactivity by the low-mixing ratio isomers β -phellandrene and limonene, which react quickly due to the presence of multiple double bonds and contribute twice as much to reactivity as they do to mixing ratio. Together, these two species account for roughly one-third of OH reactivity, the abundant but less-reactive α -pinene account for another \sim one-third, and the remaining

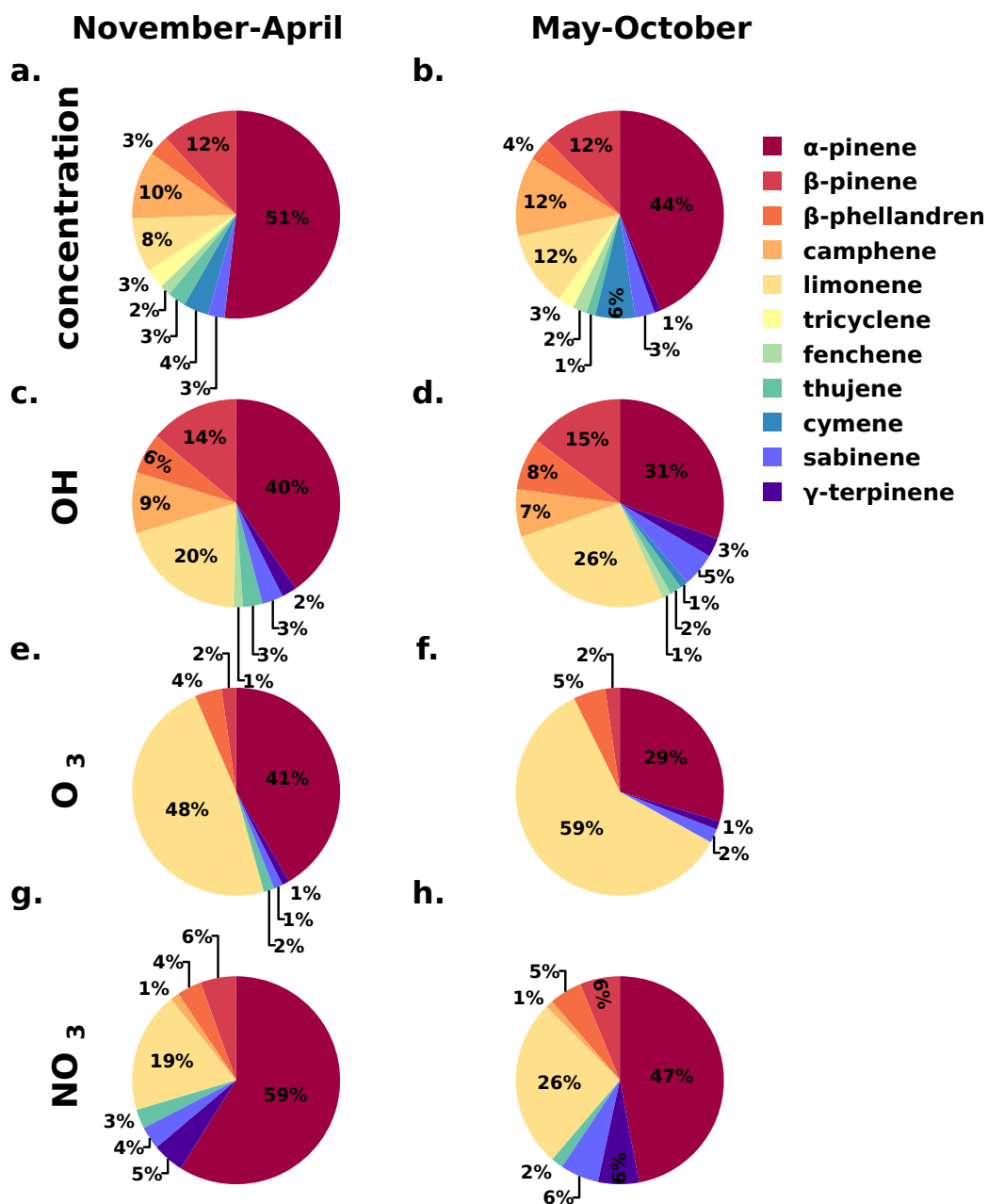


Figure 3.8 A breakdown of detected monoterpene isomers in the growing and non-growing seasons for (a-b) concentration, (c-d) OH reactivity, (e-f) ozone reactivity, (g-h) nitrate reactivity. Values are rounded to the nearest percent and values below 1% are not depicted.

monoterpenes account for the remainder (mostly β -pinene, camphene, and γ -terpinene). The stability of the mixing ratios and OH reactivity across a year of measurements suggests that the observed distribution of isomers is a reasonable average representation of monoterpenes in this ecosystem. While α -pinene is the dominant isomer by far, its lower reaction rate relative to other isomers suggest that it is not necessarily a good representative proxy species for the broader monoterpene compound class. Instead, a more general quantitative description of the rate at which monoterpenes react with OH (or any other oxidant) would allow a measurement or estimate of bulk monoterpenes to more accurately be converted into an estimate of their impact on reactivity. Correlations between calculated monoterpene oxidant reactivity and detected monoterpene mixing ratio (Fig. B.2) suggest a bulk monoterpene reaction rate of $k_{\text{OH}+\text{MT}} = 6.9 \times 10^{-11} \text{ cm}^3 \cdot \text{molec}^{-1} \cdot \text{s}^{-1}$, $\sim 30\%$ greater than the reaction rate of α -pinene, and this average rate is relatively temporally stable. It should also be noted that Fig. 3.8 suggests that OH reaction with faster-reacting, poly-unsaturated, lower-mixing ratio isomers is as likely as reaction with α -pinene.

The role of structure on atmospheric reactions is even more apparent and critical when considering the reactivity of monoterpenes with ozone. Despite its relatively low mixing ratio, limonene is the greatest contributor to reactivity with ozone at 59% and 48% in the growing and non-growing season respectively due to an ozone reaction rate 8 times faster than that of the more abundant isomers (Fig. 3.8e-f). Nearly all the rest of ozone reactivity is contributed by the dominant isomer α -pinene (30% and 41%), with a minor contribution from β -phellandrene (5% and 4%), β -pinene (2% and 2%), and γ -terpinene (1% and 1%), while the other isomers are either not reactive with ozone (cymene, tricyclene) or react very slowly with ozone (camphene). Though the general breakdown of ozone reactivity is qualitatively similar during both the growing and non-growing seasons, there are significant quantitative differences. Due to the greater contribution of limonene in the growing season compared to the non-growing season, the relative importance of limonene compared to α -

pinene increases substantially in the growing season, from 1.3:1 to 2.1:1. In other words, reactions of monoterpenes with ozone, at least in this canopy, are dominated by reactions with limonene, with a smaller but significant contribution from α -pinene. The bulk O_3 reaction rate with monoterpenes (i.e., the rate that best converts hourly mixing ratio to reactivity) is $k_{O_3+MT} = 1.1 \times 10^{-16} \text{ cm}^3 \cdot \text{molec}^{-1} \cdot \text{s}^{-1}$, $\sim 25\%$ faster than α -pinene. However, while this average rate is relatively stable across seasons, there are periods in the growing season during which the average reaction rate of monoterpenes is substantially faster, which could have impacts during these periods (Fig. B.2).

Isomer-dependence of nitrate reactivity is somewhere between O_3 and OH, with an outsized impact of limonene, but with a more even split of reactivity across monoterpenes species. These trends may be explained by the reaction behavior of nitrate. Like the OH radical, nitrate can react with alkenes by either addition to a double bond or abstract a hydrogen, but it has a stronger tendency to add across a double bond, analogous to O_3 (Lee et al. 2014; Pfrang et al. 2006). Similar to OH reactivity, limonene contributes an outsized amount to NO_3 reactivity in both the growing and non-growing season (26% and 19%). However, for nitrate reactivity, α -pinene remains the dominant component, contributing 48% to reactions with nitrate in the growing season and 59% in the non-growing season. The average reaction rate of α -pinene is about ~ 10 -20% faster than the bulk reaction rate of monoterpenes with nitrate radicals.

3.5 Conclusion

Long-term BVOC measurements are imperative for understanding interannual trends in the formation and loss of ozone and SOA, and for improving existing models of BVOC emissions and oxidation. These measurements are difficult, however, without robust measurement techniques that do not require significant maintenance. The use of an automated GC-FID adapted to collect air samples makes it possible to do long-term collection of BVOCs in an

unmonitored location. Using this method, we have collected and are continuing to measure a range of BVOCs in the canopy of a forest representative of the Southeastern U.S., with periodic coupling of a mass spectrometer to allow for identification of the species of interest. The relative ease of this method gives it great potential for additional long-term BVOC monitoring sites to be set up in more locations.

From this study we have gained a greater understanding of the seasonality of BVOCs ranging from isoprene, isoprene oxidation products, monoterpenes, and sesquiterpenes. Isoprene is important for OH reactivity, but monoterpenes prevail as the most important BVOC class for ozone and nitrate reactivities. Monoterpenes are observed to be a diverse class of BVOCs with 11 identified compounds detected at the site year-round. While α -pinene is the most dominant species, a few species with lower mixing ratios but high reactivities (particularly limonene and β -phellandrene) were found to be important contributors to atmospheric reactivity. This finding is most evident for ozone reactivity but is also the case for OH and nitrate reactivity. The distribution of monoterpenes is qualitatively stable throughout the year, though some important quantitative differences are observed. Consequently, the distribution measured here may be a useful description of the “typical” monoterpene chemical class observed in mixed, temperate forests. The bulk reaction rates of the monoterpene class with major atmospheric oxidants presented here therefore provide an improved means to estimate the reactions and impacts of monoterpenes in cases where isomer-resolved measurements are not available (e.g., when measured using direct-air-sampling mass spectrometers (Davison et al. 2009; Ghirardo et al. 2010)).

3.6 Acknowledgements

This research was funded by the National Science Foundation (AGS 1837882 and AGS 1837891). Temperature and downwelling solar radiation data were provided by Todd M. Scanlon. Tower maintenance and operation was supported in part by the Pace Endowment.

D.F.M. and L.E.R.B. were supported in part by Virginia Space Grant Consortium Graduate Research Fellowships. The authors gratefully acknowledge the assistance of Koong Yi, Graham Frazier, and Bradley Sutliff in their support in upkeep and maintenance of the instrument at Pace Tower. We thank Todd Scanlon for the use of the meteorological data provided in Figure S1.

3.7 References

- Arnts, Robert R., Fred L. Mowry, and Gary A. Hampton (2013). “A high-frequency response relaxed eddy accumulation flux measurement system for sampling short-lived biogenic volatile organic compounds”. In: *Journal of Geophysical Research Atmospheres* 118.10, pp. 4860–4873. ISSN: 21698996. DOI: [10.1002/jgrd.50215](https://doi.org/10.1002/jgrd.50215).
- Atkinson, R. et al. (2006). “Evaluated kinetic and photochemical data for atmospheric chemistry: Volume II – gas phase reactions of organic species”. In: *Atmospheric Chemistry and Physics* 6.11, pp. 3625–4055. ISSN: 1680-7324. DOI: [10.5194/acp-6-3625-2006](https://doi.org/10.5194/acp-6-3625-2006). URL: <https://acp.copernicus.org/articles/6/3625/2006/>.
- Atkinson, Roger and Janet Arey (2003a). “Atmospheric Degradation of Volatile Organic Compounds”. In: *Chemical Reviews* 103.12, pp. 4605–4638. ISSN: 0009-2665. DOI: [10.1021/cr0206420](https://doi.org/10.1021/cr0206420). URL: <https://pubs.acs.org/doi/10.1021/cr0206420>.
- (2003b). “Gas-phase tropospheric chemistry of biogenic volatile organic compounds: A review”. In: *Atmospheric Environment* 37.SUPPL. 2, pp. 197–219. ISSN: 13522310. DOI: [10.1016/S1352-2310\(03\)00391-1](https://doi.org/10.1016/S1352-2310(03)00391-1).
- Atkinson, Roger, Sara M Aschmann, and Janet Arey (1990). *Rate constants for the gas-phase reactions of OH and NO₃ Radicals and O₃ with sabinene and camphene*.
- Atkinson, Roger et al. (1992). “Formation of OH Radicals in the Gas Phase Reactions of Ozone with a Series of Terpenes”. In: 97.92, pp. 6065–6073.

- Avnery, Shiri et al. (2011a). “Global crop yield reductions due to surface ozone exposure: 1. Year 2000 crop production losses and economic damage”. In: *Atmospheric Environment* 45.13, pp. 2284–2296. ISSN: 13522310. DOI: [10.1016/j.atmosenv.2010.11.045](https://doi.org/10.1016/j.atmosenv.2010.11.045). URL: <http://dx.doi.org/10.1016/j.atmosenv.2010.11.045>.
- (2011b). “Global crop yield reductions due to surface ozone exposure: 2. Year 2030 potential crop production losses and economic damage under two scenarios of O₃ pollution”. In: *Atmospheric Environment* 45.13, pp. 2297–2309. ISSN: 13522310. DOI: [10.1016/j.atmosenv.2011.01.002](https://doi.org/10.1016/j.atmosenv.2011.01.002). URL: <http://dx.doi.org/10.1016/j.atmosenv.2011.01.002>.
- Biesenthal, Thomas A. and Paul B. Shepson (1997). “Observations of anthropogenic inputs of the isoprene oxidation products methyl vinyl ketone and methacrolein to the atmosphere”. In: *Geophysical Research Letters* 24.11, pp. 1375–1378. ISSN: 00948276. DOI: [10.1029/97GL01337](https://doi.org/10.1029/97GL01337).
- Chan, WS (2011). “The Fate of Biogenic Hydrocarbons within a Forest Canopy: Field Observation and Model Results”. PhD thesis. University of Virginia.
- Claeys, Magda et al. (2004). “Formation of secondary organic aerosols from isoprene and its gas-phase oxidation products through reaction with hydrogen peroxide”. In: 38, pp. 4093–4098. DOI: [10.1016/j.atmosenv.2004.06.001](https://doi.org/10.1016/j.atmosenv.2004.06.001).
- Corchnoy, Stephanie B. and Roger Atkinson (1990). “Kinetics of the Gas-Phase Reactions of OH and NO₃ Radicals with 2-Carene, 1,8-Cineole, p-Cymene, and Terpinolene”. In: *Environmental Science and Technology* 24.10, pp. 1497–1502. ISSN: 15205851. DOI: [10.1021/es00080a007](https://doi.org/10.1021/es00080a007).
- Davison, B. et al. (2009). “Concentrations and fluxes of biogenic volatile organic compounds above a Mediterranean Macchia ecosystem in western Italy”. In: *Biogeosciences* 6.8, pp. 1655–1670. ISSN: 17264189. DOI: [10.5194/bg-6-1655-2009](https://doi.org/10.5194/bg-6-1655-2009).

- Demetillo, Mary Angelique G. et al. (2019). *Observing Severe Drought Influences on Ozone Air Pollution in California*. DOI: [10.1021/acs.est.8b04852](https://doi.org/10.1021/acs.est.8b04852).
- Faiola, C. L. et al. (2012). “Quantification of biogenic volatile organic compounds with a flame ionization detector using the effective carbon number concept”. In: *Atmospheric Measurement Techniques* 5.8, pp. 1911–1923. ISSN: 18671381. DOI: [10.5194/amt-5-1911-2012](https://doi.org/10.5194/amt-5-1911-2012).
- Faiola, C. L. et al. (2018). “Terpene Composition Complexity Controls Secondary Organic Aerosol Yields from Scots Pine Volatile Emissions”. In: *Scientific Reports* 8.1, pp. 1–13. ISSN: 20452322. DOI: [10.1038/s41598-018-21045-1](https://doi.org/10.1038/s41598-018-21045-1).
- Faiola, Celia L. et al. (2019). “Secondary Organic Aerosol Formation from Healthy and Aphid-Stressed Scots Pine Emissions”. In: *ACS Earth and Space Chemistry* 3.9, pp. 1756–1772. ISSN: 24723452. DOI: [10.1021/acsearthspacechem.9b00118](https://doi.org/10.1021/acsearthspacechem.9b00118).
- Fares, Silvano et al. (2010). “Ozone uptake by citrus trees exposed to a range of ozone concentrations”. In: *Atmospheric Environment* 44.28, pp. 3404–3412. ISSN: 13522310. DOI: [10.1016/j.atmosenv.2010.06.010](https://doi.org/10.1016/j.atmosenv.2010.06.010).
- Friedman, Beth and Delphine K. Farmer (2018). “SOA and gas phase organic acid yields from the sequential photooxidation of seven monoterpenes”. In: *Atmospheric Environment* 187. January, pp. 335–345. ISSN: 18732844. DOI: [10.1016/j.atmosenv.2018.06.003](https://doi.org/10.1016/j.atmosenv.2018.06.003). URL: <https://doi.org/10.1016/j.atmosenv.2018.06.003>.
- Fuentes, JD et al. (1999). “Biogenic Hydrocarbons in the Atmospheric Boundary Layer: A Review”. In.
- Geron, Chris et al. (2000). “A review and synthesis of monoterpene speciation from forests in the United States”. In: *Atmospheric Environment* 34.11, pp. 1761–1781. ISSN: 13522310. DOI: [10.1016/S1352-2310\(99\)00364-7](https://doi.org/10.1016/S1352-2310(99)00364-7).
- Ghirardo, Andrea et al. (2010). “Determination of de novo and pool emissions of terpenes from four common boreal/alpine trees by ^{13}C labelling and PTR-MS analysis”. In:

- Plant, Cell & Environment* 33.5, pp. 781–792. ISSN: 01407791. DOI: [10.1111/j.1365-3040.2009.02104.x](https://doi.org/10.1111/j.1365-3040.2009.02104.x). URL: <https://onlinelibrary.wiley.com/doi/10.1111/j.1365-3040.2009.02104.x>.
- Gilman, Jessica B. et al. (2009). “Measurements of volatile organic compounds during the 2006 TexAQS/GoMACCS campaign: Industrial influences, regional characteristics, and diurnal dependencies of the OH reactivity”. In: *Journal of Geophysical Research* 114.7, D00F06. ISSN: 0148-0227. DOI: [10.1029/2008JD011525](https://doi.org/10.1029/2008JD011525). URL: <http://doi.wiley.com/10.1029/2008JD011525>.
- Goldstein, A H et al. (2004). “Forest thinning experiment confirms ozone deposition to forest canopy is dominated by reaction with biogenic VOCs”. In: 31.June 2000, pp. 2–5. DOI: [10.1029/2004GL021259](https://doi.org/10.1029/2004GL021259).
- Goldstein, Allen H and Ian Galbally (2007). “Known and unexplored organic constituents in the earth’s atmosphere”. In: *Environmental Science & Technology*.
- Greenberg, J. P. et al. (2003). “Eddy flux and leaf-level measurements of biogenic VOC emissions from mopane woodland of Botswana”. In: *Journal of Geophysical Research: Atmospheres* 108.13, pp. 1–9. ISSN: 01480227. DOI: [10.1029/2002jd002317](https://doi.org/10.1029/2002jd002317).
- Guenther, A. et al. (1996). “Leaf, branch, stand and landscape scale measurements of volatile organic compound fluxes from U.S. woodlands”. In: *Tree Physiology* 16.1-2, pp. 17–24. ISSN: 0829318X. DOI: [10.1093/treephys/16.1-2.17](https://doi.org/10.1093/treephys/16.1-2.17).
- Guenther, A. B. et al. (2012). “The model of emissions of gases and aerosols from nature version 2.1 (MEGAN2.1): An extended and updated framework for modeling biogenic emissions”. In: *Geoscientific Model Development* 5.6, pp. 1471–1492. ISSN: 1991959X. DOI: [10.5194/gmd-5-1471-2012](https://doi.org/10.5194/gmd-5-1471-2012).
- Guenther, Alex (1997). “Seasonal and spatial variations in natural volatile organic compound emissions”. In: *Ecological Applications* 7.1, pp. 34–45. ISSN: 10510761. DOI: [10.1890/1051-0761](https://doi.org/10.1890/1051-0761).

- Guenther, Alex et al. (1995). “A global model of natural volatile organic compound emissions”. In: *J. Geophys. Res.* 100.94, pp. 8873–8892.
- Hallquist, Mattias, Ingvar Wängberg, and Evert Ljungström (1997). “Atmospheric Fate of Carbonyl Oxidation Products Originating from α -Pinene and Δ^3 -Carene: Determination of Rate of Reaction with OH and NO₃ Radicals, UV Absorption Cross Sections, and Vapor Pressures”. In: *Environmental Science & Technology* 31.11, pp. 3166–3172. ISSN: 0013-936X. DOI: [10.1021/es970151a](https://doi.org/10.1021/es970151a). URL: https://www.google.com/search?tbm=bks&hl=en&q=reaction+rate+constants&gws_rd=sslhttps://pubs.acs.org/doi/10.1021/es970151a.
- Hellén, Heidi et al. (2018). “Long-term measurements of volatile organic compounds highlight the importance of sesquiterpenes for the atmospheric chemistry of a boreal forest”. In: *Atmospheric Chemistry and Physics* 18.19, pp. 13839–13863. ISSN: 16807324. DOI: [10.5194/acp-18-13839-2018](https://doi.org/10.5194/acp-18-13839-2018).
- Helmig, Detlev et al. (2006). “Sesquiterpene emissions from loblolly pine and their potential contribution to biogenic aerosol formation in the Southeastern US”. In: *Atmospheric Environment* 40.22, pp. 4150–4157. ISSN: 13522310. DOI: [10.1016/j.atmosenv.2006.02.035](https://doi.org/10.1016/j.atmosenv.2006.02.035). URL: <https://linkinghub.elsevier.com/retrieve/pii/S1352231006002421>.
- Hoffmann, Thorsten et al. (1997). “Formation of Organic Aerosols from the Oxidation of Biogenic Hydrocarbons”. In: 1, pp. 189–222.
- Holdren, M W H, H H Westberg, and P R Zimmerman (1979). “Analysis of Monoterpene Hydrocarbons in Rural Atmospheres”. In: 84.9, pp. 1–6.
- Holopainen, Jarmo K et al. (2018). “Climate Change Effects on Secondary Compounds of Forest Trees in the Northern Hemisphere”. In: *Frontiers in Plant Science* 9.October, pp. 1–10. ISSN: 1664-462X. DOI: [10.3389/fpls.2018.01445](https://doi.org/10.3389/fpls.2018.01445). URL: <https://www.frontiersin.org/article/10.3389/fpls.2018.01445/full>.

- Holzke, C. et al. (2006). “Diurnal and seasonal variation of monoterpene and sesquiterpene emissions from Scots pine (*Pinus sylvestris* L.)” In: *Atmospheric Environment* 40.17, pp. 3174–3185. ISSN: 13522310. DOI: [10.1016/j.atmosenv.2006.01.039](https://doi.org/10.1016/j.atmosenv.2006.01.039).
- Hunter, James F. et al. (2017). “Comprehensive characterization of atmospheric organic carbon at a forested site”. In: *Nature Geoscience* 10.10, pp. 748–753. ISSN: 1752-0894. DOI: [10.1038/ngeo3018](https://doi.org/10.1038/ngeo3018). URL: <http://www.nature.com/articles/ngeo3018>.
- Isaacman-VanWertz, Gabriel et al. (2017). “Automated single-ion peak fitting as an efficient approach for analyzing complex chromatographic data”. In: *Journal of Chromatography A* 1529, pp. 81–92. ISSN: 0021-9673. DOI: [10.1016/j.chroma.2017.11.005](https://doi.org/10.1016/j.chroma.2017.11.005). URL: <http://dx.doi.org/10.1016/j.chroma.2017.11.005>.
- Kalogridis, C. et al. (2014). “Concentrations and fluxes of isoprene and oxygenated VOCs at a French Mediterranean oak forest”. In: *Atmospheric Chemistry and Physics* 14.18, pp. 10085–10102. ISSN: 16807324. DOI: [10.5194/acp-14-10085-2014](https://doi.org/10.5194/acp-14-10085-2014).
- Kerdouci, Jamila, Bénédicte Picquet-Varrault, and Jean François Doussin (2010). “Prediction of rate constants for gas-phase reactions of nitrate radical with organic compounds: A new structure-activity relationship”. In: *ChemPhysChem* 11.18, pp. 3909–3920. ISSN: 14397641. DOI: [10.1002/cphc.201000673](https://doi.org/10.1002/cphc.201000673).
- Kesselmeier, J and M Staudt (1999). “An Overview on Emission, Physiology and Ecology.pdf”. In: *Journal of Atmospheric Chemistry* 33, pp. 23–88. ISSN: 01677764. DOI: [10.1023/A:1006127516791](https://doi.org/10.1023/A:1006127516791). arXiv: 0005074v1 [arXiv:astro-ph]. URL: <https://link-springer-com.ez27.periodicos.capes.gov.br/content/pdf/10.1023/2FA/3A1006127516791.pdf>.
- King, Martin D., Carlos E. Canosa-Mas, and Richard P. Wayne (1999). “A structure-activity relationship (SAR) for predicting rate constants for the reaction of NO₃, OH and O₃ with monoalkenes and conjugated dienes”. In: *Physical Chemistry Chemical Physics* 1.9, pp. 2239–2246. ISSN: 14639076. DOI: [10.1039/a901193e](https://doi.org/10.1039/a901193e).

- Kramer, L. J. et al. (2015). “Seasonal variability of atmospheric nitrogen oxides and non-methane hydrocarbons at the GEOSummit station, Greenland”. In: *Atmospheric Chemistry and Physics* 15.12, pp. 6827–6849. ISSN: 1680-7324. DOI: [10.5194/acp-15-6827-2015](https://doi.org/10.5194/acp-15-6827-2015). URL: <https://acp.copernicus.org/articles/15/6827/2015/>.
- Kroll, Jesse H. and John H. Seinfeld (2008). “Chemistry of secondary organic aerosol: Formation and evolution of low-volatility organics in the atmosphere”. In: *Atmospheric Environment* 42.16, pp. 3593–3624. ISSN: 13522310. DOI: [10.1016/j.atmosenv.2008.01.003](https://doi.org/10.1016/j.atmosenv.2008.01.003).
- Kurpius, Meredith R and Allen H Goldstein (2003). “Gas-phase chemistry dominates ozone loss to a forest, implying a source of aerosols and hydroxyl radicals to the atmosphere”. In: 30.7, pp. 2–5. DOI: [10.1029/2002GL016785](https://doi.org/10.1029/2002GL016785).
- Kwok, Eric S.C. and Roger Atkinson (1995). “Estimation of hydroxyl radical reaction rate constants for gas-phase organic compounds using a structure-reactivity relationship: An update”. In: *Atmospheric Environment* 29.14, pp. 1685–1695. ISSN: 13522310. DOI: [10.1016/1352-2310\(95\)00069-B](https://doi.org/10.1016/1352-2310(95)00069-B).
- Lamb, Brian et al. (1987). “A national inventory of biogenic hydrocarbon emissions”. In: *Atmospheric Environment (1967)* 21.8, pp. 1695–1705. ISSN: 00046981. DOI: [10.1016/0004-6981\(87\)90108-9](https://doi.org/10.1016/0004-6981(87)90108-9). URL: <https://linkinghub.elsevier.com/retrieve/pii/S0004698187901089>.
- Laothawornkitkul, Jullada et al. (2009). “Biogenic volatile organic compounds in the Earth system: Tansley review”. In: *New Phytologist* 183.1, pp. 27–51. ISSN: 0028646X. DOI: [10.1111/j.1469-8137.2009.02859.x](https://doi.org/10.1111/j.1469-8137.2009.02859.x).
- Lee, Anita et al. (2006). “Gas-phase products and secondary aerosol yields from the ozonolysis of ten different terpenes”. In: 111.Ci, pp. 1–18. DOI: [10.1029/2005JD006437](https://doi.org/10.1029/2005JD006437).
- Lee, Lance et al. (2014). *On rates and mechanisms of OH and O₃ reactions with isoprene-derived hydroxy nitrates*. DOI: [10.1021/jp4107603](https://doi.org/10.1021/jp4107603).

- Lerdau, Manuel, Alex Guenther, and Russ Monson (1997). “Plant Production and Emission of Volatile Organic Compounds”. In: *BioScience* 47.6, pp. 373–383. ISSN: 00063568. DOI: [10.2307/1313152](https://academic.oup.com/bioscience/article-lookup/doi/10.2307/1313152). URL: <https://academic.oup.com/bioscience/article-lookup/doi/10.2307/1313152>.
- Lim, Stephen S. et al. (2012). “A comparative risk assessment of burden of disease and injury attributable to 67 risk factors and risk factor clusters in 21 regions, 1990-2010: A systematic analysis for the Global Burden of Disease Study 2010”. In: *The Lancet* 380.9859, pp. 2224–2260. ISSN: 1474547X. DOI: [10.1016/S0140-6736\(12\)61766-8](https://doi.org/10.1016/S0140-6736(12)61766-8).
- Ling, Zhenhao et al. (2019). “Sources of methacrolein and methyl vinyl ketone and their contributions to methylglyoxal and formaldehyde at a receptor site in Pearl River Delta”. In: *Journal of Environmental Sciences* 79, pp. 1–10. ISSN: 10010742. DOI: [10.1016/j.jes.2018.12.001](https://doi.org/10.1016/j.jes.2018.12.001). URL: <https://linkinghub.elsevier.com/retrieve/pii/S1001074218328419>.
- Maria Yanez-Serrano, Ana et al. (2018). “Monoterpene chemical speciation in a tropical rainforest: variation with season, height, and time of day at the Amazon Tall Tower Observatory (ATTO)”. In: *Atmospheric Chemistry and Physics* 18.5, pp. 3403–3418. ISSN: 16807324. DOI: [10.5194/acp-18-3403-2018](https://doi.org/10.5194/acp-18-3403-2018).
- Matsumoto, Jun (2014). “Measuring biogenic volatile organic compounds (BVOCs) from vegetation in terms of ozone reactivity”. In: *Aerosol and Air Quality Research* 14.1, pp. 197–206. ISSN: 16808584. DOI: [10.4209/aaqr.2012.10.0275](https://doi.org/10.4209/aaqr.2012.10.0275).
- Millet, Dylan B. et al. (2005). “Atmospheric volatile organic compound measurements during the Pittsburgh Air Quality Study: Results, interpretation, and quantification of primary and secondary contributions”. In: *Journal of Geophysical Research Atmospheres* 110.7, pp. 1–17. ISSN: 01480227. DOI: [10.1029/2004JD004601](https://doi.org/10.1029/2004JD004601).

- Ortega, John et al. (2007). “Flux estimates and OH reaction potential of reactive biogenic volatile organic compounds (BVOCs) from a mixed northern hardwood forest”. In: 41, pp. 5479–5495. DOI: [10.1016/j.atmosenv.2006.12.033](https://doi.org/10.1016/j.atmosenv.2006.12.033).
- Panopoulou, Anastasia et al. (2020). “Yearlong measurements of monoterpenes and isoprene in a Mediterranean city (Athens): Natural vs anthropogenic origin”. In: *Atmospheric Environment* 243, July, p. 117803. ISSN: 13522310. DOI: [10.1016/j.atmosenv.2020.117803](https://doi.org/10.1016/j.atmosenv.2020.117803). URL: <https://linkinghub.elsevier.com/retrieve/pii/S1352231020305379>.
- Park, Changhyoun, Gunnar W. Schade, and Ian Boedeker (2010). “Flux measurements of volatile organic compounds by the relaxed eddy accumulation method combined with a GC-FID system in urban Houston, Texas”. In: *Atmospheric Environment* 44, 21–22, pp. 2605–2614. ISSN: 13522310. DOI: [10.1016/j.atmosenv.2010.04.016](https://doi.org/10.1016/j.atmosenv.2010.04.016). URL: <http://dx.doi.org/10.1016/j.atmosenv.2010.04.016>.
- Peake, E and H S Sandhu (1983). “The formation of ozone and peroxyacetyl nitrate (PAN) in the urban atmospheres of Alberta”. In: *Canadian Journal of Chemistry* 61, 5, pp. 927–935. ISSN: 0008-4042. DOI: [10.1139/v83-166](https://doi.org/10.1139/v83-166). URL: <http://www.nrcresearchpress.com/doi/10.1139/v83-166>.
- Pfrang, Christian et al. (2006). “Structure–activity relations (SARs) for gas-phase reactions of NO₃, OH and O₃ with alkenes: An update”. In: *Atmospheric Environment* 40, 6, pp. 1180–1186. ISSN: 13522310. DOI: [10.1016/j.atmosenv.2005.09.080](https://doi.org/10.1016/j.atmosenv.2005.09.080). URL: <https://linkinghub.elsevier.com/retrieve/pii/S1352231005009763>.
- Pinto, Delia M. et al. (2007). “The effects of increasing atmospheric ozone on biogenic monoterpene profiles and the formation of secondary aerosols”. In: *Atmospheric Environment* 41, 23, pp. 4877–4887. ISSN: 13522310. DOI: [10.1016/j.atmosenv.2007.02.006](https://doi.org/10.1016/j.atmosenv.2007.02.006). URL: <https://linkinghub.elsevier.com/retrieve/pii/S1352231007001410>.
- Plass-Dülmer, C et al. (2002). “C₂–C₈ Hydrocarbon measurement and quality control procedures at the Global Atmosphere Watch Observatory Hohenpeissenberg”. In: *Journal of*

- Chromatography A* 953.1-2, pp. 175–197. ISSN: 00219673. DOI: [10.1016/S0021-9673\(02\)00128-0](https://doi.org/10.1016/S0021-9673(02)00128-0). URL: <https://linkinghub.elsevier.com/retrieve/pii/S0021967302001280>.
- Pollmann, Jan, John Ortega, and Detlev Helmig (2005). “Analysis of atmospheric sesquiterpenes: Sampling losses and mitigation of ozone interferences”. In: *Environmental Science and Technology* 39.24, pp. 9620–9629. ISSN: 0013936X. DOI: [10.1021/es050440w](https://doi.org/10.1021/es050440w).
- Porter, William C., Sarah A. Safieddine, and Colette L. Heald (2017). “Impact of aromatics and monoterpenes on simulated tropospheric ozone and total OH reactivity”. In: *Atmospheric Environment* 169, pp. 250–257. ISSN: 18732844. DOI: [10.1016/j.atmosenv.2017.08.048](https://doi.org/10.1016/j.atmosenv.2017.08.048).
- Pratt, K. A. et al. (2012). “Contributions of individual reactive biogenic volatile organic compounds to organic nitrates above a mixed forest”. In: *Atmospheric Chemistry and Physics* 12.21, pp. 10125–10143. ISSN: 1680-7324. DOI: [10.5194/acp-12-10125-2012](https://doi.org/10.5194/acp-12-10125-2012). URL: <https://acp.copernicus.org/articles/12/10125/2012/>.
- Pusede, S E et al. (2014). “On the temperature dependence of organic reactivity, nitrogen oxides, ozone production, and the impact of emission controls in San Joaquin Valley, California”. In: 2010, pp. 3373–3395. DOI: [10.5194/acp-14-3373-2014](https://doi.org/10.5194/acp-14-3373-2014).
- Read, K. A. et al. (2009). “Intra-annual cycles of NMVOC in the tropical marine boundary layer and their use for interpreting seasonal variability in CO”. In: *Journal of Geophysical Research Atmospheres* 114.21, pp. 1–14. ISSN: 01480227. DOI: [10.1029/2009JD011879](https://doi.org/10.1029/2009JD011879).
- Sadiq, Mehliyar et al. (2017). “Effects of ozone – vegetation coupling on surface ozone air quality via biogeochemical and meteorological feedbacks”. In: pp. 3055–3066. DOI: [10.5194/acp-17-3055-2017](https://doi.org/10.5194/acp-17-3055-2017).
- Scanlon, J. T. and D. E. Willis (1985). “Calculation of Flame Ionization Detector Relative Response Factors Using the Effective Carbon Number Concept”. In: *Journal of Chromatographic Science* 23.8, pp. 333–340. ISSN: 0021-9665. DOI: [10.1093/chromsci/23](https://doi.org/10.1093/chromsci/23).

8.333. URL: <https://academic.oup.com/chromsci/article-lookup/doi/10.1093/chromsci/23.8.333>.

Schade, Gunnar W. and Allen H. Goldstein (2001). “Fluxes of oxygenated volatile organic compounds from a ponderosa pine plantation”. In: *Journal of Geophysical Research Atmospheres* 106.D3, pp. 3111–3123. ISSN: 01480227. DOI: [10.1029/2000JD900592](https://doi.org/10.1029/2000JD900592).

— (2003). “Increase of monoterpene emissions from a pine plantation as a result of mechanical disturbances”. In: *Geophysical Research Letters* 30.7, pp. 10–13. ISSN: 00948276. DOI: [10.1029/2002GL016138](https://doi.org/10.1029/2002GL016138).

Schade, Gunnar W., Allen H. Goldstein, and Mark S. Lamanna (1999). “Are Monoterpene Emissions influenced by Humidity?” In: *Geophysical Research Letters* 26.14, pp. 2187–2190. ISSN: 00948276. DOI: [10.1029/1999GL900444](https://doi.org/10.1029/1999GL900444).

Shu, Yonghui and Roger Atkinson (1994). “Rate constants for the gas-phase reactions of O₃ with a series of Terpenes and OH radical formation from the O₃ reactions with Sesquiterpenes at 296 ± 2 K”. In: *International Journal of Chemical Kinetics* 26.12, pp. 1193–1205. ISSN: 10974601. DOI: [10.1002/kin.550261207](https://doi.org/10.1002/kin.550261207).

Simpson, Isobel J. et al. (2012). “Long-term decline of global atmospheric ethane concentrations and implications for methane”. In: *Nature* 488.7412, pp. 490–494. ISSN: 00280836. DOI: [10.1038/nature11342](https://doi.org/10.1038/nature11342). URL: <http://dx.doi.org/10.1038/nature11342>.

Stein, Stephen E and Donald R Scott (1994). “ScienceDirect - Journal of the American Society for Mass Spectrometry : Optimization and testing of mass spectral library search algorithms for compound identification”. In: *Journal of the American Society for Mass Spectrometry* 5, pp. 859–866. ISSN: 1044-0305. URL: <http://www.sciencedirect.com/science/article/pii/S1044030594870098>{\%}5Cnpapers2://publication/uuid/4C2DAA2D-87B3-4A05-B306-B1877FBDCA3B.

The Intergovernmental Panel on Climate Change (2013). *Climate Change 2013: The Physical Science basis*, p. 1552. ISBN: 9781107661820.

- Trainer, M et al. (1993). “Correlation of ozone with NO_y in photochemically aged air”. In: 98, pp. 2917–2925.
- U.S. EPA (2012). *Estimation Programs Interface Suite™ for Microsoft® Windows, v 4.11*. URL: <https://www.epa.gov/tsca-screening-tools/epi-suitetm-estimation-program-interface>.
- Wolfe, G. M. and J. A. Thornton (2011). “The Chemistry of Atmosphere-Forest Exchange (CAFE) Model - Part 1: Model description and characterization”. In: *Atmospheric Chemistry and Physics* 11.1, pp. 77–101. ISSN: 16807316. DOI: [10.5194/acp-11-77-2011](https://doi.org/10.5194/acp-11-77-2011).
- Wolfe, G. M. et al. (2011). “The chemistry of atmosphere-forest exchange (CAFE) model-part 2: Application to BEARPEX-2007 observations”. In: *Atmospheric Chemistry and Physics* 11.3, pp. 1269–1294. ISSN: 16807324. DOI: [10.5194/acp-11-1269-2011](https://doi.org/10.5194/acp-11-1269-2011).
- Worton, David R. et al. (2017). *Improved molecular level identification of organic compounds using comprehensive two-dimensional chromatography, dual ionization energies and high resolution mass spectrometry*. DOI: [10.1039/c7an00625j](https://doi.org/10.1039/c7an00625j).
- Yee, Lindsay D. et al. (2018). “Observations of sesquiterpenes and their oxidation products in central Amazonia during the wet and dry seasons”. In: *Atmospheric Chemistry and Physics* 18.14, pp. 10433–10457. ISSN: 16807324. DOI: [10.5194/acp-18-10433-2018](https://doi.org/10.5194/acp-18-10433-2018).
- Zheng, Yiqi et al. (2017). “Drought impacts on photosynthesis, isoprene emission and atmospheric formaldehyde in a mid-latitude forest”. In: 167, pp. 190–201. DOI: [10.1016/j.atmosenv.2017.08.017](https://doi.org/10.1016/j.atmosenv.2017.08.017).
- Zimmerman, P. R. (1979). *Testing of hydrocarbone emissions from vegetation, leaf litter and aquatic surfaces, and development of a methodology for compiling biogenic emissions inventories*. Tech. rep., pp. 1–112. URL: <http://ci.nii.ac.jp/naid/10004472642/en/>.

Chapter 4

Minor contributions of daytime monoterpenes are major contributors to atmospheric reactivity

Deborah F. McGlynn¹, Graham Frazier¹, Laura E.R. Barry², Manuel T. Lerdau^{2,3}, Sally E. Pusede², Gabriel Isaacman-VanWertz¹

¹Civil and Environmental Engineering, Virginia Tech, Blacksburg, VA, 24061, USA

²Department of Environmental Sciences, University of Virginia, Charlottesville, VA, 22904, USA

³Department of Biology, University of Virginia, Charlottesville, VA, 22904, USA

4.1 Abstract

Emissions from natural sources are driven by various external stimuli such as sunlight, temperature, and soil moisture. Once biogenic volatile organic compounds (BVOCs) are emitted into the atmosphere, they rapidly react with atmospheric oxidants, which has significant impacts on ozone and aerosol budgets. However, diurnal, seasonal, and interannual variability of these species are poorly captured in emissions models due to a lack of long-term, speciated measurements. Therefore, increasing the monitoring of these emissions will improve the modeling of ozone and secondary organic aerosol concentrations. Using two years of speciated hourly BVOC data collected at the Virginia Forest Lab, in Fluvanna County,

Virginia, we examine how minor changes in the composition of monoterpenes between seasons are found to have profound impacts on ozone reactivity. The concentration of a range of BVOCs in the summer were found to have two different diurnal profiles, largely driven by temperature- versus light-dependent emissions. Factor analysis was used to separate the two observed diurnal profiles and determine the contribution from each driver. Highly reactive BVOCs were found to have a large influence on atmospheric reactivity in the summer, particularly during the daytime. These findings reveal a need to monitor species with high atmospheric reactivity but have low concentrations and to more accurately capture their emission trends in models.

4.2 Introduction

Biogenically emitted volatile organic compounds (BVOCs) are important precursors for reactions with atmospheric oxidants and secondary organic aerosol (SOA) formation (Atkinson and Arey 2003b; Guenther et al. 1995, 2000; Kroll and Seinfeld 2008). Their emissions are primarily driven by the species of plants present and by changes in temperature and light, with secondary effects of other ecological factors. Light dependent or *de novo* biosynthesis emissions are produced within the leaves of plants and emitted shortly after formation through plant stomata (Niinemets and Monson 2013). These emissions tend to increase with temperature (Guenther 1997; Guenther et al. 2006) but also require light. The dominant *de novo* BVOC emitted is isoprene, though some monoterpenes can be emitted in this manner (Ghirardo et al. 2010; Staudt and Seufert 1995; Taipale et al. 2011; Tingey et al. 1979). In contrast, other emissions occur independently of light from a wide variety of vegetation and therefore occur year-round primarily with a temperature dependence (Ghirardo et al. 2010; Guenther, Monson, and Fall 1991; Niinemets and Monson 2013). Monoterpenes, sesquiterpenes, and diterpenes are largely emitted in a temperature dependent manner through volatilization from storage pools or resin ducts from within the plant

(Lerdau and Gray 2003; Lerdau, Guenther, and Monson 1997; Niinemets and Monson 2013; Zimmerman 1979). The rate of volatilization is determined by the compound's vapor pressure (Lerdau and Gray 2003).

The diurnal concentration profile individual species (i.e., the observed average variability within a 24-hour period) is a function of the drivers of emissions, the concentrations of atmospheric oxidants, and meteorology. For isoprene, which is emitted from plants in a light-dependent manner (Bouvier-Brown et al. 2009; Ghirardo et al. 2010; Guenther, Monson, and Fall 1991; Niinemets and Monson 2013), the diurnal profile is well established and relatively consistent across environments (Delwiche and Sharkey 1993; Guenther et al. 2000; Niinemets and Monson 2013; Rinne et al. 2002). Due to strong daytime emissions, concentrations peak midday to late afternoon, when incoming solar radiation and temperatures are greatest. Nighttime emissions of *de novo* emitted BVOCs drop to near zero due to the lack of light (Ghirardo et al. 2010; Guenther et al. 1996; Niinemets and Monson 2013; Panopoulou et al. 2020; Rinne et al. 2002). Concentrations of *de novo* emitted species concomitantly drop as suspended gases are depleted by atmospheric oxidation.

The diurnal variation of monoterpenes is substantially more variable and complex. Because their emissions are predominantly temperature dependent, emissions peak in the afternoon but continue throughout the night. Consequently, monoterpene concentrations are often greatest during the evening hours (Bouvier-Brown et al. 2009; Hakola et al. 2012; Panopoulou et al. 2020), when oxidation by photochemically formed hydroxyl radicals is minimal and boundary height is reduced, decreasing dilution through atmospheric mixing (Bouvier-Brown et al. 2009; Haapanala et al. 2007; Panopoulou et al. 2020). However, some plants do produce and emit monoterpenes in a light-dependent manner (Guenther et al. 2012; Harley et al. 2014; Staudt et al. 1999; Staudt and Seufert 1995; Taipale et al. 2011; Yu et al. 2017). Despite these findings, light dependent monoterpene emission have largely been deemed to contribute minimally to total monoterpene emissions. (Bouvier-Brown et al.

2009; Lerdau and Gray 2003). This lack of contribution to total flux occurs because they are emitted from only a handful of plant taxa and the emission rates themselves have not been overwhelming (Loreto et al. 1998; Staudt et al. 1999; Staudt and Seufert 1995). Interestingly, a few studies find that many trees emit low levels of monoterpenes in a light dependent manner, and these studies have found that this emission activity is seasonal and changes with phenological patterns. (Fischbach et al. 2002; Ghirardo et al. 2010) (Ghirardo et al. 2010; Steinbrecher et al. 1999; Taipale et al. 2011). Despite representation of light dependent and independent monoterpene emissions, discrepancies exist between this representation and the literature. (Bouvier-Brown et al. 2009; Fischbach et al. 2002; Ghirardo et al. 2010; Guenther et al. 2012; Kesselmeier and Staudt 1999; Rinne et al. 2002; Staudt and Seufert 1995; Steinbrecher et al. 1999; Taipale et al. 2011; Tingey et al. 1979).

The explanation for these discrepancies among studies appears to lie in the fact that for some plant species, e.g., members of the genus *Pinus*, monoterpene emissions are largely not light dependent, though this also tends to vary with season (Harley et al. 2014; Kesselmeier and Staudt 1999; Niinemets et al. 2002). While for other plants species, e.g., *Fagus* and the European live oaks (sub-genus *Cerris*), emissions are largely light dependent (Niinemets and Monson 2013; Schuh et al. 1997). The observed variability appears to be a function of both plant species and terpenes species (Ghirardo et al. 2010; Niinemets et al. 2002; Staudt and Seufert 1995; Steinbrecher et al. 1999). That is, the same terpenoid compound may be light dependent in one species but light independent in another. From the perspective of atmospheric processes, though, the impacts of monoterpenes depend on their absolute fluxes, the timing and control over these fluxes, and their specific reactivities. A major goal of the present work is to understand the potential role that the minor contribution of light dependent emissions and/or individual compounds with differing temporal variability may play in the atmosphere. Certain monoterpenes that are often emitted at low levels and/or in a light dependent manner have extremely high reactivities, raising the question of whether

or not chemical impact may be disproportionate to flux magnitude.

A lack of understanding of how individual compounds are emitted from vegetative sources makes emission modeling difficult and more uncertain. This is largely due to the impact the structure of a BVOC has on its aerosol formation potential and its reaction rates with atmospheric oxidants, particularly for reactions involving ozone. For example, endocyclic monoterpenes (e.g., limonene and 3-carene) and sesquiterpenes (e.g., α -humulene and β -caryophyllene) have a greater aerosol formation potential and tend to react faster than compounds with exocyclic double bonds (e.g. α -pinene, α -cedrene). Consequently, long-term measurements of speciated BVOCs can assist in modeling BVOC emissions and in understanding their contribution to ozone modulation and SOA formation (Porter, Safieddine, and Heald 2017). These impacts extend further to the importance of individual fast-reacting isomers, which can represent substantial fractions of total reactivity even at low concentrations (Yee et al. 2018). In this context, a detailed understanding of the different drivers of isomer emissions and the temporal variability of composition is critical for interpreting such data.

Using two years of chemically resolved concentration measurements of in-canopy, biogenic volatile organic compound (BVOC) concentration data, we examine the contribution of individual monoterpene compounds to ozone reactivity on diurnal, seasonal, and interannual timescales. We elucidate the impact of temporal variability on ozone reactivity on scales from hours to years by identifying two varying components in the data, which we identify as coming from light dependent and independent emissions and quantifying their chemical impacts on each timescale. Factor analysis is used to quantitatively separate these observed profiles and their contributions to total monoterpene concentration and ozone reactivity. Our findings highlight the need to better understand the drivers of emissions with isomer-level chemical resolution and improve their representation in emissions models as they have significant atmospheric impact.

4.3 Methods

4.3.1 Data collection and preparation

We measured in-canopy BVOC concentrations at the Virginia Forest Research Lab (VFRL) (37.9229 °N, 78.2739 °W) in Fluvanna County, Virginia. The VFRL sits on the east side of the Blue Ridge Mountains and is about 25 km east-southeast of Charlottesville, VA. The site houses a 40-meter meteorological tower, with a climate-controlled, internet-connected lab at the bottom that is supplied by line power. The BVOC concentrations were measured using a gas chromatography flame ionization detector (GC-FID) adapted for automated collection and analysis of air samples from mid-canopy (~ 20 m) of the VFRL. Additional details pertaining to the measurement location, instrument operation, and data analyses can be seen in McGlynn et al. (2021). To identify analytes in the samples, a mass spectrometer (MS, Agilent 5977) was deployed in October 2019, September 2020, and June 2021 in parallel with the FID. Retention times of analytes detected by the two detectors were aligned using the retention time of known analytes. Analytes were identified by mass spectral matching with the 2011 NIST MS Library and reported retention indices (Mass Spectrometry Data Center, NIST, 2022). The chromatographic data were analysed using the freely-available TERN software packaged by Isaacman-VanWertz et al. (2017) within the Igor Pro 8 programming environment (Wavemetrics, Inc.). The measurement period included in this work extends from September 15, 2019, to September 14, 2021. This work presents all isoprene and monoterpene data collected during the measurement period but focuses largely on the monoterpenes between the months of May-September.

4.3.2 Positive Matrix Factorization

Positive matrix factorization (PMF) has been widely used for source apportionment problems (Kuang et al. 2015; Norris et al. 2014; Ulbrich et al. 2009). A large number of variables

can be reduced by the PMF algorithm to the main sources or factors that drive the observed variability (Norris et al. 2014). Application of PMF to multi-variable data generates two matrices, the factor contributions and factor profiles (Norris et al. 2014), which for environmental data represent timeseries as a set of covarying variables (e.g., chemical species).

This work employed EPA’s PMF 5.0 program to support the identification in the observational data of two apparent sources or drivers of BVOC concentration variability. Specifically, a two-factor PMF solution was examined to better understand and quantify the profiles and temporal variability of each observed factor. The two years of monoterpene data were run separately (“2020”: September 15th, 2019-September 14th, 2020, and “2021”: September 15th, 2020- September 14th, 2021), with uncertainty, u , in the data calculated using the equation provided by (Norris et al. 2014):

$$u = \sqrt{(0.15 \times \text{concentration})^2 + (0.5 \times MDL)^2} \quad (4.1)$$

The method detection limit, MDL, is 2.2 ppt for monoterpenes (McGlynn et al. 2021). Values below the method detection limit were substituted with MDL/2 in both the concentration and uncertainty file. Missing data are excluded from the data processing (Norris et al. 2014). Factor contributions are returned from the PMF program as normalized values, which are converted to concentration by multiplying returned values by the sum of the concentrations of species in the factor profiles.

4.3.3 Ozone reactivity calculations

Reactivity of an individual BVOC with ozone (O_3R) is calculated as the sum of the products of the concentration and oxidation reaction rate of each BVOC, i :

$$O_3R_{tot}(s^{-1}) = \sum (k_{O_3+BVOC_i} [BVOC_i]) \quad (4.2)$$

All rate constants (units: $\text{cm}^3 \text{ molec}^{-1} \text{ s}^{-1}$) used in this work listed in Table D.1 (Atkinson et al. 2006; Atkinson and Arey 2003a; Atkinson, Aschmann, and Arey 1990; Pinto et al. 2007; Pratt et al. 2012; Shu and Atkinson 1994). A temperature of 298 K is assumed for all rate constants, representing the approximate midpoint between day and night temperatures in the summer at this site, which vary by roughly 10°C (McGlynn et al. 2021). Taking the temperature dependence of rate constants into account would increase daytime OH reactivity by 5-8%, and decrease nighttime OH reactivity by approximately the same amount (National Institute for Standards and Technology 2019). These differences suggest the true difference between the light dependent (daytime) and light independent (nighttime) mixtures is $\sim 10\%$ higher than calculated, but this effect is not included quantitatively because temperature dependence is not known for many of monoterpene reaction rates.

4.4 Results and discussion

At the Virginia Forest Research Lab, concentrations of a wide range of species, including anthropogenic and other VOCs, are measured hourly. The BVOCs measured include isoprene, methyl vinyl ketone, methacrolein, 11 monoterpenes, and 2 sesquiterpenes. This work focuses primarily on monoterpenes, which contribute the dominant fraction of speciated ozone reactivity from BVOCs (McGlynn et al. 2021) at the research site throughout the year.

4.4.1 Monoterpene seasonality

To understand the drivers of monoterpene variability, we first examine diurnal and seasonal patterns in two monoterpenes found at the site, α -pinene and limonene, that exhibit features of two different concentration profiles. Seasonal averages are defined as: December, January, and February (Winter); March, April, May (Spring); June, July, August (Summer); and September, October, November (Fall). Diurnal trends in these species demonstrate some

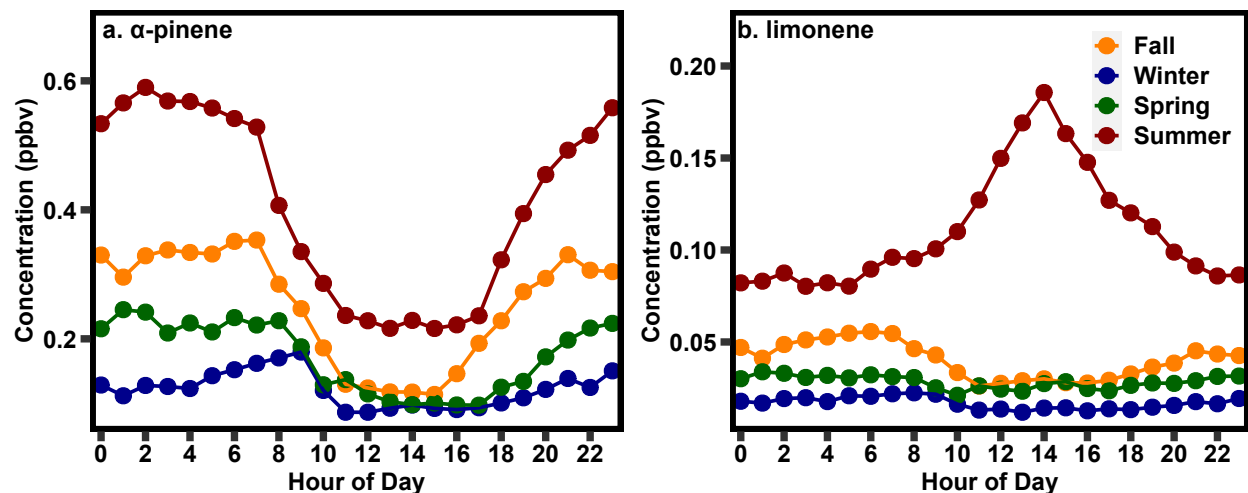


Figure 4.1 The mean (a) α -pinene and (b) limonene concentration in the four seasons of the northern hemisphere between September 2019 and September 2021.

clear differences in their concentration patterns (Figure 4.1). α -pinene concentrations were lowest in the daytime winter hours at about 0.05 ppb and highest in the evening summer hours, at 0.60 ppb. In all seasons, α -pinene concentrations were highest at night and decreased in the morning hours, following “typical” patterns of temperature-driven monoterpene concentrations (Bouvier-Brown et al. 2009) due to the higher planetary boundary layer and increased concentrations of oxidants during the day. Concentrations were lowest in the middle of the day, between 10:00 and 17:00 and highest between 20:00 and 8:00 (Figure 4.1a). Concentrations transitions between these periods vary somewhat by season in accordance with the changing temperature and daylight hours of a subtropical climate zone.

In contrast, while limonene concentrations were similarly lowest in the daytime winter hours, at 0.01 ppb, they were highest during the daytime summer hours, at 0.2 ppb. In fall, winter, and spring, limonene exhibited the same seasonality as α -pinene with daytime lows and night-time highs, though with weaker diurnal variability (Figure 4.1b). In summer, however, diurnal trends in limonene concentrations are very different, with a peak in the mid to late afternoon. To reach daytime peaks in concentration, daytime emissions of limonene

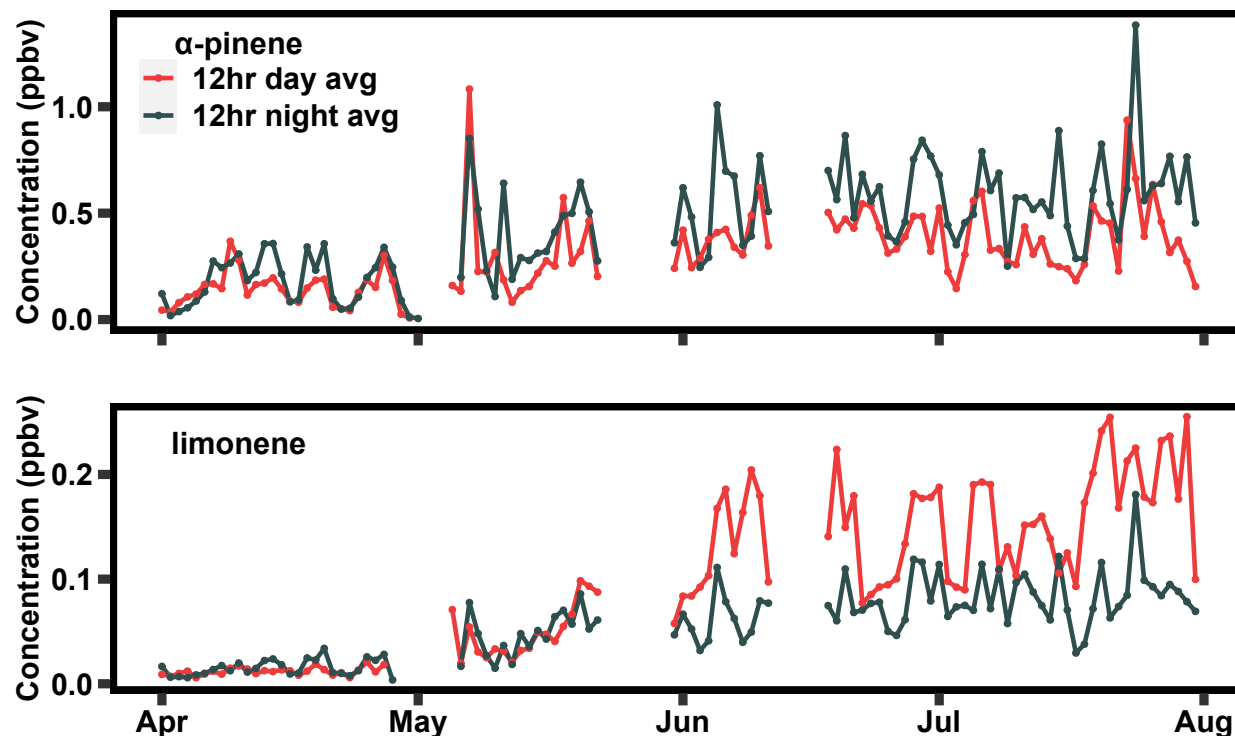


Figure 4.2 The 12-hour average of α -pinene and limonene between April 2021 and August 2021. The averaging period for each compound was between 7 AM and 7 PM.

must be high, particularly given that the reaction rate of limonene with OH radical, ozone, and nitrate is 3, 2.3, and 1.3 times as fast, respectively, as those of α -pinene.

The seasonal rise and fall in the observed daytime peak of limonene, in contrast to the relative stability of α -pinene, is apparent in a spring/summertime comparison of daytime (7AM - 7PM) and night-time (7PM - 7AM) average concentrations (Figure 4.2). The full two-year time series of this plot can be found in the supplemental document (Figure D.1). As observed in the diurnal profiles, α -pinene evening concentrations are higher than daytime concentrations throughout the year; while concentrations increase in the summer, this increase is observed in both daytime and nighttime concentrations (Figure 4.2a). In contrast, while concentrations of limonene are highest at night throughout the early spring, concentrations begin to peak in the daytime in late-May (Figure 4.2b). From late-May

through mid-September, concentrations are highest during the day, suggesting a strong daytime source of limonene specifically in the summer, which may be co-emitted with other monoterpenes but is not a strong feature for α -pinene. The daytime peak in limonene is unique to summer and occurs in both years (Figures 4.1, 4.2, and D.1). Interestingly, while the daytime peak in summer is relatively consistent across years, nighttime concentrations of limonene in the summer area substantially lower in 2021 compared to 2020 (Figure D.1), suggesting sources for daytime and nighttime limonene that differ in their interannual variation. However, additional years of data are likely necessary to better understand the driver of this interannual variability. We demonstrate below that the timing of the rise and fall of the strong daytime source of limonene correlates with concentrations of isoprene, a known *de novo* emitted BVOC species, and appears to be a component of a set of light-dependent monoterpene emissions.

4.4.2 Light dependent and light independent monoterpene concentration

To better characterize the observed light-dependent monoterpenes and quantify their impacts, the observed patterns in monoterpenes were deconvolved as two factors using PMF. The determined factors demonstrate a clear separation between a set of monoterpenes that exhibit only nighttime peaks in concentration, and a set of compounds that exhibit a tendency to have high daytime concentrations. Quantitative assessment of the uncertainty of the two-factor solution is performed using bootstrapping, in which 100 runs are performed using arbitrary subsets of data; 95% of bootstrap runs reproduce both factors (Table D.2) with no unmapped base factors. An unmapped base factor indicates that one or more bootstrap runs did not correlate with a determined factor from the base model run (Norris et al. 2014). The Pearson correlation coefficient threshold used for this analysis was the EPA PMF default value of 0.6 (Norris et al. 2014).

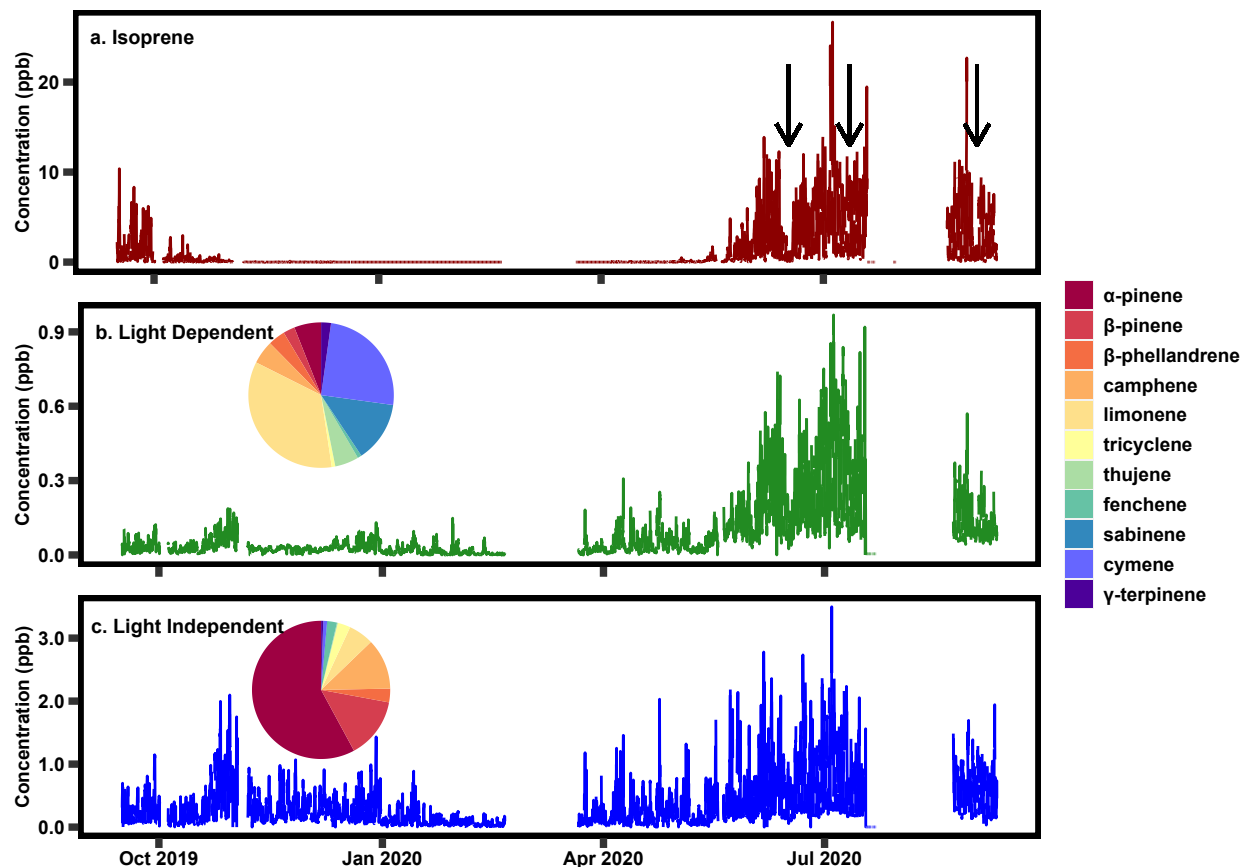


Figure 4.3 Time series of isoprene concentration, the two positive matrix factorization factors between September 2019 and September 2020 and the breakdown of the monoterpene species that contribute to each factor.

A “light dependent” factor is present primarily during the summer, characterized by daytime peaks that roughly coincide with the seasonality and variability of isoprene (Figure 4.3, results from 2020 shown, results from 2021 in Figure D.1). This factor even mirrors transient decreases in concentrations observed in isoprene, such as those observed in June 2020, July 2020, and September 2020, denoted with black arrows in Figure 4.3a, b. The largest contributor to the light dependent factor is limonene (roughly one-third), followed by cymene, sabinene, and a relatively small contribution from α -pinene, denoted by the pie charts above each factor time series. A table indicating the percent contribution for the species in each factor can be found in Table D.1. A more dominant factor contains most

of the α - and β -pinene and exhibits a diurnal pattern and seasonality more in line with what is typical for temperature-driven monoterpenes; this factor is referred to as “light independent” to distinguish it and because the dominant biogenic emission model (MEGAN) distinguishes between emission pathways as light dependent (i.e., *de novo*) vs. independent (i.e., temperature-driven volatilization from stored pools) (Guenther et al. 2012). Interpretation of factors is further supported by their diurnal trends, a representative sample of which is shown in Figure 4.4. The light dependent factor peaks mid-day, following a similar temporal pattern as isoprene. We infer these monoterpenes to be emitted through similar processes as isoprene and attribute them to *de novo* emissions. In contrast, the higher-concentration monoterpene factor peaks in the evening to early morning hours, following more typical monoterpene diurnal patterns. We attribute these monoterpene concentrations to temperature-driven light independent emissions of monoterpenes.

Overall, the light dependent factor accounts for $\sim 25\%$ of summertime monoterpene concentration, but at times the light dependent factor may contribute significantly or even dominate concentrations due to their differing diurnal variability in emissions. Interestingly, greater than 85% of the most dominant monoterpenes, including α -pinene, β -pinene, tricyclene, fenchene, and camphene are found almost entirely in the light independent factor (Table 4.1). Conversely greater than 85% of cymene, sabinene, and thujene are found in the light dependent factor (Table 4.1). A small number of species are more split, with larger percentages of their concentrations attributed to light dependent emissions than light independent emission in the summer months. These species include, β -phellandrene, limonene, and γ -terpinene (Table 4.1).

4.4.3 Ozone and OH reactivity

Despite the low contribution of the light dependent factor to total monoterpene concentration, this factor has a large impact on ozone and OH reactivity. Comparing the stacked

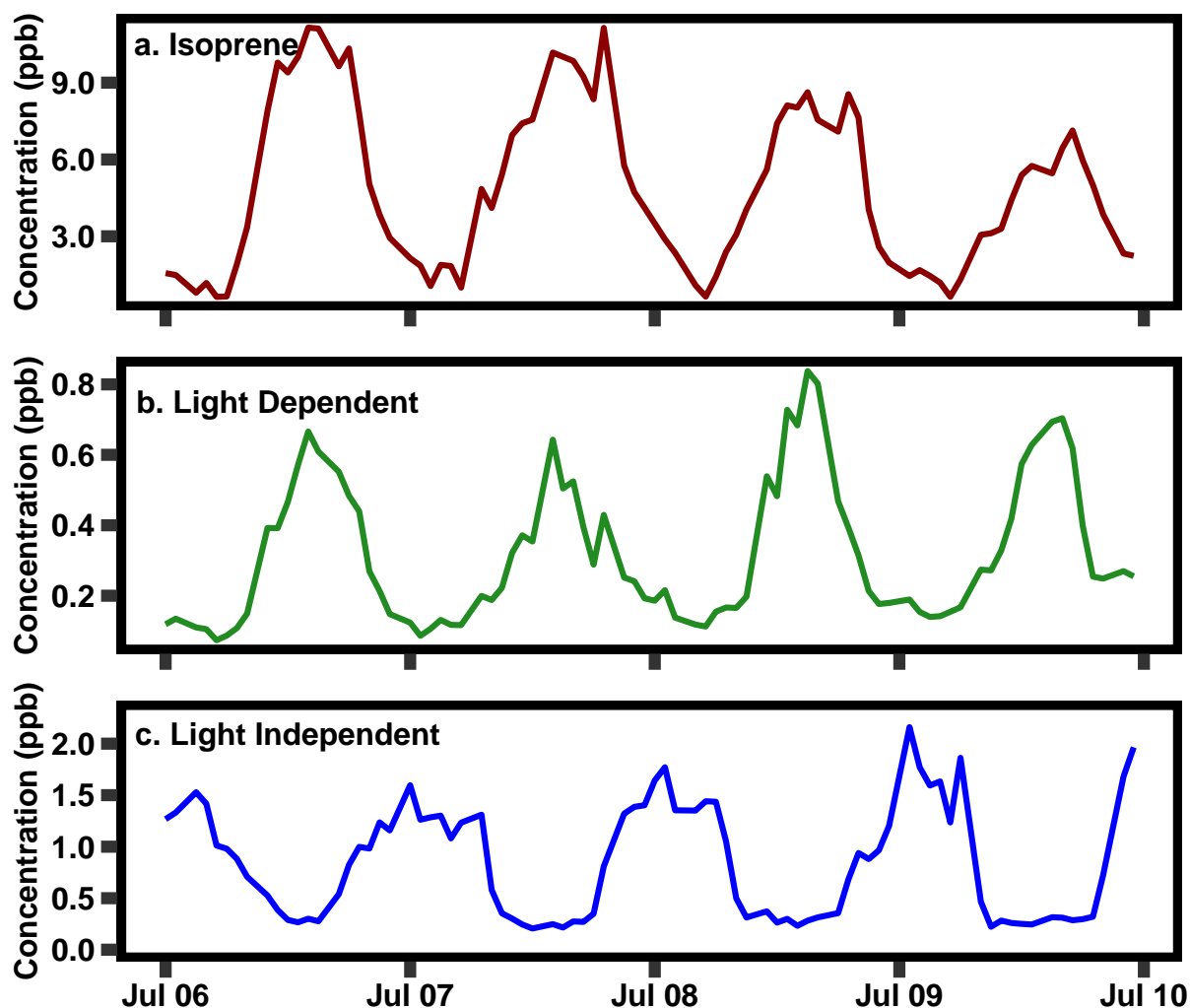


Figure 4.4 A four-day period in July 2020 of isoprene, and the two PMF factors (Light Dependent and Light Independent).

diurnal concentration profile (Fig. 4.5a) to the stacked ozone and OH reactivity diurnal profile (Fig. 4.5b, c) in summer illuminate's clear differences in their variability. While the concentration profile shows that the majority of species peak at night, there is a slight increase in the middle of the day, owing to the contribution from light dependent emissions. When this profile is multiplied by respective reaction rate constant for each species and oxidant, there is a clear mid-day peak that prevails as the dominant contributor to ozone and OH reactivity in the summer. Further, the largest contributor to total ozone and OH

Table 4.1 Percent of concentrations attributed to de novo and pool emissions by compound for 2019-2020

compound	Annual		Summer	
	% LIF	% LDF	% LIF	% LDF
α -pinene	97.7	2.3	96.6	3.4
β -pinene	96.1	3.9	94.2	5.8
tricyclene	94.3	5.7	91.8	8.2
fenchene	92.1	7.9	88.6	11.4
camphene	91.0	9.0	87.2	12.8
β -phellandrene	78.9	21.1	71.5	28.5
γ -terpinene	48.5	51.5	38.6	61.4
limonene	43.0	57.0	33.5	66.5
thujene	14.6	85.4	10.2	89.8
cymene	14.0	86.0	9.8	90.2
sabinene	0.0	100.0	0.0	100.0

reactivity is limonene despite its lower contribution to total concentration due to its high reaction rate with each atmospheric oxidant.

A majority of the highly reactive isomer limonene is associated with light dependent monoterpenes (57%), while the more dominant α -pinene concentrations are almost entirely attributed to pool emissions (98%) Table 4.1. Sabinene is also notable contributor to the light dependent mixture, contributing approximately 30% to concentration, 25% to ozone reactivity, and 33% to OH reactivity; it is not found in the light independent mixture. The major contribution of limonene and sabinene to the light dependent monoterpene mixture makes light driven emissions particularly reactive, with a reaction rate roughly 1.5 times that of the light independent mixture for both ozone and OH reactivity. This daytime peak has an enormous impact on daytime ozone and OH reactivity (Fig. 4.5e, f), such that calculated summertime ozone and OH reactivity consequently have little diurnal pattern and is roughly uniform throughout the day (average: $1.4\text{-}2.4 \times 10^{-6} \text{ s}^{-1}$ for ozone reactivity and $1\text{-}2 \text{ s}^{-1}$ for OH reactivity) during the summer months. Even in the summer, when concentrations of light dependent monoterpenes are highest, the diurnal profile of the total

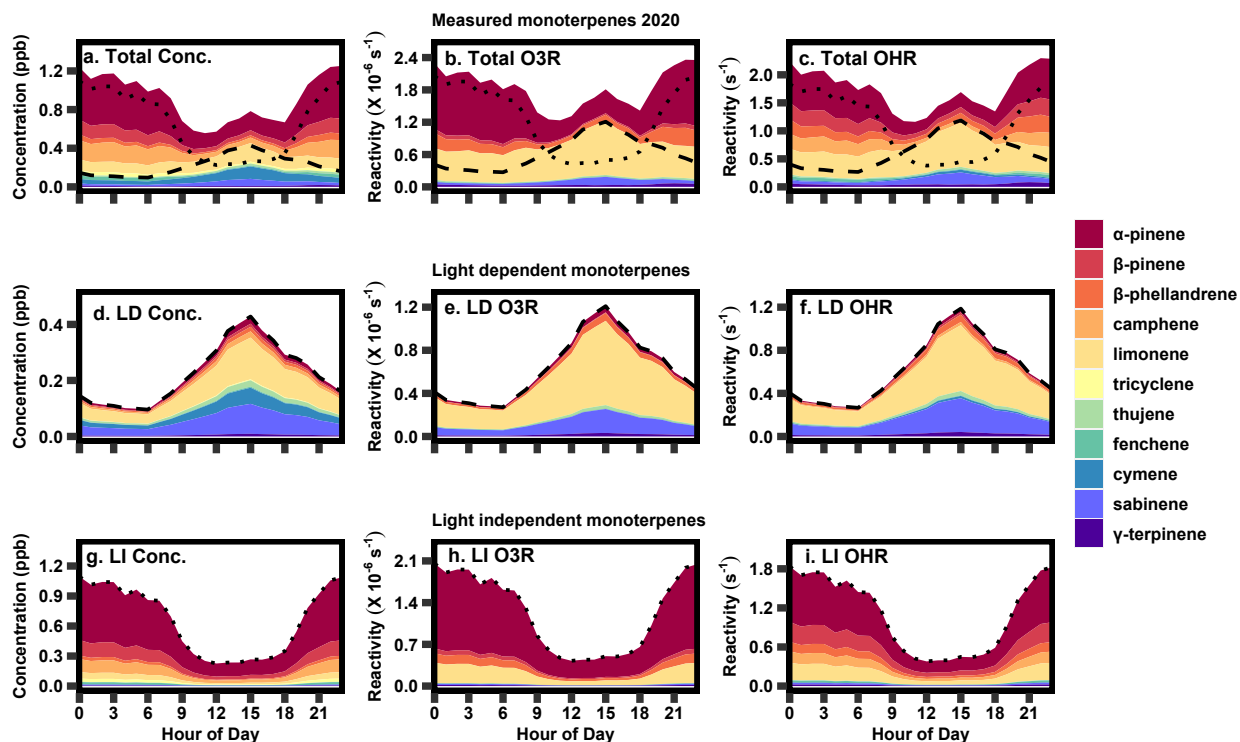


Figure 4.5 The 2020 summer diurnal profile of (a) measured concentration, (b) calculated monoterpene ozone reactivity and (c) OH reactivity, as well as light dependent(LD) (d) concentrations, (e) ozone reactivity, and (f) OH reactivity, and light independent (LI) (g) concentration, (h) ozone reactivity, (i) OH reactivity.

monoterpene chemical class (Figure 4.5a) roughly follows that of α -pinene (Figure 4.5a) with only moderate daytime concentrations. However, this average profile is a combination of a night-time peak dominated by light independent compounds (Figure 4.5g) and a daytime peak dominated by light dependent compounds (Figure 4.5d). Consequently, understanding light dependent monoterpenes is critical, not only to better characterize the carbon cycle and predict long-term trends, but also because it has immediate and substantial impacts on the atmospheric oxidant budget in the summer that would be overlooked when considering monoterpenes as a bulk compound class.

4.5 Conclusion

Using two years of hourly speciated BVOC concentrations collected at a meteorological tower in Central Virginia, we identify and quantify diurnal and seasonal variability of monoterpenes and isoprene. Though a majority of monoterpene concentrations exhibit temporal behaviour expected from pool emissions whose flux rates are independent of light, we identify a minor (in mass terms) contribution from monoterpenes with seasonality and diurnal variability that show a strong light dependence and resemble *de novo* emissions. These light dependent monoterpene emissions are strongest in the summer, where they contribute $\sim 25\%$ to total monoterpene concentrations, with smaller contributions in other seasons. However, the minor contribution to total monoterpene mass belies their major impact on ozone and OH reactivity. Due to differences in the temporal variability of the two monoterpene classes and the significantly higher reaction rates of the light dependent mixture, we observe high ozone and OH reactivity in the summer daytime that is not well captured by bulk monoterpene concentration. This reactivity is dominated by limonene, which contributes $\sim 80\%$ and $\sim 65\%$ to light dependent sourced ozone and OH reactivity and $\sim 20\%$ to light independent sourced ozone and OH reactivity. In a changing climate, these BVOC emission sources may vary. For example, drought may decrease vegetative growth which could increase per-unit-leaf-area in emissions for stored (i.e., light independent) monoterpenes, even as canopy leaf area declines (Funk, Mak, and Lerdau 2004; Lewinsohn et al. 1993). But, increased precipitation can decrease photosynthesis, causing a decrease in *de novo* (i.e., light dependent) emissions (Funk, Mak, and Lerdau 2004; Lewinsohn et al. 1993). These findings highlight the need for speciated long-term monitoring studies with a focus on capturing low concentration but highly reactive species.

A significant implication of this work is that the unique drivers of each monoterpene isomer challenge our ability to view this class monolithically or simplify its variability. Mea-

surement studies focused on total BVOC classes may be sufficient to gain an understanding of total BVOC concentrations but demonstrate a need for isomer-resolved understanding of oxidant reactivity. For example, while this work supports the general conclusion that light dependent monoterpenes are a minor component (reflected in current emission models (Guenther et al. 2012) and supported by measurement studies (Bouvier-Brown et al. 2009; Davison et al. 2009; Kesselmeier and Staudt 1999; Niinemets et al. 2002; Rinne et al. 2002; Taipale et al. 2011; Tingey et al. 1979), the composition and temporal variability of light dependent monoterpenes, as well as their high per-molecule reactivity, drive strong atmospheric impacts. It is clear that drivers of limonene emissions are particularly critical for understanding this ecosystem (see also McGlynn et al. (2021)). Capturing the detail of this or any monoterpene in emissions models is difficult, as the light dependent fraction depends on plant species and other ecological variables, but it is clear there is some disconnect between the results here and dominant models that, for example, estimate α -pinene as more strongly light dependent than limonene (Guenther et al. 2012) and do not tend to vary light dependent fraction by plant function type. Small gaps such as these in our understanding of what drives monoterpene emissions may lead to significant uncertainty in models or outcomes. Furthermore, oxidation of these compounds ultimately leads to SOA formation, but the impacts on this process of the different long- and short-term temporal trends of each isomer is difficult to assess. It is clear from existing literature that SOA yields vary significantly by isomer and are dependent on structure (Faiola et al. 2018; Friedman and Farmer 2018; Lee et al. 2006; Lim and Ziemann 2009). Consequently, we anticipate that light dependent and independent monoterpenes vary in their average SOA yields, and the seasonal and interannual variability observed in this work has significant regional impacts on aerosol loadings. Unfortunately, these differences are difficult to quantify, with previous studies even disagreeing on whether α -pinene or limonene has a higher SOA yield (Faiola et al. 2018; Friedman and Farmer 2018). Enhanced monitoring of BVOC concentrations

and emissions needs to be supplemented by improved chemically-resolved measurements of SOA concentrations and formation processes in order to enhance our understanding of the contribution of these emissions to SOA mass loadings.

4.6 Acknowledgements

This research was funded by the National Science Foundation (AGS 1837882 and AGS 1837891). Tower maintenance and operation was supported in part by the Pace Endowment. D.F.M. and L.E.R.B. were supported in part by Virginia Space Grant Consortium Graduate Research Fellowships. The authors gratefully acknowledge the assistance of Koong Yi, and Bradley Sutliff in their support in upkeep and maintenance of the instrument at Pace Tower.

4.7 References

- Atkinson, R. et al. (2006). “Evaluated kinetic and photochemical data for atmospheric chemistry: Volume II – gas phase reactions of organic species”. In: *Atmospheric Chemistry and Physics* 6.11, pp. 3625–4055. ISSN: 1680-7324. DOI: [10.5194/acp-6-3625-2006](https://doi.org/10.5194/acp-6-3625-2006). URL: <https://acp.copernicus.org/articles/6/3625/2006/>.
- Atkinson, Roger and Janet Arey (2003a). “Atmospheric Degradation of Volatile Organic Compounds”. In: *Chemical Reviews* 103.12, pp. 4605–4638. ISSN: 0009-2665. DOI: [10.1021/cr0206420](https://doi.org/10.1021/cr0206420). URL: <https://pubs.acs.org/doi/10.1021/cr0206420>.
- (2003b). “Gas-phase tropospheric chemistry of biogenic volatile organic compounds: A review”. In: *Atmospheric Environment* 37.SUPPL. 2, pp. 197–219. ISSN: 13522310. DOI: [10.1016/S1352-2310\(03\)00391-1](https://doi.org/10.1016/S1352-2310(03)00391-1).
- Atkinson, Roger, Sara M Aschmann, and Janet Arey (1990). *Rate constants for the gas-phase reactions of OH and NO₃ Radicals and O₃ with sabinene and camphene*.
- Bouvier-Brown, N. C. et al. (2009). “In-situ ambient quantification of monoterpenes, sesquiterpenes, and related oxygenated compounds during BEARPEX 2007: implications for gas-

- and particle-phase chemistry”. In: *Atmospheric Chemistry and Physics* 9.15, pp. 5505–5518. ISSN: 1680-7324. DOI: [10.5194/acp-9-5505-2009](https://doi.org/10.5194/acp-9-5505-2009). URL: <https://acp.copernicus.org/articles/9/5505/2009/>.
- Davison, B. et al. (2009). “Concentrations and fluxes of biogenic volatile organic compounds above a Mediterranean Macchia ecosystem in western Italy”. In: *Biogeosciences* 6.8, pp. 1655–1670. ISSN: 17264189. DOI: [10.5194/bg-6-1655-2009](https://doi.org/10.5194/bg-6-1655-2009).
- Delwiche, C. F. and T. D. Sharkey (1993). “Rapid appearance of ^{13}C in biogenic isoprene when $^{13}\text{CO}_2$ is fed to intact leaves”. In: *Plant, Cell and Environment* 16.5, pp. 587–591. ISSN: 0140-7791. DOI: [10.1111/j.1365-3040.1993.tb00907.x](https://doi.org/10.1111/j.1365-3040.1993.tb00907.x). URL: <https://onlinelibrary.wiley.com/doi/10.1111/j.1365-3040.1993.tb00907.x>.
- Faiola, C. L. et al. (2018). “Terpene Composition Complexity Controls Secondary Organic Aerosol Yields from Scots Pine Volatile Emissions”. In: *Scientific Reports* 8.1, pp. 1–13. ISSN: 20452322. DOI: [10.1038/s41598-018-21045-1](https://doi.org/10.1038/s41598-018-21045-1).
- Fischbach, Robert Josef et al. (2002). “Seasonal pattern of monoterpene synthase activities in leaves of the evergreen tree *Quercus ilex*”. In: *Physiologia Plantarum* 114.3, pp. 354–360. ISSN: 00319317. DOI: [10.1034/j.1399-3054.2002.1140304.x](https://doi.org/10.1034/j.1399-3054.2002.1140304.x). URL: <http://doi.wiley.com/10.1034/j.1399-3054.2002.1140304.x>.
- Friedman, Beth and Delphine K. Farmer (2018). “SOA and gas phase organic acid yields from the sequential photooxidation of seven monoterpenes”. In: *Atmospheric Environment* 187. January, pp. 335–345. ISSN: 18732844. DOI: [10.1016/j.atmosenv.2018.06.003](https://doi.org/10.1016/j.atmosenv.2018.06.003). URL: <https://doi.org/10.1016/j.atmosenv.2018.06.003>.
- Funk, J. L., J. E. Mak, and M. T. Lerdau (2004). “Stress-induced changes in carbon sources for isoprene production in *Populus deltoides*”. In: *Plant, Cell and Environment* 27.6, pp. 747–755. ISSN: 0140-7791. DOI: [10.1111/j.1365-3040.2004.01177.x](https://doi.org/10.1111/j.1365-3040.2004.01177.x). URL: <https://onlinelibrary.wiley.com/doi/10.1111/j.1365-3040.2004.01177.x>.

- Ghirardo, Andrea et al. (2010). “Determination of de novo and pool emissions of terpenes from four common boreal/alpine trees by ^{13}C CO₂ labelling and PTR-MS analysis”. In: *Plant, Cell & Environment* 33.5, pp. 781–792. ISSN: 01407791. DOI: [10.1111/j.1365-3040.2009.02104.x](https://doi.org/10.1111/j.1365-3040.2009.02104.x). URL: <https://onlinelibrary.wiley.com/doi/10.1111/j.1365-3040.2009.02104.x>.
- Guenther, A. et al. (1996). “Leaf, branch, stand and landscape scale measurements of volatile organic compound fluxes from U.S. woodlands”. In: *Tree Physiology* 16.1-2, pp. 17–24. ISSN: 0829318X. DOI: [10.1093/treephys/16.1-2.17](https://doi.org/10.1093/treephys/16.1-2.17).
- Guenther, A. B. et al. (2012). “The model of emissions of gases and aerosols from nature version 2.1 (MEGAN2.1): An extended and updated framework for modeling biogenic emissions”. In: *Geoscientific Model Development* 5.6, pp. 1471–1492. ISSN: 1991959X. DOI: [10.5194/gmd-5-1471-2012](https://doi.org/10.5194/gmd-5-1471-2012).
- Guenther, Alex (1997). “Seasonal and spatial variations in natural volatile organic compound emissions”. In: *Ecological Applications* 7.1, pp. 34–45. ISSN: 10510761. DOI: [10.1890/1051-0761](https://doi.org/10.1890/1051-0761).
- Guenther, Alex et al. (1995). “A global model of natural volatile organic compound emissions”. In: *J. Geophys. Res.* 100.94, pp. 8873–8892.
- Guenther, Alex et al. (2000). “Natural emissions of non-methane volatile organic compounds, carbon monoxide, and oxides of nitrogen from North America”. In: 34.
- Guenther, Alex et al. (2006). “Estimates of global terrestrial isoprene emissions using MEGAN (Model of Emissions of Gases and Aerosols from Nature)”. In: DOI: [10.5194/acp-6-3181-2006](https://doi.org/10.5194/acp-6-3181-2006).
- Guenther, Alex B., Russell K. Monson, and Ray Fall (1991). “Isoprene and monoterpene emission rate variability: Observations with eucalyptus and emission rate algorithm development”. In: *Journal of Geophysical Research* 96.D6, p. 10799. ISSN: 0148-0227. DOI: [10.1029/91jd00960](https://doi.org/10.1029/91jd00960).

- Haapanala, S. et al. (2007). “Boundary layer concentrations and landscape scale emissions of volatile organic compounds in early spring”. In: *Atmospheric Chemistry and Physics* 7.7, pp. 1869–1878. ISSN: 16807324. DOI: [10.5194/acp-7-1869-2007](https://doi.org/10.5194/acp-7-1869-2007).
- Hakola, H. et al. (2012). “In situ measurements of volatile organic compounds in a boreal forest”. In: *Atmospheric Chemistry and Physics* 12.23, pp. 11665–11678. ISSN: 1680-7324. DOI: [10.5194/acp-12-11665-2012](https://doi.org/10.5194/acp-12-11665-2012). URL: <https://acp.copernicus.org/articles/12/11665/2012/>.
- Harley, Peter et al. (2014). “Observations and models of emissions of volatile terpenoid compounds from needles of ponderosa pine trees growing in situ: Control by light, temperature and stomatal conductance”. In: *Oecologia* 176.1, pp. 35–55. ISSN: 00298549. DOI: [10.1007/s00442-014-3008-5](https://doi.org/10.1007/s00442-014-3008-5).
- Isaacman-VanWertz, Gabriel et al. (2017). “Automated single-ion peak fitting as an efficient approach for analyzing complex chromatographic data”. In: *Journal of Chromatography A* 1529, pp. 81–92. ISSN: 0021-9673. DOI: [10.1016/j.chroma.2017.11.005](https://doi.org/10.1016/j.chroma.2017.11.005). URL: <http://dx.doi.org/10.1016/j.chroma.2017.11.005>.
- Kesselmeier, J and M Staudt (1999). “An Overview on Emission, Physiology and Ecology.pdf”. In: *Journal of Atmospheric Chemistry* 33, pp. 23–88. ISSN: 01677764. DOI: [10.1023/A:1006127516791](https://doi.org/10.1023/A:1006127516791). arXiv: 0005074v1 [arXiv:astro-ph]. URL: <https://link-springer-com.ez27.periodicos.capes.gov.br/content/pdf/10.1023/2FA/3A1006127516791.pdf>.
- Kroll, Jesse H. and John H. Seinfeld (2008). “Chemistry of secondary organic aerosol: Formation and evolution of low-volatility organics in the atmosphere”. In: *Atmospheric Environment* 42.16, pp. 3593–3624. ISSN: 13522310. DOI: [10.1016/j.atmosenv.2008.01.003](https://doi.org/10.1016/j.atmosenv.2008.01.003).
- Kuang, B Y et al. (2015). “Sources of humic-like substances in the Pearl River Delta, China: positive matrix factorization analysis of PM2.5 major components and source markers”. In: *Atmospheric Chemistry and Physics* 15.4, pp. 1995–2008. ISSN: 1680-7324. DOI: [10.5194/acp-15-1995-2008](https://doi.org/10.5194/acp-15-1995-2008).

5194/acp-15-1995-2015. URL: <https://acp.copernicus.org/articles/15/1995/2015/>.

Lee, Anita et al. (2006). “Gas-phase products and secondary aerosol yields from the ozonolysis of ten different terpenes”. In: 111.Ci, pp. 1–18. DOI: [10.1029/2005JD006437](https://doi.org/10.1029/2005JD006437).

Lerdau, Manuel and Dennis Gray (2003). “Ecology and evolution of light-dependent and light-independent phytogenic volatile organic carbon”. In: *New Phytologist* 157.2, pp. 199–211. ISSN: 0028-646X. DOI: [10.1046/j.1469-8137.2003.00673.x](https://doi.org/10.1046/j.1469-8137.2003.00673.x). URL: <https://onlinelibrary.wiley.com/doi/10.1046/j.1469-8137.2003.00673.x>.

Lerdau, Manuel, Alex Guenther, and Russ Monson (1997). “Plant Production and Emission of Volatile Organic Compounds”. In: *BioScience* 47.6, pp. 373–383. ISSN: 00063568. DOI: [10.2307/1313152](https://doi.org/10.2307/1313152). URL: <https://academic.oup.com/bioscience/article-lookup/doi/10.2307/1313152>.

Lewinsohn, Efraim et al. (1993). “Oleoresinosis in Grand Fir (*Abies grandis*) Saplings and Mature Trees (Modulation of this Wound Response by Light and Water Stresses)”. In: *Plant Physiology* 101.3, pp. 1021–1028. ISSN: 0032-0889. DOI: [10.1104/pp.101.3.1021](https://doi.org/10.1104/pp.101.3.1021). URL: <https://academic.oup.com/plphys/article/101/3/1021-1028/6066090>.

Lim, Yong B. and Paul J. Ziemann (2009). “Effects of Molecular Structure on Aerosol Yields from OH Radical-Initiated Reactions of Linear, Branched, and Cyclic Alkanes in the Presence of NO_x”. In: *Environmental Science & Technology* 43.7, pp. 2328–2334. ISSN: 0013-936X. DOI: [10.1021/es803389s](https://doi.org/10.1021/es803389s). URL: <https://pubs.acs.org/doi/10.1021/es803389s>.

Loreto, Francesco et al. (1998). “On the monoterpene emission under heat stress and on the increased thermotolerance of leaves of *Quercus ilex* L. fumigated with selected monoterpenes”. In: *Plant, Cell and Environment* 21.1, pp. 101–107. ISSN: 01407791. DOI: [10.1046/j.1365-3040.1998.00268.x](https://doi.org/10.1046/j.1365-3040.1998.00268.x).

- McGlynn, Deborah F. et al. (2021). “Measurement report: Variability in the composition of biogenic volatile organic compounds in a Southeastern US forest and their role in atmospheric reactivity”. In: *Atmospheric Chemistry and Physics* 21.20, pp. 15755–15770. ISSN: 1680-7324. DOI: [10.5194/acp-21-15755-2021](https://doi.org/10.5194/acp-21-15755-2021). URL: <https://acp.copernicus.org/articles/21/15755/2021/>.
- National Institute for Standards and Technology (2019). *NIST Chemical Kinetics Database*. URL: <https://kinetics.nist.gov/kinetics/index.jsp> (visited on 05/05/2020).
- Niinemets, Ülo and Russell K. Monson, eds. (2013). *Biology, Controls and Models of Tree Volatile Organic Compound Emissions*. Vol. 5. Tree Physiology. Dordrecht: Springer Netherlands. ISBN: 978-94-007-6605-1. DOI: [10.1007/978-94-007-6606-8](https://doi.org/10.1007/978-94-007-6606-8). URL: <http://link.springer.com/10.1007/978-94-007-6606-8>http://link.springer.com/10.1007/978-94-007-6606-8{_}16.
- Niinemets, Ülo et al. (2002). “Stomatal constraints may affect emission of oxygenated monoterpenoids from the foliage of *Pinus pinea*”. In: *Plant Physiology* 130.3, pp. 1371–1385. ISSN: 00320889. DOI: [10.1104/pp.009670](https://doi.org/10.1104/pp.009670).
- Norris, Gary et al. (2014). *EPA positive matrix factorization (PMF) 5.0 fundamentals and user guide*. US Environmental Protection Agency EPA/600/R-14/108, pp. 1–136.
- Panopoulou, Anastasia et al. (2020). “Yearlong measurements of monoterpenes and isoprene in a Mediterranean city (Athens): Natural vs anthropogenic origin”. In: *Atmospheric Environment* 243.July, p. 117803. ISSN: 13522310. DOI: [10.1016/j.atmosenv.2020.117803](https://doi.org/10.1016/j.atmosenv.2020.117803). URL: <https://linkinghub.elsevier.com/retrieve/pii/S1352231020305379>.
- Pinto, Delia M. et al. (2007). “The effects of increasing atmospheric ozone on biogenic monoterpene profiles and the formation of secondary aerosols”. In: *Atmospheric Environment* 41.23, pp. 4877–4887. ISSN: 13522310. DOI: [10.1016/j.atmosenv.2007.02.006](https://doi.org/10.1016/j.atmosenv.2007.02.006). URL: <https://linkinghub.elsevier.com/retrieve/pii/S1352231007001410>.

- Porter, William C., Sarah A. Safieddine, and Colette L. Heald (2017). “Impact of aromatics and monoterpenes on simulated tropospheric ozone and total OH reactivity”. In: *Atmospheric Environment* 169, pp. 250–257. ISSN: 18732844. DOI: [10.1016/j.atmosenv.2017.08.048](https://doi.org/10.1016/j.atmosenv.2017.08.048).
- Pratt, K. A. et al. (2012). “Contributions of individual reactive biogenic volatile organic compounds to organic nitrates above a mixed forest”. In: *Atmospheric Chemistry and Physics* 12.21, pp. 10125–10143. ISSN: 1680-7324. DOI: [10.5194/acp-12-10125-2012](https://doi.org/10.5194/acp-12-10125-2012). URL: <https://acp.copernicus.org/articles/12/10125/2012/>.
- Rinne, H. J.I. et al. (2002). “Isoprene and monoterpene fluxes measured above Amazonian rainforest and their dependence on light and temperature”. In: *Atmospheric Environment* 36.14, pp. 2421–2426. ISSN: 13522310. DOI: [10.1016/S1352-2310\(01\)00523-4](https://doi.org/10.1016/S1352-2310(01)00523-4).
- Schuh, G. et al. (1997). “Emissions of volatile organic compounds from Sunflower and Beech: dependence on temperature and light intensity”. In: *Journal of Atmospheric Chemistry* 27, pp. 291–318. DOI: [10.1023/A:1005850710257](https://doi.org/10.1023/A:1005850710257).
- Shu, Yonghui and Roger Atkinson (1994). “Rate constants for the gas-phase reactions of O₃ with a series of Terpenes and OH radical formation from the O₃ reactions with Sesquiterpenes at 296 ± 2 K”. In: *International Journal of Chemical Kinetics* 26.12, pp. 1193–1205. ISSN: 10974601. DOI: [10.1002/kin.550261207](https://doi.org/10.1002/kin.550261207).
- Staudt, M. et al. (1999). “Seasonal Variation in Amount and Composition of Monoterpenes Emitted by Young Pinus pinea Trees – Implications for Emission Modeling”. In: *Plant, Cell and Environment* 35, pp. 77–99. ISSN: 0140-7791. DOI: <https://doi.org/10.1023/A:1006233010748>.
- Staudt, Michael and Guenther Seufert (1995). “Light-dependent Emission of Monoterpenes by Holm Oak (*Quercus ilex* L.)” In: 2, pp. 89–92.
- Steinbrecher, R. et al. (1999). “A revised parameterisation for emission modelling of isoprenoids for boreal plants”. In: *Air Pollution research report* 70.3, pp. 29–44.

- Taipale, R et al. (2011). “Role of de novo biosynthesis in ecosystem scale monoterpene emissions from a boreal Scots pine forest”. In: *Biogeosciences* 8.8, pp. 2247–2255. ISSN: 1726-4189. DOI: [10.5194/bg-8-2247-2011](https://doi.org/10.5194/bg-8-2247-2011). URL: <https://bg.copernicus.org/articles/8/2247/2011/>.
- Tingey, David T. et al. (1979). “The Influence of Light and Temperature on Isoprene Emission Rates from Live Oak”. In: *Physiologia Plantarum* 47.2, pp. 112–118. ISSN: 0031-9317. DOI: [10.1111/j.1399-3054.1979.tb03200.x](https://doi.org/10.1111/j.1399-3054.1979.tb03200.x). URL: <https://onlinelibrary.wiley.com/doi/10.1111/j.1399-3054.1979.tb03200.x>.
- Ulbrich, I M et al. (2009). “Interpretation of organic components from Positive Matrix Factorization of aerosol mass spectrometric data”. In: *Atmospheric Chemistry and Physics* 9.9, pp. 2891–2918. ISSN: 1680-7324. DOI: [10.5194/acp-9-2891-2009](https://doi.org/10.5194/acp-9-2891-2009). URL: <https://acp.copernicus.org/articles/9/2891/2009/>.
- Yee, Lindsay D. et al. (2018). “Observations of sesquiterpenes and their oxidation products in central Amazonia during the wet and dry seasons”. In: *Atmospheric Chemistry and Physics* 18.14, pp. 10433–10457. ISSN: 16807324. DOI: [10.5194/acp-18-10433-2018](https://doi.org/10.5194/acp-18-10433-2018).
- Yu, Haofei et al. (2017). “Airborne measurements of isoprene and monoterpene emissions from southeastern U.S. forests”. In: *Science of the Total Environment* 595, pp. 149–158. ISSN: 18791026. DOI: [10.1016/j.scitotenv.2017.03.262](https://doi.org/10.1016/j.scitotenv.2017.03.262).
- Zimmerman, P. R. (1979). *Testing of hydrocarbon emissions from vegetation, leaf litter and aquatic surfaces, and development of a methodology for compiling biogenic emissions inventories*. Tech. rep., pp. 1–112. URL: <http://ci.nii.ac.jp/naid/10004472642/en/>.

Chapter 5

Conclusions

Biogenic volatile organic compounds widely vary in their physical and chemical properties, which has implications for both the ozone budget and secondary organic aerosol composition. Furthermore, the VOC composition of a particular region will heavily depend on emission sources, which for BVOCs, depend on vegetative composition. Therefore, increased monitoring and the use of instrumentation that can successfully capture a range of species at normal atmospheric concentrations is vital to understanding the role of these compounds in the atmosphere and in how their impact will vary in a changing climate. This dissertation focused on three objectives to improve our understanding of the role of BVOCs in the atmosphere. These include:

1. The development and validation of an automated, online, gas-chromatography flame ionization detector for detection of atmospheric volatile organic compounds across the volatility range of most BVOC classes.
2. Increase our understanding of atmospheric reactivity of BVOC species and how it varies intra-annually.
3. Understand the biological drivers of diurnal, seasonal, and interannual changes in BVOC concentrations and their impacts on atmospheric reactivity.

A major advance of this work is to provide a detailed description and validation of a gas chromatograph/flame ionization detector for remote and automated monitoring of VOCs

ranging from volatile to semi-volatile, which provides a foundation for broadening the availability of these data. The instrument was deployed for two years in a forest in central Virginia, with the data collected made publicly available for the use of future researchers. In this work we have gained significant new insights in the impacts of BVOCs on the local and regional atmospheric chemistry. While isoprene is an important compound for atmospheric reactivity due to its high atmospheric concentration in the summer, monoterpenes are the main compound class reacting with atmospheric oxidants in the other 9 months of the year. Furthermore, monoterpenes are also a dominant reactant in the summer months, accounting for 50% of reactivity with ozone and nitrate. There is also high temporal variability in the importance of individual monoterpenes throughout the year. These findings highlight the importance of long term monitoring individual compounds at high temporal resolution. Additional data sets such as the one developed here can be used to inform emission and atmospheric composition models.

5.1 Outcomes of objective 1

Adaptation of a GC-FID for remote monitoring of VOCs

A gas chromatography flame ionization detector was adapted for automated sampling and analysis through the use of a newly developed sample trap by Aerosol Dynamics. The use of this trap allowed for the collection of volatile species such as pentane and isoprene without sample cooling. In this work we also developed a specialized electronics box and labview software program to interface with the GC-FID, which enabled the system to run every hour without user interaction. This work then outlines additional developments in data transfer and chromatogram integration to mitigate the time required to analyze the amount of data collected by an automated GC. Finally, we provide suggestions to mitigate downtime of the instrument to enable future replication while limiting potential setbacks.

We deployed this instrument for two years at a meteorological tower in central Virginia. In

this work, we provide an overview of the hardware components, sample flow, and electronic box components as well as the instrument stability over a 4 month period and discuss the calibration methods.

5.2 Outcomes of objective 2

The role of biogenic volatile organic compounds in atmospheric reactivity intra-annually

In this work, we use the BVOC data collected from the first year of sampling in the canopy of a forest representative of the Southeastern U.S. The use of an automated GC-FID adapted to collect air samples made it possible to do long-term collection of BVOCs in an unmonitored location.

We have gained a greater understanding of the seasonality of the major BVOC classes. Isoprene was found to be important for OH reactivity in the summer, but monoterpenes were found to be an important BVOC class for ozone and nitrate reactivities year round and for OH reactivity outside of the summer months. Given the importance of monoterpenes, this class was investigated on a species specific basis. 11 monoterpenes are detected at the site year-round with α -pinene being the most dominant species. A few species with lower mixing ratios but high reactivities (particularly limonene and β -phellandrene) were found to be important contributors to atmospheric reactivity. This finding highlights the importance of structure and concentration in assessing the impact of VOCs on atmospheric composition.

5.3 Outcomes of objective 3

Understanding the biological drivers of diurnal, seasonal, and interannual changes in BVOC concentrations and their impacts on atmospheric reactivity.

In this work we have increased our understanding of diurnal, seasonal, and interannual variability of BVOC concentrations at the VFL. This work was done using two years of hourly speciated BVOC concentrations collected at the VFL to quantify diurnal and seasonal vari-

ability of monoterpenes and isoprene. We identified minor contributors to monoterpene mass as being major contributors to atmospheric reactivity. Many very reactive monoterpenes have seasonality and diurnal variability that resemble *de novo* emissions. This emission source is strongest in the summer, where it contributes 25% to total monoterpene concentrations. However, the reactivity of some species in the mixture (i.e. limonene, sabinene) is a major contributor to ozone and OH reactivity. As such, we observe high ozone and OH reactivity in the summer daytime that is not well captured by bulk monoterpene concentration. These findings highlight the need for speciated monitoring studies with a focus on capturing low concentration but highly reactive species. Comparing this work to the representation of light dependent emissions in BVOC emission models identified a differences that may lead to uncertainty in models.

5.4 Recommendations for future work

From this work, we improved our understanding of BVOC composition and determined their reactivity with atmospheric oxidants at a site in Southeastern US. We found that some lower concentration species are important for reactivity. To better understand how these and other compounds impact SOA formation or ozone budgets would require collection of BVOC emissions. Emission data would enable improved understanding of the impact of these compounds on an ecosystem scale and facilitate the quantification of the impact of these emissions on SOA formation. However, collection of BVOC emissions requires additional resources. Therefore, if emission data is not available, the collected concentration data could still be used to check or improve current emission (MEGAN) and chemical models (F0AM) (Guenther et al. 2012; Wolfe et al. 2016). This would be done through the calculation of BVOC emissions using MEGAN and available leaf area index and meteorological data. The calculated emission data could then be propagated through F0AM to get BVOC concentrations. The results could be compared to the observational concentration

data. Work such as this could identify possible improvements of such models.

This work included two years of BVOC monitoring, and interannual variability was notable. With only two years of data, it was not possible to determine the mechanistic processes behind the observed variability. Additional years of data and investigations into the cause of the variability would assist in understanding the impact of meteorological and ecological drivers and improve our understanding of climate changes on a per variable basis. For example, drought may decrease vegetative growth which could increase per-unit-leaf-area in emissions for stored monoterpenes, even as canopy leaf area declines. But, increased precipitation can decrease photosynthesis, causing a decrease in *de novo* emissions.

In this work, we identified the impact of light dependent emissions on reactivity. Knowing this, it would be useful to understand the biologic source of the emissions. Determining the source of the emissions could assist models such as MEGAN in better representing light dependent emissions given that this model considers vegetative composition in its calculations.

Appendices

Appendix A

Supplemental Information for

Chapter 2

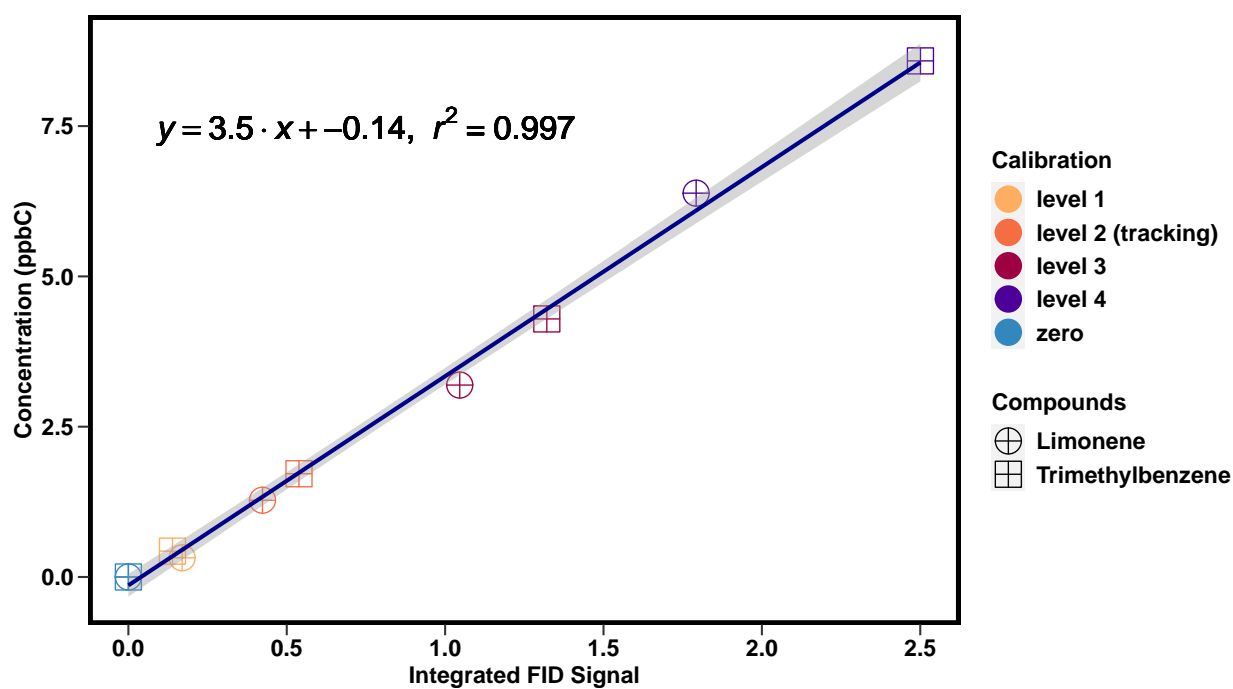


Figure A.1 A linear regression plot between the integrated FID signal and the calibrant concentration for one-week of Limonene and TMB calibrations. The shading represents the standard error (3.5 ± 0.07) of the residuals to account for the uncertainty of the slope of the linear regression. Colors represent different calibration levels (i.e., different dilution flows) and symbols represent calibrants.

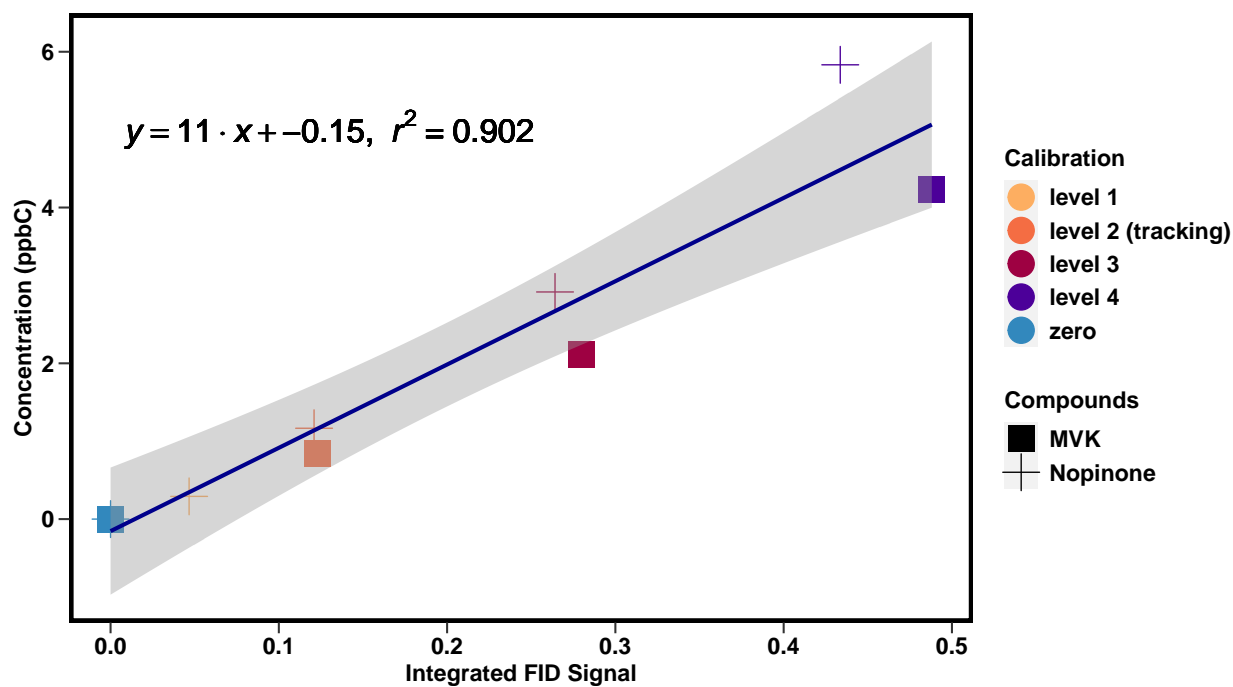


Figure A.2 A linear regression plot between the integrated FID signal and the calibrant concentration for one-week of MVK and Nopinone calibrations. The shading represents the standard error (11 ± 1.3) of the residuals to account for the uncertainty of the slope of the linear regression. Colors represent different calibration levels (i.e., different dilution flows) and symbols represent calibrants.

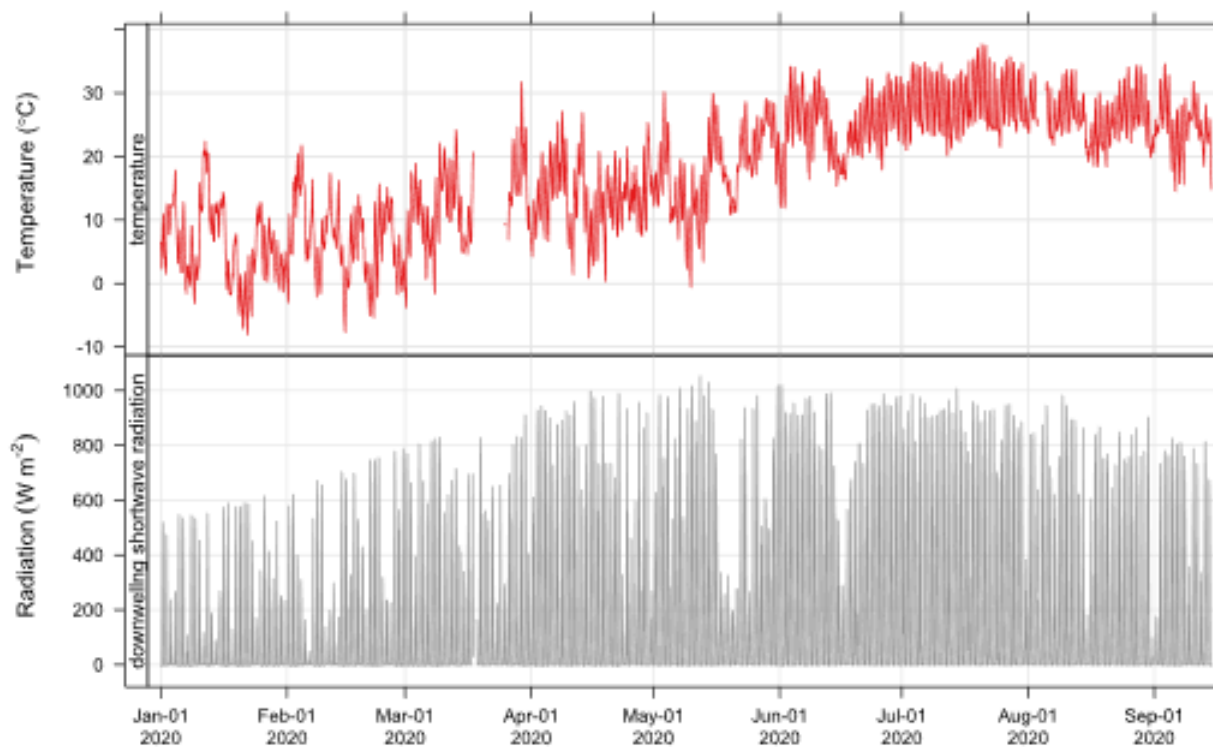
Appendix B

Supplemental Information for

Chapter 3

Table B.1 Composition and pure concentration of the multi-component calibrant

Compound	Concentration (ppbv)
Pentane	15.40
Isoprene	40.30
Methyl Vinyl Ketone	17.50
Hexane	9.96
Benzene	15.00
α -Pinene	17.60
1,3,5-Trimethylbenzne	12.40
Limonene	8.30
Nopinone	8.92
α -Cedrene	4.35
α -Humulene	4.40

Figure B.1 Ambient temperature ($^{\circ}\text{C}$) and downwelling shortwave radiation (W m^{-2}) for January 1st 2020 – September 15th, 2020.

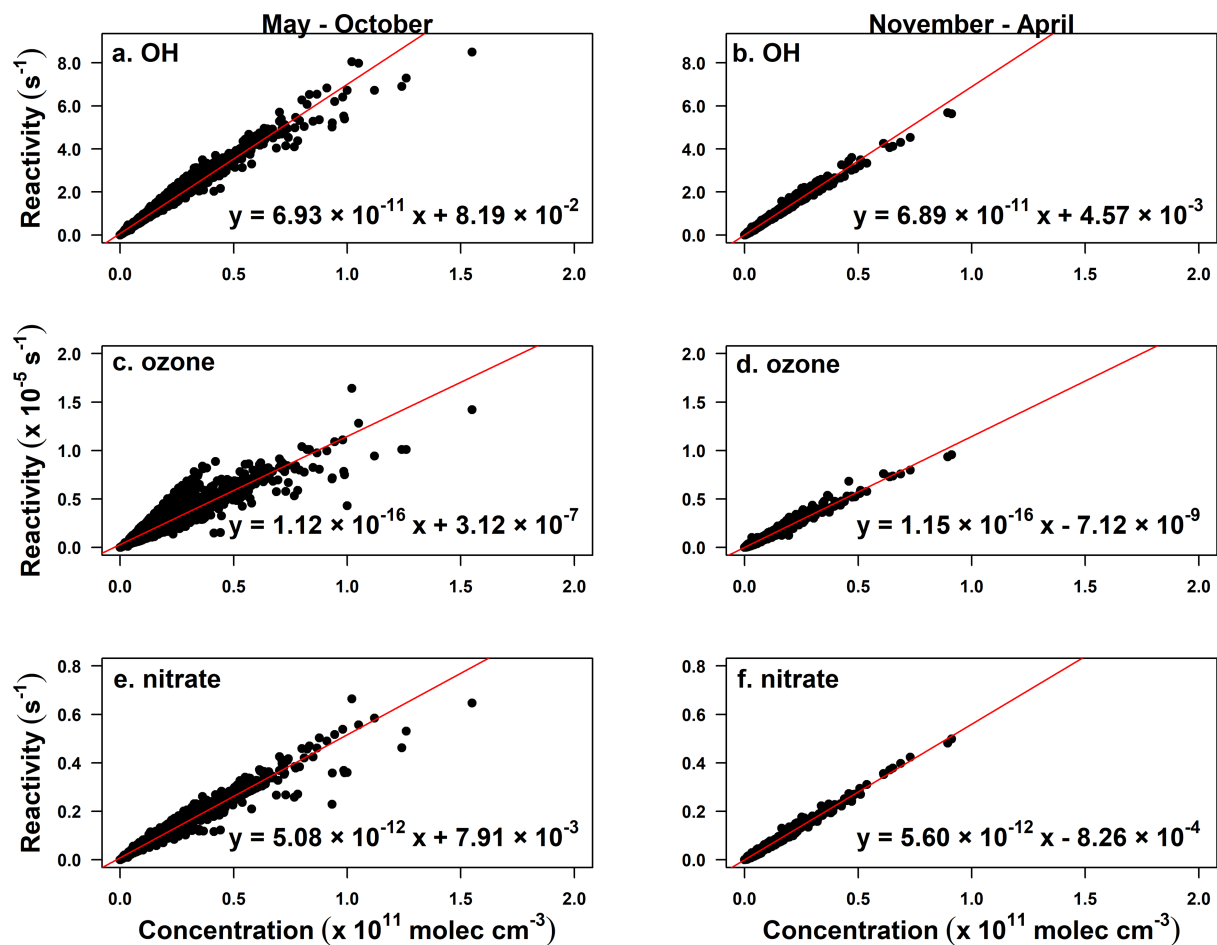


Figure B.2 Concentration plotted against reactivity to yield the rate constant for OH (a-b), Ozone (c-d), nitrate (e-f) in the growing and non-growing season. The slope in each equation is the average reaction rate of each oxidant with total monoterpenes.

Appendix C

Figures associated with the updated
ozone reaction rate constant with
limonene in chapter 3

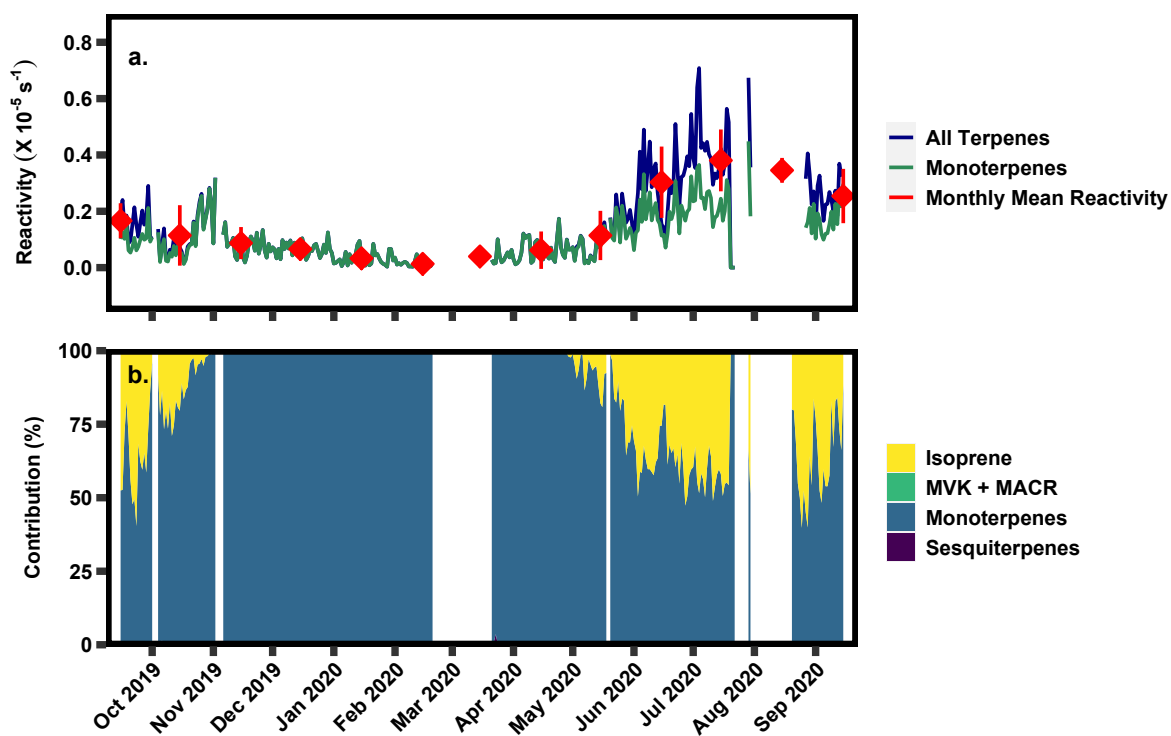


Figure C.1 (a) Timeseries of 24-hour averaged calculated ozone reactivity of all terpene classes and the monoterpene class, as well as the monthly mean of calculated ozone reactivity. (b) Relative contribution of each of the BVOC classes to ozone reactivity.

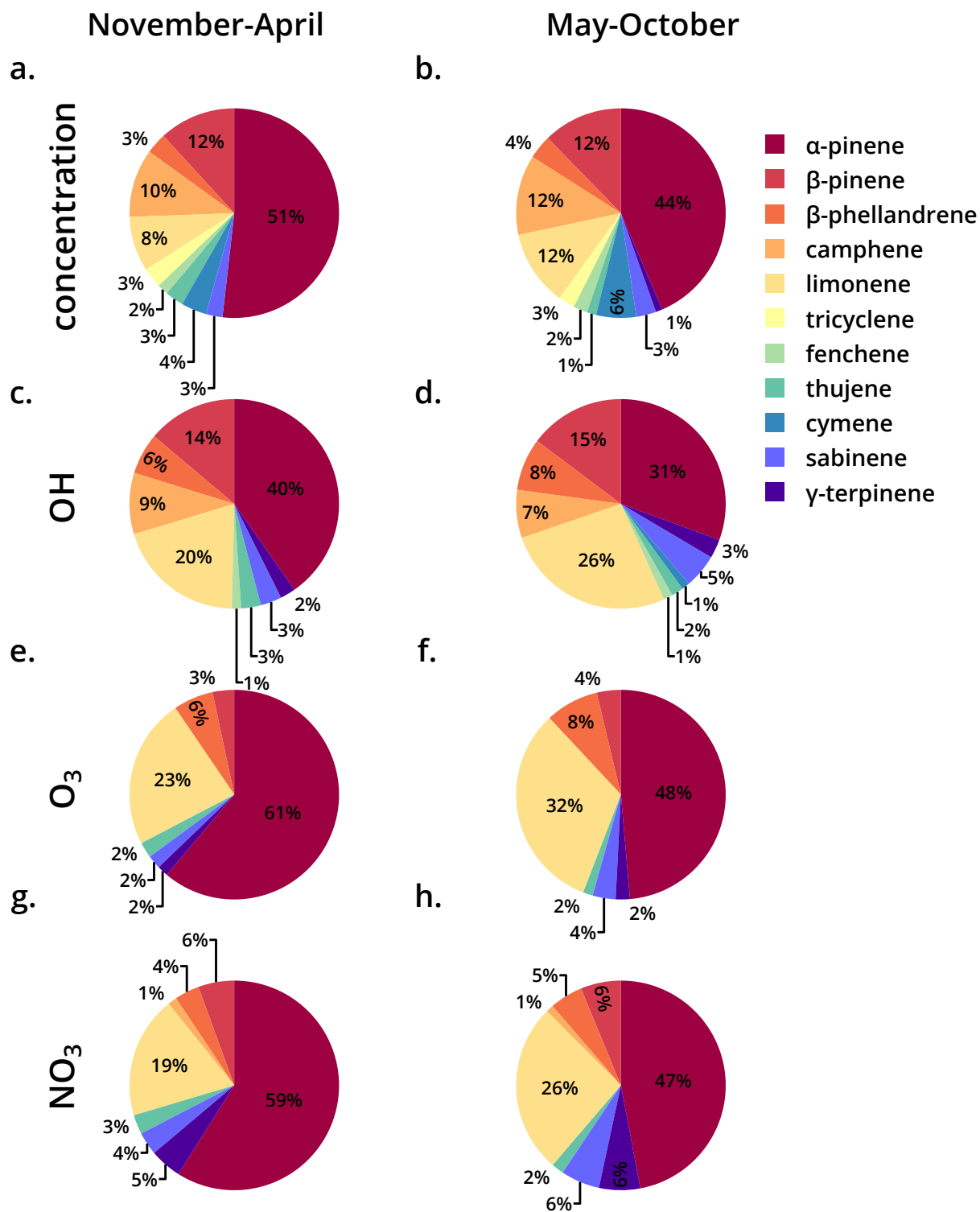


Figure C.2 A breakdown of detected monoterpene isomers in the growing and non-growing seasons for (a-b) concentration, (c-d) OH reactivity, (e-f) ozone reactivity, (g-h) nitrate reactivity. Values are rounded to the nearest percent and values below 1% are not depicted

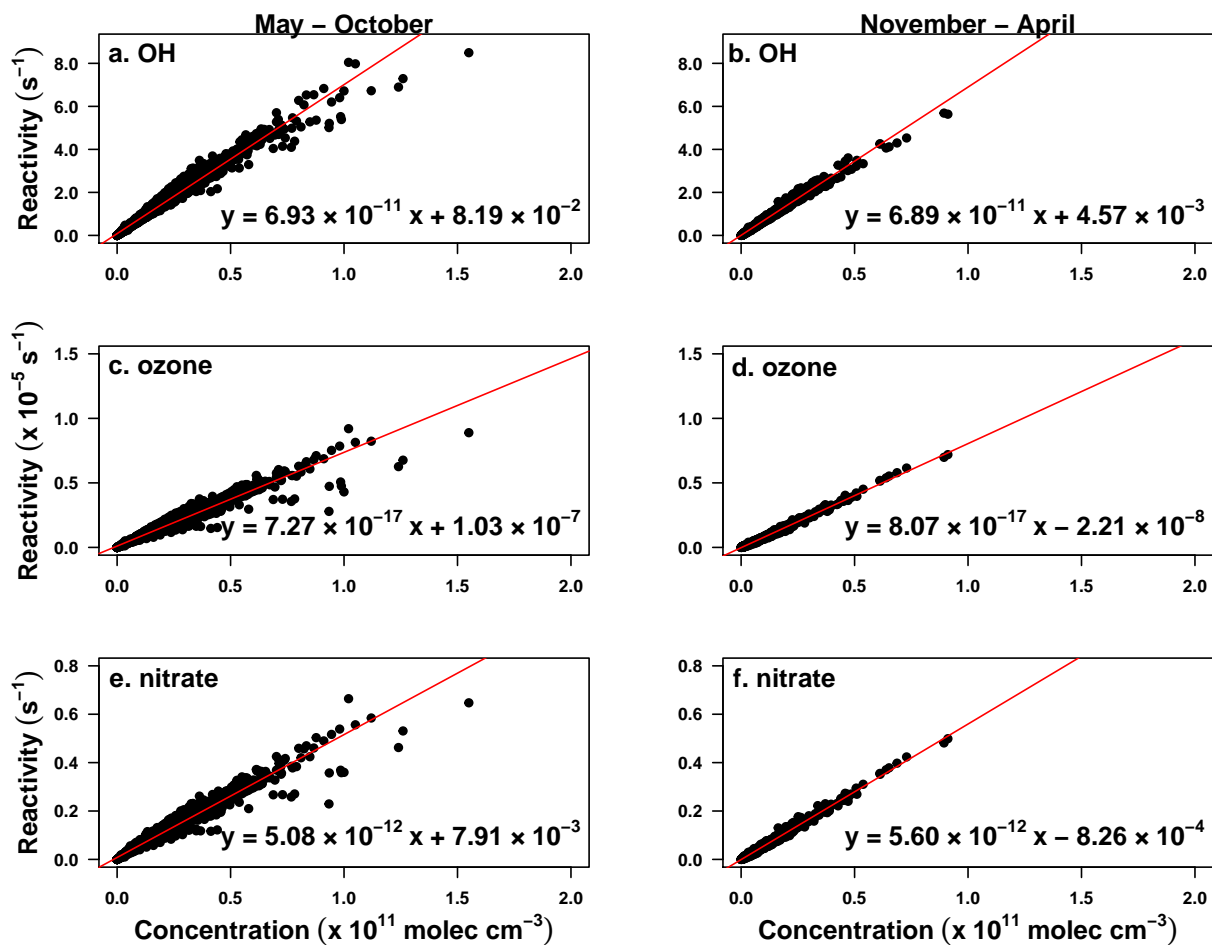


Figure C.3 Concentration plotted against reactivity to yield the rate constant for OH (a-b), Ozone (c-d), nitrate (e-f) in the growing and non-growing season. The slope in each equation is the average reaction rate of each oxidant with total monoterpenes.

Appendix D

Supplemental Information for

Chapter 4

Table D.1 Ozone rate constants and associated compounds

Compound	$k_{O_3}(cm^3molec^{-1}s^{-1})$
thujene	$6.20 \times 10^{-17,a}$
tricyclene	0
α -pinene	$9.00 \times 10^{-17,b}$
fenchene	$1.20 \times 10^{-17,c}$
camphene	$9.00 \times 10^{-19,a}$
sabinene	$8.30 \times 10^{-17,d}$
β -pinene	$2.10 \times 10^{-17,d}$
cymene	0
limonene	$2.10 \times 10^{-16,d}$
β -phellandrene	$1.80 \times 10^{-16,d}$
γ -terpinene	$1.40 \times 10^{-16,d}$

^aPinto et al. (2007), ^bAtkinson et al. (2006),
^cAtkinson et al. (1990), ^dAtkinson and Arey
(2003)

Table D.2 Mapping of bootstrap factors to base factors for 2019-2020 data

Bootstrapping run	Base Factor 1	Base Factor 2	Unmapped
Boot Factor 1	95	5	0
Boot Factor 2	0	100	0

Table D.3 Percent of factor attributed to light independent (%LI) and light dependent (%LD) emissions by compound for 2019-2020 data

compound	%LI	%LD
α -pinene	57.9	6.0
β -pinene	14.2	2.6
β -phellandrene	3.2	3.8
camphene	11.9	5.2
limonene	5.9	34.8
tricyclene	3.0	0.8
thujene	0.2	5.3
fenchene	2.3	0.9
sabinene	0.0	13.5
cymene	0.9	25.0
γ -terpinene	0.5	2.2

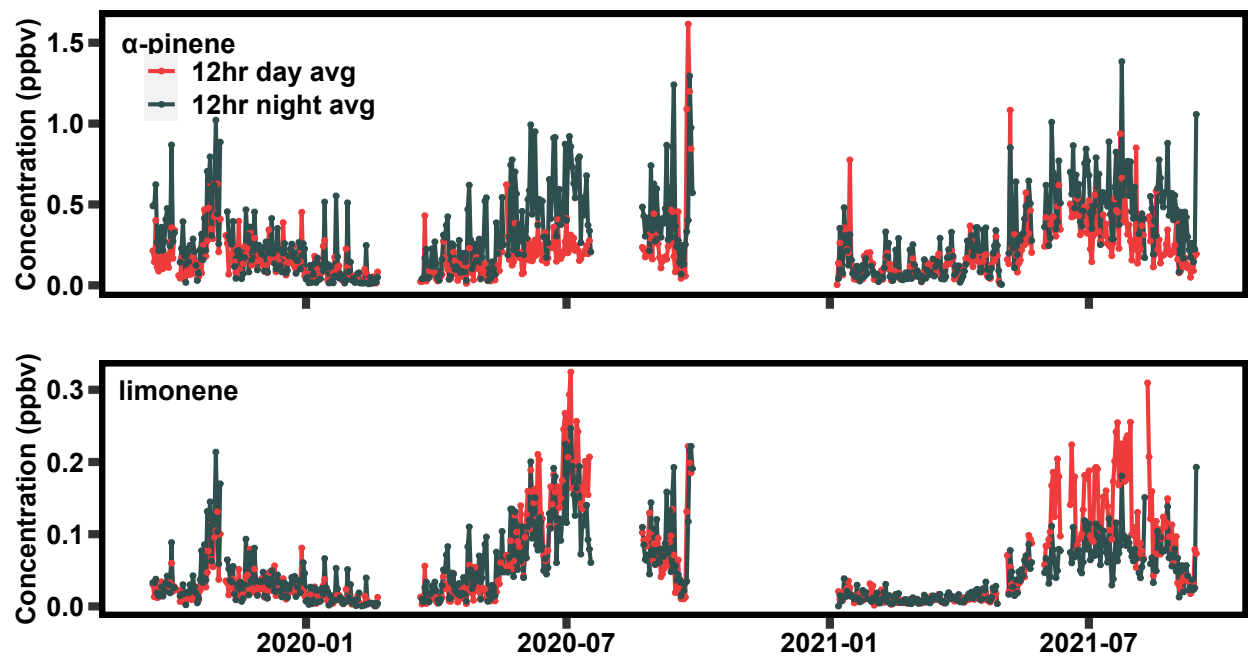


Figure D.1 The 12-hour average of α -pinene and limonene between September 2019 and September 2021. The averaging period for each compound was between 7 AM and 7 PM.

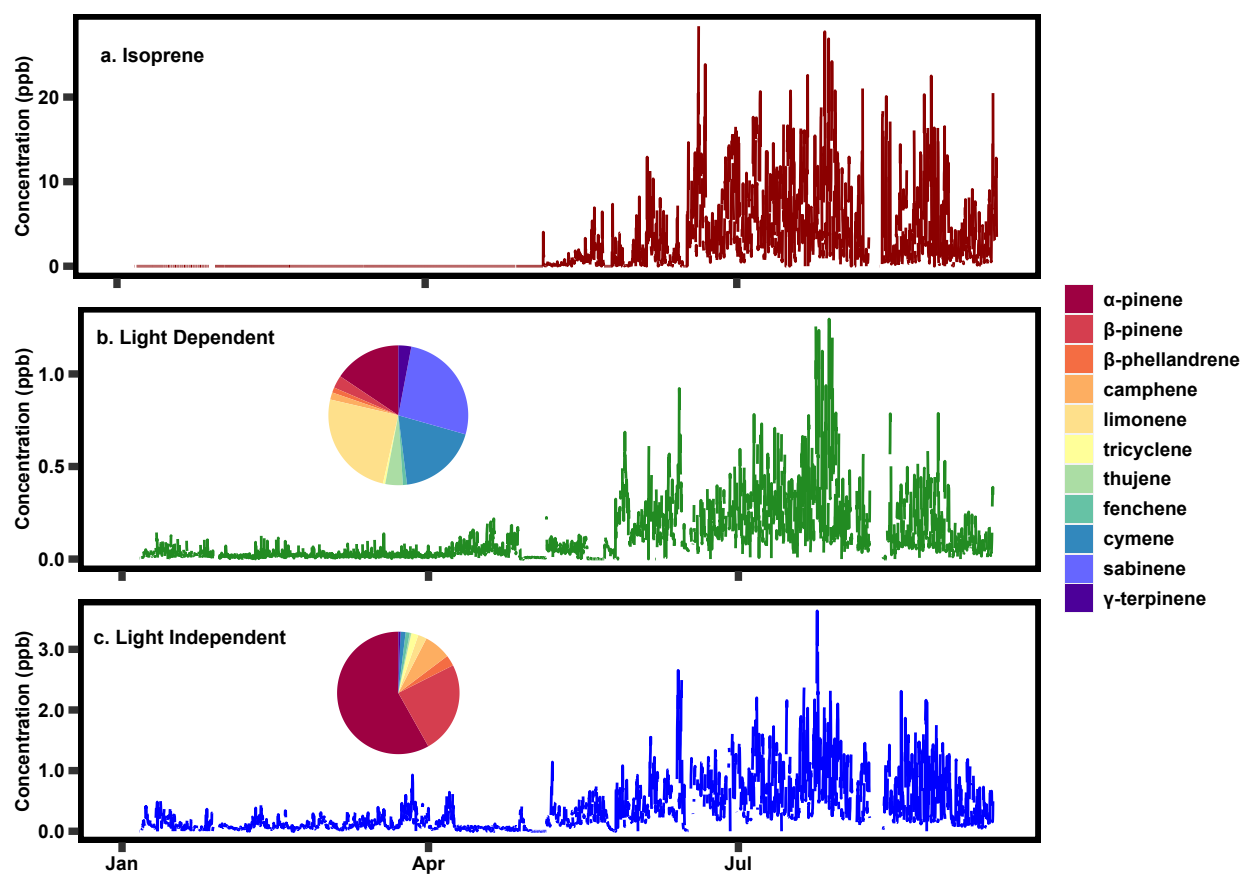


Figure D.2 Time series of isoprene concentration, the two positive matrix factorization factors between January 2021 and September 2021 and the breakdown of the monoterpane species that contribute to each factor.

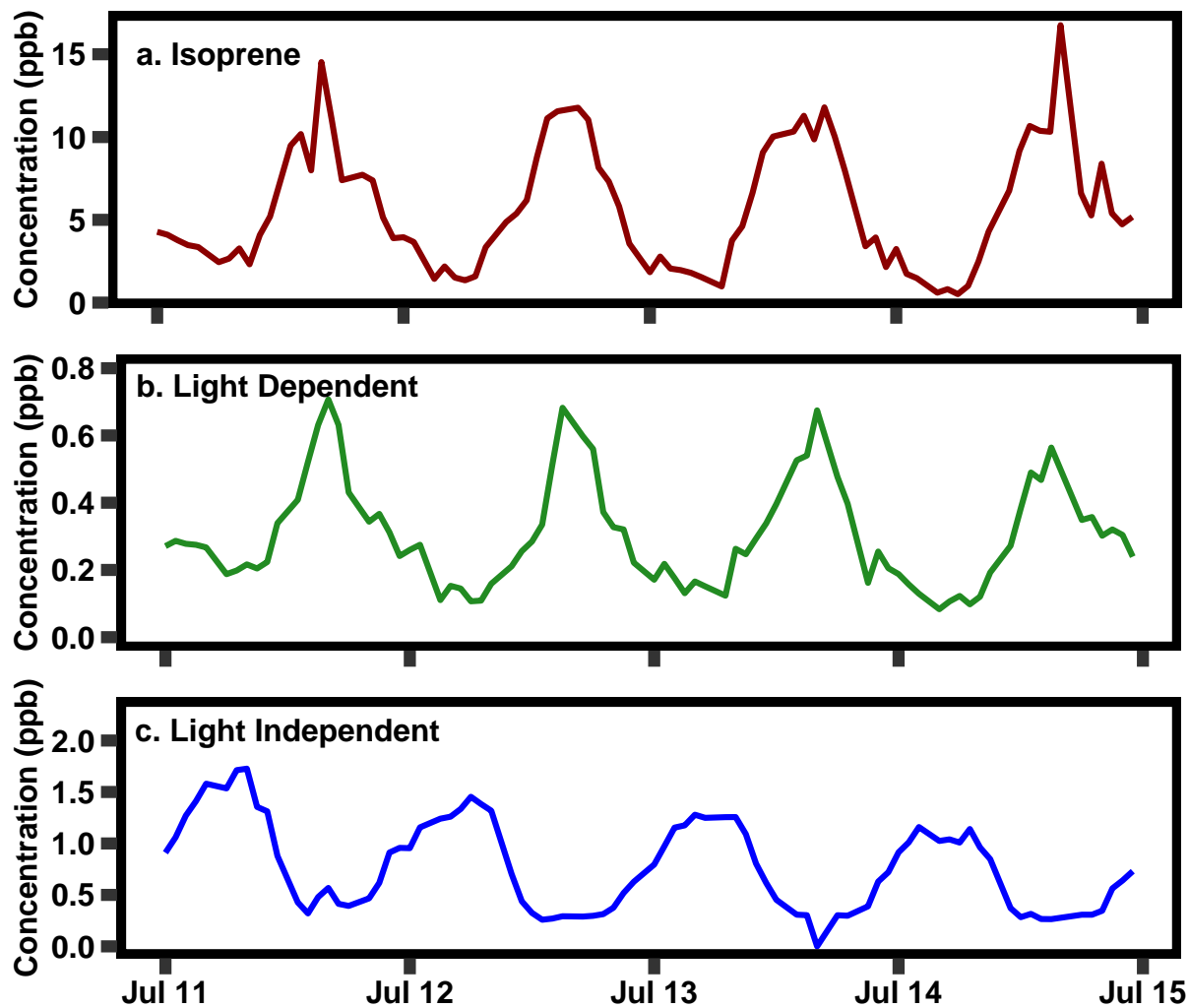


Figure D.3 A four-day period in July 2021 of isoprene, and the two PMF factors (Light Dependent and Light Independent).

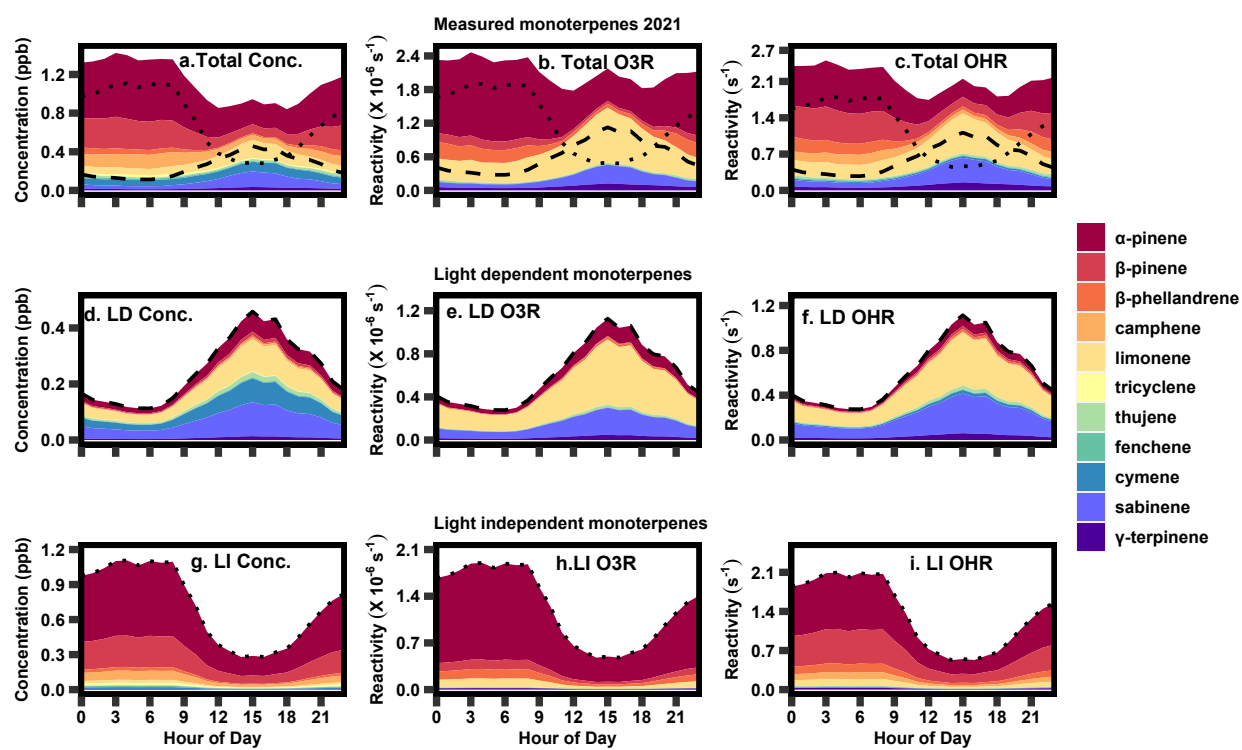


Figure D.4 The diurnal profile of (a) measured monoterpene concentration and (b) ozone reactivity, (c) factor 1 monoterpene concentration and (d) ozone reactivity, and (e) factor 2 monoterpene concentration and (f) ozone reactivity for summer 2021.